Detection of dementia (Alzheimer's disease) marker tau using a four gold microband electrode impedance sensor

Desiree E. Acha
(M00505823)

Submitted to Middlesex University in partial fulfilment of the requirements for PhD in Biomedical Science

Supervisors

Prof Richard Bayford

Prof Ajit Shah

Dr Frank Hills

Prof Ivan Riott

Detection of dementia (Alzheimer's disease) marker tau protein using a four gold microband electrode impedance sensor

By

Desiree E. Acha
(M00505823)

A thesis submitted in partial fulfilment of the requirements for the degree of

Doctor of Philosophy

October 2020

Faculty of Science and Technology

Middlesex University

London

Declaration

I, Desiree E. Acha confirm that the work presented in this thesis is my own. Where information has been derived from other sources, I confirm that this has been referenced in the thesis.

Abstract

Alzheimer's disease (AD) is the most common form of dementia, with an estimated 37 million sufferers worldwide and expected to affect 115 million by 2050. At present, there is no reliable technique or method for the diagnosis of AD in the early stages. There is an urgent demand to produce a reliable, cost-effective, objective testing and monitoring method in order to diagnose and then indicate treatment of Alzheimer's Disease. This study presents for the first time a four-electrode impedimetric biosensor system for the detection of tau protein, which is one of the most sensitive markers for the prediction of Alzheimer's and the level of this marker in the plasma has been found to correlate with cerebro-spinal fluid (CSF) load. The biosensor is based on the formation of stable antibody–antigen complexes on golden microband electrodes covered with a layer of a self-assembled monolayer (SAM) and protein G. Specific antibodies were immobilized on the surface of the gold electrode by interacting with protein G. Electrochemical impedance spectroscopy (EIS), where the impedance is measured as a function of frequency, was employed to analyze the impedance change, which revealed a linear response when the antigens/biomarkers bind to the antibodies with increasing concentrations. The assay is fast (30 mins for incubation and measurement) and very sensitive. The biosensor system demonstrated that it could detect the concentration down to 0.2 pM for the full-length 2N4R tau protein which is clinically relevant. This concentration is unaltered when the assay was processed in bovine serum albumin or human serum and is significantly below the detection limit of conventional detection methods such as ELISAs as demonstrated in this study. The specificity of the biosensor explored in this project was confirmed by means of Western blotting.

This method could be adapted for the detection of an array of biomarkers to provide a multiple assay which could increase the specificity and accuracy for the diagnosis of AD. The future commercialization of the biosensor system could be a revolutionary improvement for the early diagnosis and monitoring of AD progression in a point of care setting.

Acknowledgements

The work conducted so far together with this thesis is dedicated to my Mother my heroine, source of inspiration, motivation and courage that has helped me throughout my life especially in this difficult and challenging period. You have single-handedly raised me and my brothers after the demise of our father when we were as young as months old. Thank you so much, for giving me everything I ever needed and for always being there for me. I hope I will become the woman you always wanted me to be. Thank you mother so much, for being that rock solid shoulder I have had to lean on all these years. Thank you for all the invaluable advice and for tolerating my attitude every time I wasn't feeling well. Mother thank you for all the prayers, when I couldn't find the strength to pray, I knew within me that you were praying for me. And finally dad, though in death I know you are watching over me and guiding me with love, thank you.

I would like to thank my brothers Frank and Nico, for all the moral and financial support. Many thanks also to my cousin Eric, his wife Collette and their Kids Rosie and Darlene for making their home a place of escape when I needed to reset my brain and for their support and help over these years.

Thank you all so much for always being there listening to me, for your unconditional love, support and encouragement, for all the advice, all the hour-long phone calls, and patience. A very big thanks to Mrs Kadjija for all the invaluable scientific discussions I had with her over the years and for proof-reading most of what I wrote. A million thanks to Miss Tem Farlon, Mrs Millisen Malum , Mr Daba Agyingi , Mr Aristide Afunchwenchi for their non-stop support, the frequent phone calls during the past years, for their love and sweetness, for believing in me, for listening to me, for putting up with me for so long and for their advice and support.

I would like to express my greatest thanks and my outmost respect to my Director of Studies Professor Richard Bayford, whom I have known since 2014, for his guidance, supervision, help, support and understanding throughout all these years. Thank you so much, for taking me under your wing since day one, for being a mentor and a father figure to me, for allowing me to be your student and for believing in me. Thank you for your support, for your pressure for sitting next to me in the lab and in the office to help me understand new concepts, for your honest professional interest, your guidance and for all the invaluable advice you have

TABLE OF CONTENT

LIST OF TABLES

LIST OF FIGURES

Chapter 1

1.0   Introduction

The brain comprises many different parts including the cerebellum, cerebrum, frontal lobe and temporal lobe. These parts all have different functions as shown on Fig 1.1, for example, the hippocampus is responsible for long term memory. However, these parts all work together to order the body to perform its daily activities such as memory, thinking, problem solving, language, personality etc. Dementia is a general term used to describe a decline in brain function caused by different diseases (Table 1.1 and Fig. 1.2). Alzheimer's disease (AD) is the most common of these diseases (Fig 1.2).
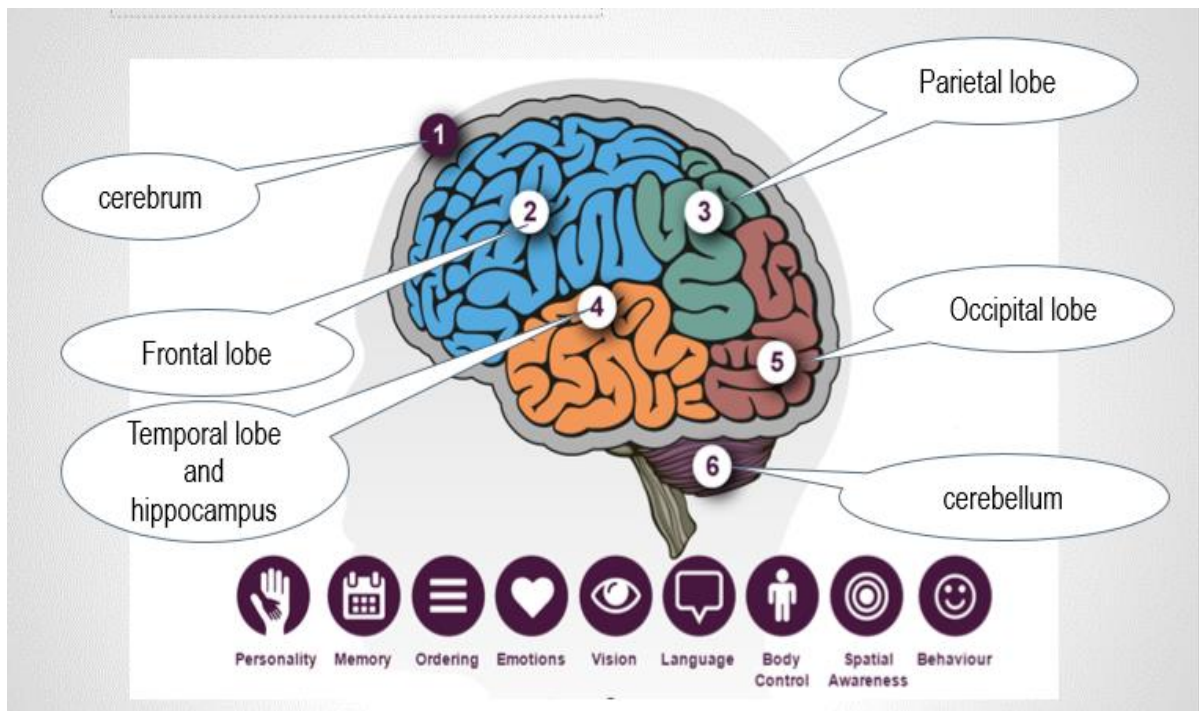
Figure 1.1 Major parts of the brain and a list of some of the functions they control.

Source: Adapted from Alzheimer's society, 2017

Table 1.1: Types of dementias, their signs and symptoms, pathology/imaging. The common symptom of all dementias is memory impairment

Type of dementia	Brief description	Signs and symptoms	Pathology
Alzheimer's disease	-Most common form of dementia -Accounts for about 60% to 80 % of all dementia -Gradual, progressive onset	-memory loss especially for names and recent events -Impaired visuospatial skills And later symptoms include -disorientation -confusion -Difficulty speaking, swallowing and walking -behaviour symptoms such as aggression	-Neurofibrillary tangles -amyloid beta plaques -Brain atrophy
Vascular dementia	-previously known as multi-infarct or post-stroke dementia - second most common form of dementia -abrupt or gradual onset	- impaired judgement -memory loss -mood swings	-strokes -lacunar infarcts -white matter lesions -vulnerable to cerebrovascular events
Lewy body dementia (DLB)	-insidious onset and progressive with fluctuations	-sleep disturbances -visual hallucinations -Fluctuating memory and thinking problems -muscle rigidity -tremors and falls	-Abnormal protein (alpha synuclein) called Lewy body accumulation in midbrain -general brain atrophy
Parkinson's disease	-As Parkinson's disease progresses, it will progress similar to Lewy body dementia and Alzheimer's disease	-first symptoms are problems with movement -similar symptoms as in dementia with Lewy body	-Abnormal protein (alpha synuclein)called Lewy body accumulation in midbrain
Korsakoff syndrome	-Most common cause is alcohol misuse	- strikingly severe memory problems whereas other functions such as thinking and social skills maybe relatively unaffected	-Deficiency of thiamine (Vitamin B-1) resulting in chronic memory loss

Type of dementia	Brief description	Signs and symptoms	Pathology
Creutzfeldt-Jakob disease (CJD)	-Most common human form of a group of rare fatal brain disorders affecting both humans and other mammals -variant of CJD (mad cows disease) common in cattle has been transmitted to humans in some circumstance	-impaired memory -behaviour changes -rapidly fatal	-Presence of Prion protein in the brain
Mixed dementia	-Abnormality common to more than one type of dementia occurs in simultaneously the brain	-depend on disease involved	-Depends on diseases involved
Fronto-temporal dementia (FTD)	-Includes dementias such as behavioural variant FTD (bvFTD), primary progressive aphasia, pick's disease and progressive supranuclear palsy -Insidious onset -typically 50s and 60s -Rapid progression	-disinhibition -socially inappropriate behaviour -poor judgement -apathy, decreased motivation -poor executive function	-Pick cells and pick bodies in cortex -Frontal and temporal atrophy

Source: (Alzheimer's society 2017; Holmes & Amin 2016)

Types of dementias and their percentages
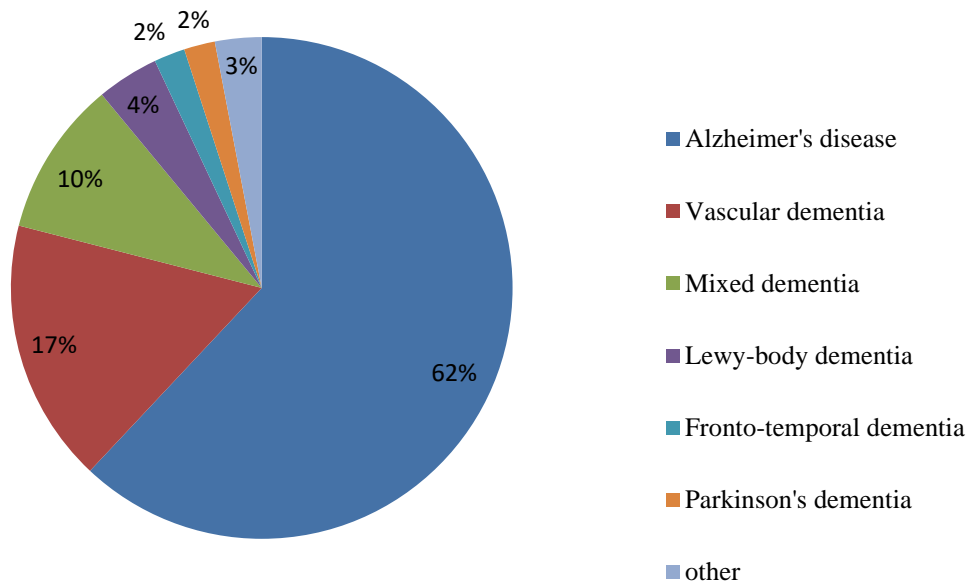
Figure 1.2: **Representation of the incidence of the different types of dementias in the UK in percentages (Adapted from Alzheimer's society, 2017).**

1.1. Dementia statistics

There was an estimated 50 million people in the world living with dementia in 2019, and this number is projected to double every 20 years, reaching over 75 million by 2030 and about 152 million by 2050 (World Alzheimer Report, 2019; Livingston *et al.*, 2020). It is believed that someone develops dementia every three seconds. Much of the increasing rate of dementia is in the developing countries particularly China, India and their south Asian and Western Pacific neighbours. In the UK, there are over 850,000 people living with dementia and this number is predicted to rise up to 1.6 million by the year 2040 (Alzheimer's society, 2020).

Worldwide, the total estimated annual cost of care for dementia was about US $ 1 trillion in 2019, a figure set to double by 2030 (Comas-Herrera, 2019). According to the Alzheimer's society, the total cost of care for people with dementia in the UK is currently about £34.7 billion a year. This is predicted to rise over the next two decades to £94.1 billion by 2040 (Alzheimer's society, 2020). The current prevalence consensus found that there are slightly more people with dementia in the youngest (65 to 69) and oldest (90+) age bands and slightly fewer in the intermediate age groups. Over 42.000 people under the age of 65 years (working age) in the UK live with dementia (early-onset dementia, Alzheimer's society, 2020)

implying that dementia is no longer just a disease of old age as was thought of previously. Alzheimer's disease makes up 60% to 80% of the total dementia population; therefore, urgent action is needed to address the devastating effects of dementia particularly Alzheimer's disease.

1.2 Alzheimer's disease

There are about 37 million sufferers worldwide, a number expected to triple by 2050 if no effective therapeutic strategies are developed (Wimo *et al.*, 2013). AD is considered a neurodegenerative disease meaning that it causes the loss of neurons in the brain, particularly in the cortex, leading to the symptoms characteristic of dementia (Table 1.1). The cause of AD is not completely understood, however two major hallmarks that are often sighted in its progression are amyloid beta plaques and neurofibrillary tangles (Alzheimer's Association, 2019; Holmes and Amin, 2016; Kametani and Hasegawa, 2018) (See Section 1.3).

1.2.1   Risks associated with onset of AD

In addition to the hallmarks mentioned in Section 1.2, genetic factors have also been implicated in the onset of AD pathology which could be Sporadic or Familial (Holmes and Amin, 2016). Sporadic AD describes the cause of late onset AD resulting from a combination of genetic and environmental risk factors. Sporadic AD accounts for the majority of cases and the risk increases significantly with age. Apolipoprotein E gene (ApoE e4) has been highly associated with onset of AD (Coon et al., 2007). Research has shown an increase risk of developing AD with inheritance of 1 ApoE e4 allele and this risk further increases with 2 inherited ApoE e4 alleles, one from each parent (Chen, Lin and Chen, 2009) while ApoE e3 has been associated with less risk of developing disease (Alzheimer's Association, 2019).

Familial AD onset is used to describe situations where a dominant gene was inherited that speeds up the progression of the disease, sometimes referred to as early onset AD. Early onset AD accounts for about 5 to 10 % of cases and can be caused by several gene mutations. Mutations in the PSEN1, PSEN2 and APP genes on chromosomes 14 , 19 and 21 respectively have been linked to early onset AD (Wu et al., 2012; Loy et al., 2014; Alzheimer's Association, 2019). PSEN1 and PSEN2 encode for presenilin 1 and presenilin 2 which are both subunits of γ-secretase an enzyme that plays an important role in the synthesis of APP to amyloid beta. Mutations in PSEN1 or PSEN2 can alter the position where γ-secretase chops APP producing varying lengths of amyloid beta, most commonly Aβ 1-40, Aβ1-42. Aβ1-42 is the more hydrophobic form of amyloid and has been reported to be better at forming plaques (Zhang et al., 2011).

Another known risk factor of AD is Down syndrome or trisomy 21, which involves an extra copy of chromosome 21 (Jiang *et al*., 2010, Choices 2015). The gene required for synthesis of APP is located on chromosome 21 implying people with Down's syndrome have an extra APP gene leading to increased expression of APP, potentially increasing the amount of amyloid plaque build-up. It is for this reason that familial AD usually progresses by age 40 in people with Down syndrome (Trazzi *et al.*, 2013).

1.2.2 Diagnosis of AD

The diagnosis of AD is difficult due to asymptomatic onset and presentation of symptoms rather during later stages of the disease. Currently, the only way to effectively confirm clinically that a person has AD is by performing a brain biopsy after autopsy. Usually, a clinician will make a diagnosis of AD after excluding other causes of dementia such as stroke, depression, excessive alcohol, Parkinson's disease and cardiovascular disease. There is no simple diagnostic test for AD, current diagnosis is dependent on mini-mental examinations (questionnaires) and imaging (Cunningham *et al.*, 2015). These approaches can only diagnose advanced AD in patients, they cannot predict the disease onset. Furthermore, neuroimaging techniques like MRI and PET scans are only available in some hospitals and they are costly and some patients are not able to undergo these procedures. New diagnostic tests based on objective measurements for early and specific recognition of Alzheimer's disease at the prodromal stages are of crucial importance in order to find a cure for this devastating disease (Cunningham *et al.*, 2015). Current research is looking into the use of biomarkers for earlier diagnosis of AD (Mayeux and Schupf, 2011 Andreasen *et al.*, 2001; Craig-Schapiro, Fagan and Holtzman, 2009; Hampel *et al.*, 2010; Humpel, 2011; Koyama *et al.*, 2013; del Campo *et al.*, 2015; Blennow, 2017; Pekeles *et al.*, 2018)**.** A reliable, cost-effective method or device for aggressively and objectively detecting and monitoring using biomarkers to identify the onset and progression of AD for effective intervention is urgently needed as a priority identified within the **'World Alzheimer Report 2015:** The Global Impact of Dementia'. The current project aims at developing a Point-of-Care device (POC) to address this need. The method developed during this project will aim to provide a fast economical diagnostic device that provides multiple answers for use in doctors' clinics and field stations to enable immediate clinical decisions to be made without the need to wait for distant laboratories' answers, in addition, to monitoring disease progression.

1.2.3 Treatment of AD

Glutamate and acetylcholine signalling pathways are involved in learning and memory processes in healthy individuals. Neurotoxicity resulting from amyloid beta deposits has been associated with dysfunction of both glutamatergic and cholinergic signalling resulting in direct impairment of cognition and neuronal loss leading to symptoms seen in AD. While there are no medications that can cure or stop AD from progressing, there are medications (Table 1.2) that may help lessen symptoms, such as memory loss and confusion, for a limited period of time. The U.S. Food and Drug Administration (FDA) has approved two types of medications for treatment of AD: Acetylcholinesterase inhibitors (AchEI) or cholinesterase inhibitors for short which include (Donepezil (Aricept), Rivastigmine (Exelon) and Galantamine (Razadyne)), and N-methyl-D-aspartate (NMDA) receptor antagonist; memantine (Namenda) (Parsons *et al.*, 2013). The mechanism of action of cholinesterase inhibitors interfere with the cholinergic signalling pathway by inhibiting the action of acetylcholinesterase, an enzyme responsible for the breakdown of acetylcholine. Acetylcholine is a neurotransmitter which presents in lower than normal amounts in AD (Parsons *et al.*, 2013). NMDA receptor antagonists act through the glutamatergic signally pathway to block the effect of excess glutamate and prevent further damage of nerve cells in the brain. Glutamate like acetycholine is a neurotransmitter; it is well documented that the glutamatergic and cholinergic pathways influence each other, and that their joint dysfunction is central to the effects produced by AD pathology. Consequently, the combined use of memantine and an AchEI to address these two pathological aspects of AD would appear to be a highly logical and rational approach to treatment in which case Namzaric (a combination of both Donepezil and memantine) is used as a more effective treatment for severe AD (Parsons *et al.*, 2013) .

Table 1.2: Approved treatments for cognitive function and their side effects

Generic	Brand	Approved for	Side effects
Donepezil	Aricept	All stages	Nausea, vomiting, loss of appetite and increased frequency of bowel movements.
Galantamine	Razadyne	Mild to moderate	Nausea, vomiting, loss of appetite and increased frequency of bowel movements.
Memantine	Namenda	Moderate to severe	Headache, constipation, confusion and dizziness

Rivastigmine	Exelon	Mild to moderate	Nausea, vomiting, loss of appetite and increased frequency of bowel movements.
Memantine +donepezil	Namzaric	Moderate to severe	Headache, diarrhea, dizziness, loss of appetite, vomiting, nausea, and bruising

Source: (Alzheimer's society, 2017)

For other symptoms such as sleep changes and behaviour, non-drug approaches are used depending on the symptom, for example avoiding caffeine for sleeplessness. However, if symptoms don't get better then anti-depressants are prescribed to better mood and enhance sleep (Alzheimer's society, 2017).

1.3 Pathology of AD

Tangles and plaques together with other genetic factors and inflammation have been implicated in the onset of AD (Akiyama *et al*., 2000; Tanzi & Bertram 2001; Ballatore *et al*., 2007; LaFerla *et al*., 2007; Rubio-Perez & Morillas-Ruiz 2011). Central to this is a specific protein called amyloid precursor protein (APP). APP is found in the cell membrane of neurons in the brain. APP is thought to help the neuronal cell to grow and repair itself after injury. APP is processed by proteolytic enzymes called secretases through amyloidogenic or non-amyloidogenic pathways. The amyloidogenic pathway is the process of Aβ biogenesis: APP is first cleaved by β-secretase, producing soluble β-APP fragments (sAPPβ) and C-terminal β fragment (CTFβ, C99), and C99 is further cleaved by γ-secretase, generating APP intracellular domain (AICD) and Aβ also known as amyloid beta monomer. The non-amyloidogenic pathway is an innate way to prevent the generation of Aβ, as APP is first cleaved by α-secretase within Aβ domain, generating soluble α-APP fragments (sAPPα) and C-terminal fragment α (CTFα, C83), C83 is then cleaved by γ-secretase, producing non-toxic P3 and AICD fragments (Fig 1.3)(LaFerla *et al*., 2007; Zhang *et al*., 2011; Sun, Chen and Wang, 2015).
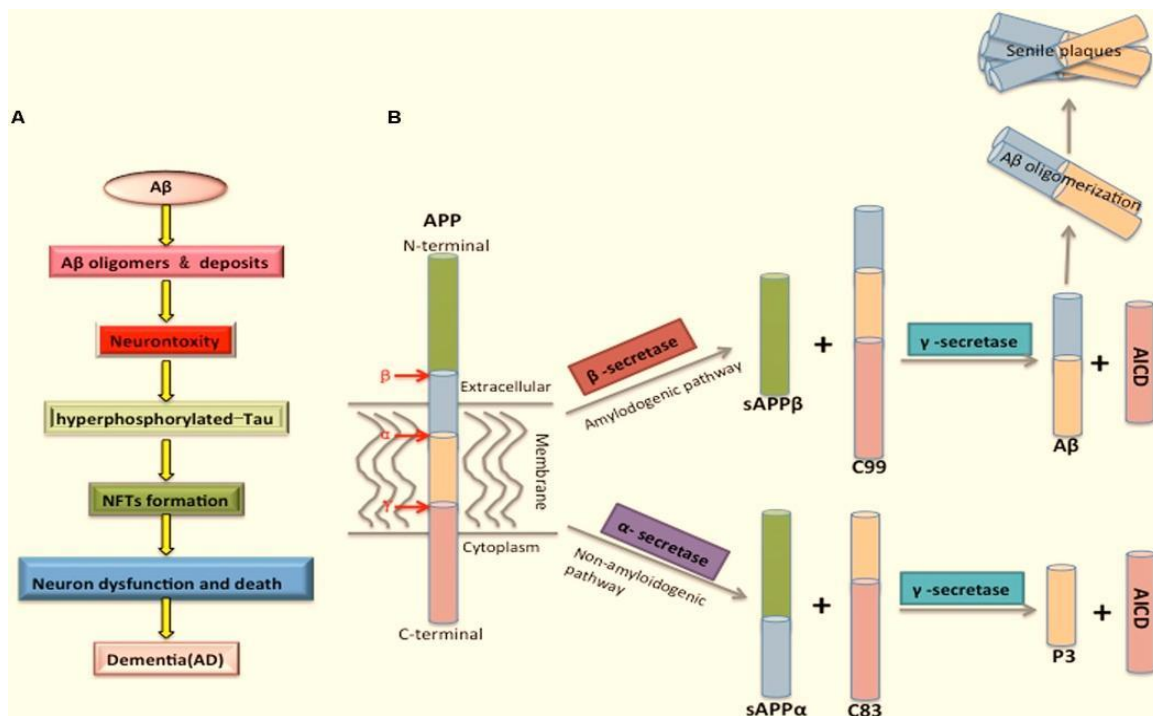
Figure 1.3 : (A) The mechanism of amyloid beta (Aβ) toxicity and the interplay between amyloid and Tau protein in the pathogenesis of AD.(B) The biogenesis of Aβ from the proteolytic processing of Amyloid precursor protein (APP)(Sun, Chen and Wang, 2015).

Aβ monomers are chemically sticky and tend to stick together outside the neurons, forming oligomers. Amyloid oligomers are a fundamental component of amyloidogenic disorders such as Alzheimer's disease, being both critical intermediates in the formation of amyloid fibrils and plaques and are the most toxic species on the protein aggregation pathway (Dear *et al.*, 2020). The series of events leading to onset of AD initiated by accumulation of Aβ has been described as the amyloid cascade hypothesis (Section 1.3.1). The second hallmark of AD is tangles which are found inside of the cells as opposed to the amyloid beta found outside the cells. Like every other cell, neurones are held together by their cytoskeleton which is partly made up of microtubules stabilized by tau protein (Ballatore, Lee and Trojanowski, 2007). Tau protein is phosphorylated protein and in the brains of AD patients, tau is deposited in a hyperphosphorylated state in inclusions which are unique twisted fibrils appearing as either paired helical filaments (PHFs) or straight filaments (SFs) (Liu and Gong, 2016). These inclusions are pathological and are referred to as neurofibrillary tangles if formed in neuronal cell bodies, otherwise called threads if formed in dendrites and axons, suggesting that tau mis-sorting might induce tau pathology (Zempel and Mandelkow, 2014). The onset of AD initiated by pathological tau has been described as tau hypothesis (Section 1.3.2).

1.3.1 Amyloid Cascade hypothesis

Once formed plaques can get between neurons which can then affect neuron to neuron signalling thus impairing brain functions such as memory (Palop and Mucke, 2010). It is also believed that plaques can start an immune response, through the activation of microglia, triggering calcium influx, causing oxidative stress and inflammation which could damage neurons (McGeer and McGeer, 2013). Amyloid plaques can also be deposited around blood vessels in the brain leading to amyloid angiopathy which weakens the walls of blood vessels causing an increased risk of haemorrhage (Akiyama *et al*., 2000).

Although it is not completely understood, one school of thought suggest that the build-up of amyloid plaques outside the neuronal cell initiate pathways inside the neurons that lead to the activation of kinases such as glycogen synthase kinase 3 (GSK3α and GSKβ), mitogen-activated protein kinase 13 (MAPK13) and microtubule-associated regulatory kinase (MARK) enzymes as well as raised levels of calcium that promote phosphorylation of tau protein (Hardy and Selkoe, 2002, Cao *et al.*, 2019). Tau protein is then believed to change in shape, developing the inability to stabilize the microtubule. The tau proteins start to aggregate with other tau protein molecules forming oligomers and further tangles called neurofibrillary tangles. Neurons with unstabilized microtubules affect signal transmission leading to apoptosis of the neuronal cell (Spillantini and Goedert, 1998; Ballatore, Lee and Trojanowski, 2007; Wang and Mandelkow 2015; Kametani and Hasegawa, 2018; Goedert, Eisenberg and Crowther, 2017). As the neurons die, changes such as shrinkage start to take place in the brain. The process of amyloid accumulation triggering the formation of neurofibrillary tangles, cell loss, vascular damage, and eventually dementia has been described as the amyloid-beta cascade hypothesis (Hardy and Higgins, 1992; Giacobini and Gold, 2013; McGeer and McGeer, 2013; Ricciarelli and Fedele, 2017) (Figure 1.2).
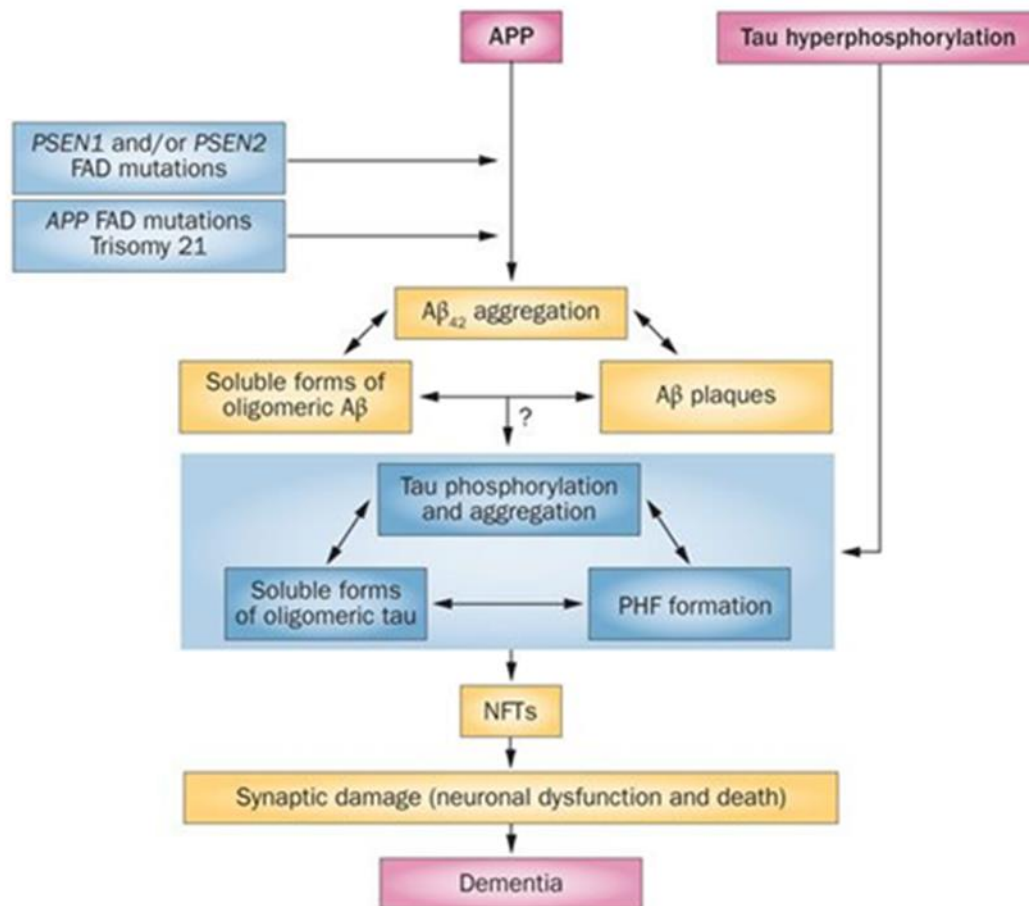
Figure 1.4: Schematic representation of the amyloid cascade hypothesis showing amyloid aggregates as the triggering event in the pathology of AD. Source: Adapted from Giacobini and Gold, 2013.

The amyloid cascade hypothesis has been greatly criticised as the triggering event in AD pathogenesis with huge opposing evidence. Aβ accumulation and deposition has been consistently shown not to correlate with neuronal loss and cognitive decline; furthermore, some studies have reported that many individuals assessed with PET scans have presented with significant amyloid plaque burden without showing symptoms of memory impairment (Delaère *et al.*, 1990; Villemagne *et al.*, 2011; Kametani and Hasegawa, 2018). Furthermore, amyloidocentric therapies have successfully brought about pharmacological reduction of Aβ without any effect on the symptoms of neuronal damage or tau load (Ostrowitzki *et al.*, 2012; Giacobini and Gold, 2013; Doody *et al.*, 2014), possibly suggesting that tau rather than amyloid causes neuronal damage.

1.3.2 Tau hypothesis

Tau protein undergoes various post-translational modifications (PTMs) (see Section 1.4.1.1.) which contribute in the regulation of tau binding to tubulin to ensure the appropriate dynamics of the system. Tau binding to MTs, as well as its propensity to aggregate, are affected by tau mutations and by tau PTMs, particularly, its hyper-phosphorylation. These pathologically modified tau molecules distort microtubule function and axonal transport, contributing to tau accumulation and neurodegeneration (Barbier *et al.*, 2019). An increased amount of modified tau has been found in a large numbers of neurodegenerative disorders referred to as tauopathies including corticobasal degeneration (CBD), frontotemporal dementia and Parkinsonism linked to chromosome 17 (FTDP-17), progressive supranuclear palsy (PSP), Pick's disease (PiD), argyrophilic grain disease (AGD), tangleonly dementia, and chronic traumatic encephalopathies (CTE) (Lee, Goedert and Trojanowski, 2001; Kovacs, 2015; Takeda, 2019) (Sergeant, Delacourte and Buée, 2005; Spillantini *et al.*, 1998; Buée *et al.*, 2000; Portelius *et al.*, 2008; Wang and Liu, 2008; Wang and Mandelkow, 2015; Goedert, Eisenberg and Crowther, 2017)**.**

It has also been demonstrated from various findings through *in vitro* and *in vivo* models that pathological forms of extracellular tau taken up by cells, can induce intracellular tau aggregates. Thus, hypothesizing that tau aggregates first form in a small number of brain cells, from where they propagate into other regions, causing neurodegeneration and thus disease. This hypothesis has recently gained attention because it has been confirmed that tau proliferates and propagates between cells (Hasegawa, 2016; Goedert, Eisenberg and Crowther, 2017; Takeda, 2019; Vogel *et al.*, 2020). The existence of several human tauopathies with distinct fibril morphologies has led to the suggestion that different molecular strains of aggregated tau exist (Goedert, Eisenberg and Crowther, 2017). Although the mechanism of transmission of tau aggregates from cell to cell is still unclear, tau pathology does spread in the brain in a well-defined manner and its distribution can be correlated strongly with the clinical stages of disease (Braak and Braak, 1991). Similar findings have been reported by Vogel et al., (2019). Recently, PET studies have closely linked spatial patterns of tau tracer binding to the patterns of neurodegeneration and clinical presentation seen in AD brains (Okamura *et al.*, 2014; Bejanin *et al.*, 2017). These findings implicate subjective cognitive decline as a sign of early tauopathy in the temporal lobe, and to a lesser extent with elevated global levels of Aβ (Buckley *et al.*, 2017). It is therefore considered that

tau pathology correlates better than Aβ pathology with clinical features of dementia (Takeda, 2019).

1.3.3   Interplay between tau and amyloid in AD

The principal role of tau, which is to modulate the stability of axonal microtubule has been reported to mediate amyloid beta toxicity which in turn, promotes tau hyper-phosphorylation and propagation (Vogel *et al.,* 2019). However, Takahashi *et al.* (2015) reported increased APP with or without familial AD mutations and that APP, not Aβ, acts as a receptor of abnormal tau fibrils and as a result promote tau aggression intracellularly. This suggests that APP rather than Aβ is responsible for the acceleration of tau hyper-phosphorylation, aggregation, accumulation and propagation (Goedert *et al.*, 2017). This contradicts previous report where amyloid peptide has been reported to drive tau hyper-phosphorylation.

Aβ oligomers are known to kill neurons *in vitro* (Kim *et al.,* 2003) and neuronal cell death has been reported to be virtually absent in APP or APP/PS1 transgenic mice modelling human AD (kin *et al.,* 2013). This suggests that high levels of endogenous Aβ peptides do not trigger neurodegeneration *in vivo*, irrespective of their assembly state. This also agrees with numerous studies where tau deficient neurons were resistant to Aβ neurotoxicity *in vitro* and endogenous tau reduction in AD mouse models which protected them from Aβ-induced synaptotoxicity and memory deficient (Rapoport *et al.,* 2002; Roberson *et al.,* 2007; Leroy *et al.,* 2012).

According to Ittner and Götz (2011), the two proteins can act in a synergistic fashion to cause cell death and Aβ is 'the trigger and tau is the bullet' in the AD pathocascade (Bloom, 2014). KJ *et al.* (2009) reported that APP and APP/PS1 mice, which produced elevated levels of Aβ, did not show evidence of tangle formation. Tangles appear to precede plaques formation and their distribution seem to correlate much better than plaques (Braak and Braak, 1991; Schönheit, Zarski and Ohm, 2004). However, Drummond and Wisniewski (2017) argue that different tau isoform profiles are expressed in mouse and human brains. Current knowledge on Aβ pathophysiology derives from transgenic AD mice, raises the question as to whether or not they can represent adequate models of the human pathology. These mice usually carry the mutations found in Familial AD (FAD) and may not be representative of a late onset Sporadic AD (SAD) that accounts for over 95 % of AD patients. Although, the anatomical features of the two forms of AD pathology are similar, it is well known that they manifest at different ages, and with distinctive cognitive symptoms and

disease progression (Komarova and Thalhauser, 2011). In addition, using a novel approach with adeno-associated viral vectors, it has been reported that *in vivo* expression of human wild type Tau4R causes cell death in cortex and hippocampal neurons in the absence of accumulation of Aβ peptides (Jaworski *et al.*, 2009, 2010) suggesting that, contrary to the amyloid cascade hypothesis, tau-induced neurodegeneration can occur independently of Aβ. This implies that the onset and progression of AD is strongly associated with tau pathology rather than amyloid and that tau is a more accurate predictor of disease severity (cook et al. 2015). It is however noteworthy that the relationship between amyloid deposits and neurofibrillary tangles remains an unresolved issue in the understanding of the pathogenesis of AD.

Both pathways lead to build up of plaques and tangles, which could commence years before neurodegeneration implying that early detection of the disease is possible. As the disease progresses, patients start to lose short term memory. Then motor skills and language are affected making movement and communication difficult. Eventually long term memory is lost, patients progressively become more disoriented and become bed-ridden in the late stages (Holmes and Amin, 2016).

1.4 Biomarkers

A biomarker is a characteristic that is objectively measured and evaluated as an indicator of normal biological processes, pathogenic processes, or pharmacologic responses to a therapeutic intervention (Strimbu and Tavel, 2011). A biomarker can serve as an indicator of health (i.e. biomarker of ageing) and disease. The sensitivity, specificity and ease-of-use are the most important factors that ultimately define the diagnostic utility of a biomarker. Some biomarkers are more reasonably viewed as risk factors rather than true disease markers. A change in the levels of biomolecules in the body can result in disease and also disease state or an alteration in normal physiology can result to abnormally high or low levels of biomarkers in the body. The effective prevention or management of a disease depends upon the ability to recognize the high-risk individuals at an early stage of the disease or long before the development of adverse events.

Biomarkers can be an objective measurement of the state of the disease in Alzheimer's patients. There is evidence that the most sensitive markers for the prediction of Alzheimer's are measured in cerebro-spinal fluid (CSF) (Blennow 2004; Craig-Schapiro *et al.*, 2009; Humpel, 2011; Hata e*t al*., 2016). However, obtaining this fluid is a highly invasive procedure with potential side effects. Other studies have looked into measuring these

biomarkers in fluids that can be obtained in a less invasive manner such as blood, plasma, serum and urine (Mayeux & Schupf 2011; Geekiyanage *et al*., 2012; Liu, Qing and Deng, 2014).Compared to CSF, these other matrices contain more contaminants, larger molecules and methods to analyse tau in these matrices are at the experimental beginning. The varying pH of urine limits it's use in biosensor measurements. For the purpose of this Study, CSF which is a more widely validated matrix is used to check that the biosensor works.

To objectively monitor the progress of Alzheimer's and provide a method of early detection, a range of parameters that indicate the degree and progression of the condition in the form of a biomarker signature is required. Analysis of peripheral biomarkers will provide an easy means for early detection and reduce the discomfort associated with techniques like lumbar puncture. Below is a comparison of levels of some of the possible AD biomarkers measured in CSF of controls and AD patients (Table 1.3) as well as various other conditions in which levels may be altered (Table 1.4) .

Table 1.3: Comparison of values of CSF markers of AD in Controls and AD state. Data was obtained by ELISA.

Biomarker	Controls: mean ±2SD (pg/ml)	AD (pg/ml)
Amyloid Beta (Aβ) (1–42)	794±20	<500
Total tau	136±89 (21–50 years)	N/A
	243±127(51–70 years)	>450 >600
	341±171 (>71 years)	
Phospho-tau-181	23±2	>60

Source: (Humpel, 2011).

From Table 1.3, Levels of CSFAβ(1–42) shows a significant reduction in AD patients compared to controls, with a cut-off of <500 pg/ml . Mollenhauer *et al.*, 2006 suggested that reduced levels of Aβ (1–42) in the CSF are caused by reduced clearance of Aβ from the brain to the blood/CSF, as well as enhanced aggregation and plaque deposition in the brain). In healthy controls, levels of total tau in the CSF increase with age (Buch et al., 1999) <300 pg/ ml (21–50 years), <450 pg/ml (51–70 years), and<500 pg/ml (>70 years). Total tau levels are significantly enhanced in AD patients as compared with age-matched control subjects with a cut off of >600 pg/ml. The detection of tau phosphorylated at position 181 is significantly enhanced in AD compared to controls with a cut-off of >60 pg/ml (Table 1.3) and the changes of CSF phospho-tau-181 levels in different diseases are given in Table1.4.

Table 1.4: Changes in the levels of some established CSF biomarkers in other various conditions which levels may be altered.

Disease	Aβ (1–42)	Total tau	Phospho-tau-181
Acute stroke	–	↑	–
Alcohol dementia	–	–	–
Alzheimer's disease (AD)	↓	↑	↑
Creutzfeldt-Jakob disease (CJD)	↓↓	↑↑↑	–
Depression	–	–	–
Frontotemporal lobar degeneration (FTLD)	↓	↑	–
Lewy body dementia (LBD)	↓	↑	↑
Neuroinflammation	↓	–	–
Normal aging	–	–	–
Parkinson's disease	–	–	–
Vascular dementia (VaD)	↓	↑	–

Source: (Humpel, 2011) Where (–) = no change; (↓) = decrease; (↑) = increase.

At present, only the analysis of Aβ (1-42), total tau and phospho-tau in CSF allows reliable, sensitive and specific diagnosis of AD, but not of other forms of dementia (Andreasen *et al.*, 2001, Hu *et al.*, 2002, Sjögren *et al*., 2001). Unfortunately, the use of CSF biomarkers as a wide screen test is limited because of the invasive method used to collect the sample and secondly because the availability of collecting CSF through spinal taps is limited in many regions in the general population. Early, fast and cheap diagnosis from body fluids using modern, ultrasensitive analytical methods will become extremely important in the future to differentiate AD from other forms of dementia (Blennow, 2017b). At present there is no clear biomarker signature defined for AD; there is therefore an urgent need to identify one that will provide an effective method of diagnosis and follow progress of treatment.

1.4.1 Tau protein

Tau protein is a protein of the microtubule associated protein (MAP) family and is mostly found in the axons of neurons in humans (Buée *et al.*, 2000). Tau protein can also be found in small amounts in other cells such as glial cells (Sergeant, Delacourte and Buée, 2005). The human tau gene is located on chromosome 17 and has sixteen exons; three (exons 2, 3 and 10) of which are adult brain specific. Alternative splicing of these three exons (2, 3 and 10) results in the appearance of six tau isoforms, which contain 0, 1 or 2 amino-terminal inserts (of 29 or 58 amino acids) and 3 or 4 microtubule-binding repeats (0N/3R, 0N/4R, 1N/3R, 1N/4R, 2N/3R and 2N/4R) (Buée *et al.*, 2000; Liu and Gong, 2008; Wang and Liu,

2008). These isoforms are made up of amino acids ranging from 352 to 441 as shown on Fig. 1.5. Their molecular weight ranges from 45 to 65 kDa (Buée *et al.,* 2000; Wang & Liu 2008). Tau isoforms are likely to have different physiological roles as they are expressed differently during human development. For instance, only one tau isoform, the shortest 0N/3R isoform is present during fetal stages, while all six isoforms are expressed during adulthood (Buée *et al.*, 2000).
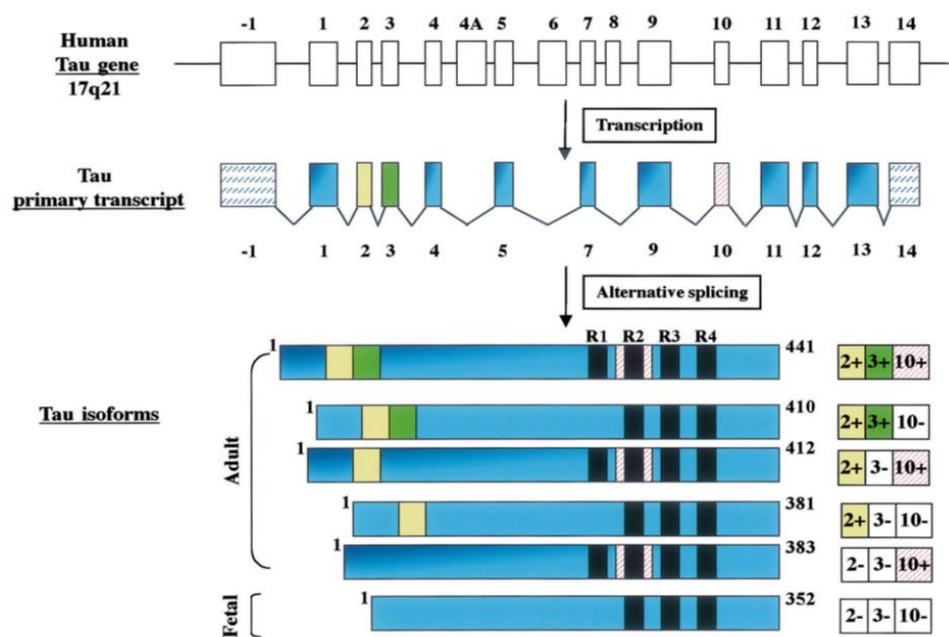
Figure 1.5: **Schematic representation of the human tau gene showing the human tau primary transcript and the six human isoforms** (Buée *et al.*, 2000).

1.4.1.1 Tau structure and function

Microtubules (MTs) are hollow cylinders formed by the lateral association of protofilaments into a regular helical lattice (Barbier *et al.*, 2019). MTs play a fundamental role in many vital processes such as cell division and neuronal activity. They are key functional and structural elements in axons, supporting neuronal cell differentiation and growth, as well as transporting motor proteins along the axons, which use MTs as support tracks. Tau is a stabilizing microtubule associated protein, whose functions are mainly regulated by phosphorylation (Barbier *et al.*, 2019). Apart from stabilizing microtubules , supporting axonal activities and neurogenesis, Tau protein has also been reported to play an essential role in other biological processes such as glucose metabolism (Gonçalves *et al.*, 2019), iron hemeostatis (Rao and Adlard, 2018), motor function (Rasul *et al.*, 2020), DNA protection (Violet *et al.*, 2014), learning and memory (Biundo *et al.*, 2018).

Each tau isoform comprise of an acidic rich N-terminal followed by a basic proline rich region (Fig 1.6). The N-terminal varies with each isoform depending on the presence of amino acid inserts and is referred to as the projection domain. The main function of the projection domain is for interaction with other cytoskeletal elements and the plasma membrane.
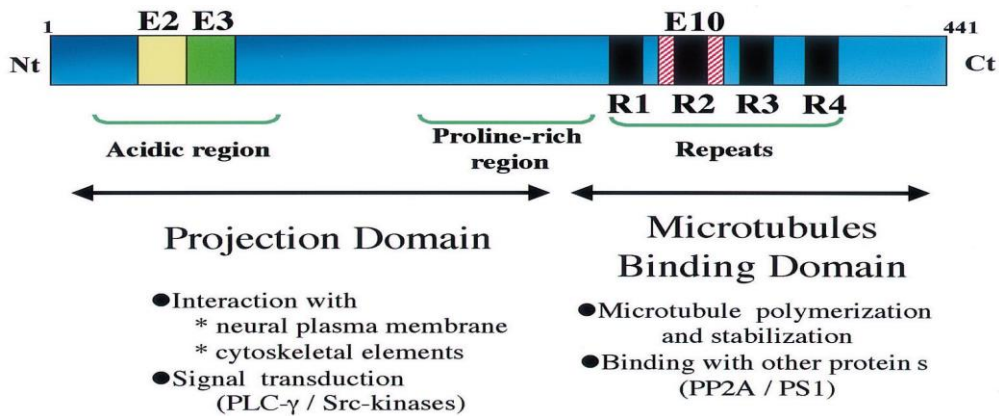
Figure 1.6: **Schematic representation of the functional domains of the longest tau isoform, tau 441 (Wang and Mandelkow, 2015).**

The N-terminal part is also involved in signal transduction pathways by interacting with proteins as phospholipase C gamma (PLC-γ) and Src-kinases. The C-terminal part, referred to as microtubules binding domain, regulates the rate of microtubules polymerization. It is also involved in the binding with functional proteins such as protein phosphatase 2A (PP2A) or presenilin 1 (PS1) (Buée *et al.*, 2000).

Tau proteins account for more than 80% of the total microtubule-associated proteins MAPs, and by means of the repeat region (R1- R4), binds to tubulin to initiate and promote microtubule assembly, elongation and stabilization (Buée *et al.,* 2000, Spillantini & Goedert 1998). During normal development, tau protein undergoes various post-translational modifications (PTMs), including phosphorylation, glycosylation, glycation, ubiquitination, truncation, and nitration (Sergeant *et al.,* 2005, Spillantini & Goedert 1998). These PTMs contribute in the regulation of tau binding to tubulin to ensure the appropriate dynamics of the system.

1.4.1.2 Total tau, phosphorylated tau and tauopathies

A lot of studies carried out on AD patients and controls have shown an increase in t-tau in AD patients by approximately 300% with a sensitivity and specificity of 80-90 %. However, in comparison with the CSF t-tau concentration of AD patients and other

neurodegenerative diseases, including fronto-temporal dementia (FTD) or vascular dementia (VaD), the specificity drops to approximately 50-60 %, thereby rendering t-tau of limited use as a diagnostic marker for differentiating AD from other dementing illnesses (Sergeant, Delacourte and Buée, 2005).

By employing antibodies that are specific in recognizing phosphorylated motifs in the tau amino acid sequence (p-tau), some p-tau isoforms (mainly p-tau181, −199 and −231) were identified and appeared to be more characteristic to AD. P-tau231 and p-tau181 can be used to distinguish AD from control groups and even from FTD, dementia with Lewy bodies (DLB), VaD and major depression. Other p-tau such as species p-tau199, p-tau199+202, as well as p-tau396+404 have also been measured, however, most studies have focused on p-tau231 and p-tau181plasma (Fossati *et al.*, 2019).

CSF t- and p-tau have been consistently demonstrated in clinical research to increase in AD compared to controls, thus, measuring these tau species proved informative for classifying AD from relevant differential diagnoses (Hampel *et al.*, 2010).

1.5   Purpose of research

The present thesis investigates the use of Electrical Impedance Spectroscopy (EIS), to measure the levels of Tau protein in buffer solution, human serum and CSF to compare with other standard laboratory methods such as the ELISA.

There is no defined single biomarker profile for diagnosis of AD; however, tau protein and amyloid beta have been extensively reported in literature as the main markers associated with AD onset and progression. Tau protein and amyloid beta levels for diagnosis of AD are currently being measured in CSF as higher levels have been detected and confirmed in CSF but not in other bodily fluids such as blood, serum, plasma and urine. However, obtaining CSF fluid is very invasive, requiring the need for techniques sensitive enough to measure levels of these markers in bodily fluids other than CSF. EIS is a technique based on the measure of the degree to which an electric circuit resists/impedes the flow of an alternating current when a voltage is applied across its terminal. It is a characterization method providing electric information of physicochemical processes occurring on the surface of electrodes, in the frequency domain (Lisdat and Schäfer, 2008). EIS technique has become more popular in the last few years and is the technique of choice for this work. EIS is chosen over other sensing techniques due to its enhanced sensitivity, rapid response, low cost and possibility for miniaturisation into a portable point of care device (Arya *et al.*, 2010). Furthermore, the use

of a very small amplitude voltage signal (5 mV) allows for measurements on the system under investigation without disturbing the properties of the material. The injection of a voltage causes variation in impedance such that it relates to the physical organisation of the substance under investigation, the chemical processes occurring within it, or a combination of both (K'Owino and Sadik, 2005). For the purpose of this study, commercially available gold electrodes were used to develop electrochemical biosensors initially for the detection of the longest isoform of microtubule associated protein tau (tau 441). Tau protein has been revealed to be more than a simple stabiliser of microtubules, reported to play a vital role in a range of biological processes including myelination, glucose metabolism, axonal transport, microtubule dynamics, iron hemeostasis, neurogenesis, motor fuction, learning and memory, neuronal excitability and DNA protection.

The successful development of a biosensor for the detection of Tau protein would have the advantage of being small in size such that it could be used by the bedside and would offer the advantage of providing real time measurements for instant results. This technology has the potential to deliver results in real time than conventional testing equipments while using a fraction of the material saving both time and money. This innovation holds great promises in medicine and research. The development of this technology is being carried out in collaboration with the University College London (UCL), where the electrical circuit boards are fabricated. Initial tests were conducted on the commercial sensors from Windsor scientific and were focused on the detection of tau in different media which was sensitive enough to be employed in the subsequent measurement of other markers in CSF as well as other matrices including blood and serum. The aim of this research is to establish the appropriate biochemistry required for further development of the biosensor on gold electrodes, and through a set of experiments, to examine factors such as reproducibility, sensitivity, and specificity.

1.6   Specific objectives

This research is based on investigations carried out to answer important questions in the development of an impedance based biosensor initially for detecting and monitoring markers of Azheimer's disease (tau protein). Work carried out in this project, to achieve the above mentioned aim included:

I.   Develop the reliability of a novel tetrapolar biosensor and the use of antibody immobilised on the surface of the biosensor for Tau

II.   Identify the limitations of specificity and sensitivity of the biosensor and provide improvements to them

1.7   Overview of thesis

Chapter 2 presents the literature review of techniques employed in measurement of biomarkers paying particular attention to the main technique used for the development of a tau biosensor. The methods of representation and interpretation of EIS data are explained. This chapter further looks at different electrode systems and materials, explaining the tetrapolar method. Chapter 3 describes the EIS experimental setup, methods results and discussions. Chapter 4 explains the in-house ELISA method developed for the detection of tau protein. The general ELISA methodology is described and the different stages in the development of the particular ELISA for this research are reported including the results and discussions. Further in this chapter comparison between the EIS and ELISA for the detection of tau in this research is presented. Chapter 5, the conclusions drawn from this research is reported and future work is proposed.

1.8   Publications and conferences

1.8.1 Journal papers

Wang, S. X., Acha, D., Shah, A. J., Hills, F., Roitt, I., Demosthenous, A., & Bayford, R. H. (2017). Detection of the tau protein in human serum by a sensitive four-electrode electrochemical biosensor. *Biosensors and Bioelectronics*, 92, p 482–488.

2.6.3   1.8.2 Conferences

Poster Presentations

I.   **Middlesex University summer conference, June 2015.**
       D.Acha, R.Bayford, X.Wang, I.Roitt, A.Shah and F.Hills ".The use of four microband gold and graphene electrodes in array of bio impedance sensors for the detection of biomarkers and the assessment of progression of dementia (Alzheimer's disease) over time"

II.   **Public Health England: Annual Proteomics and Genomics conference, June 2015**
       D.Acha, R.Bayford, X.Wang, I.Roitt, A.Shah and F.Hills . "The use of four microband gold electrodes in bio impedance sensors for the detection of biomarkers and the assessment of progression of dementia (Alzheimer's disease) over time"

III. **Royal Society of chemistry London: Sensors 2016- Wearable Smart Sensors and Technologies, June 2016 (oral presentation).**

Desiree Acha, Xiaoyan (Scarlet) Wang, Ajit Shah, Frank Hills, Ivan Roitt, Andreas Demosthenous, Richard Bayford. "Detection of Dementia Biomarkers using four gold microband electrode Impedance Sensors"

Chapter 2

2.   Literature Reviews

2.1   Detection of biomarkers

Currently, there is an enormous amount of research being done on biological molecules all with the aim of easing disease diagnoses, monitoring of disease progression and response to therapy in order to better human life. The detection and analysis of biomolecules involve characterising the biological components within a test sample using appropriate laboratory techniques. These analyses of biomolecules could be qualitative and/or quantitative. In qualitative analysis, the sample is assayed to determine whether a specific biomolecule is present or absent in the sample, whereas in quantitative assays, the quantity of a particular biomolecule is determined, very often in terms of its concentration in the sample (Reed 2007). Some of these techniques such as chromatography, X-Ray diffraction, radioisotopic and fluorescent labelling, various spectroscopic methods and electron microscopy, have led to dramatic changes in the fields of cellular and molecular biology, resulting further in more recent techniques such as immunoassays like enzyme-linked immunosorbent assays (ELISAs), molecular techniques such as polymerase chain reaction (PCR), proteomics such as mass spectrometry electrophoresis and electrochemical techniques . Although a number of analytical techniques to analyse and quantify biomarkers exist, it is very important that the best one is chosen for specific analysis, as in some cases it is not necessary to use a complex, time consuming and costly method to solve a simple problem that does not necessarily need to be highly sensitive. It is also very important to consider the principles on which these techniques operate because it is known that many procedures relying on the chemical properties of biomolecules for detection and analysis are destructive compared to those relying on the physical properties of biomolecules (Reed, 2007). The sections below give an insight on a few popular analytical techniques currently used and would hopefully explain the need to develop better techniques used for the same purpose in future.

2.2.   ELISA

ELISA is the most commonly used immunoassay technique. An immunoassay (i.e. an assay which uses antibodies or antibody-related reagents) is an affinity-based technique and essentially, detects and measures an antigen or an antibody through its specific reaction with an immobilized capture molecule, the immunoreagent (Daniels and Pourmand, 2007). Antibodies are probably the most important component of the immune system, as they are being produced in response to the presence of antigens in the body. They have the ability to

protect humans and animals against certain diseases by attacking antigens; they do so by binding to a site on a specific antigen to form an antigen-antibody complex (Reed 2007). ELISA is one of the very common and among the most important biochemical techniques used for the detection of antibodies (Indirect ELISA- Fig. 2.1) or antigens (Double antibody sandwich ELISA- Fig. 2.2) in a sample based on the specificity of antibody-antigen interactions using a chromogenic enzyme, where the enzyme is conjugated either to an antigen or antibody at a site that would not affect the binding of either component. The enzyme is then measured by reacting it with a suitable chromogenic substrate which yields a coloured product, and the intensity of that colour is then determined by a spectrophotometer (Reed 2007). In indirect ELISA (Fig.2.1), a specific antigen is bound on a solid support, such that when the antibody is added it binds to the antigen so strongly that even while rinsing, the bond stays intact. An enzyme-linked anti-immunoglobulin is then added to detect the bound antibody. The intensity of the colour is then measured and the absorbance compared to those produced from known standards such that the higher the absorbance, the more antibodies would be present. The double antibody sandwich ELISA (see Fig. 2.2) follows the same principle, but since it is used for the detection of antigens, antibodies specific to these antigens are immobilised on the solid surface so that the antigens are captured when added. An enzyme labelled antibody that binds to the antigen (to a different epitope) is then added. After any unbound enzyme-labelled antibody is washed off, the addition of a chromogenic substrate then leads to an enzyme reaction that yields a coloured product which is measured as described above. In this case the intensity of colour is proportional to the concentration of antigen in the sample.
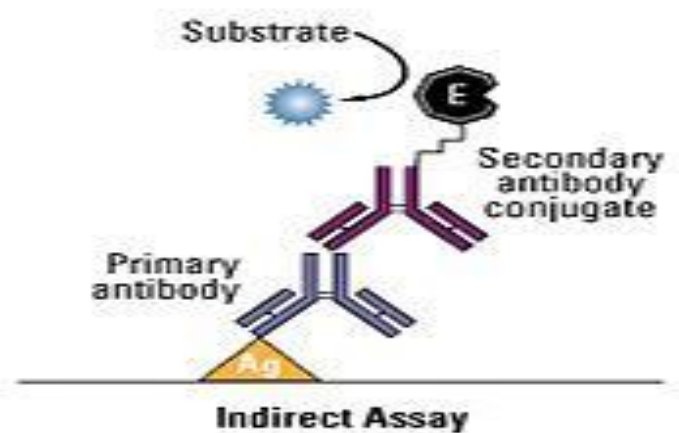
Figure 2.1: Representation of indirect ELISA. Source: http://www.studyread.com/types-of-elisa.

In the sandwich ELISA, the capture antibody is bound on the solid support, and captures the antigen of interest. An enzyme labelled antibody then binds the captured antigen at a different epitope, and a colour change is observed on the addition of a chromogenic substrate, the intensity of which would be proportional to the amount of antigen present.
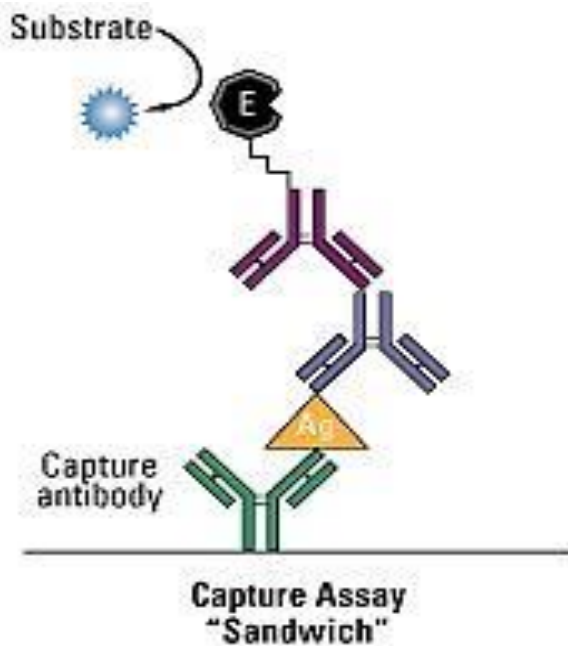
Figure 2.2: **Representation of a double antibody sandwich ELISA**. Source: http://www.studyread.com/types-of-elisa.

Due to its ease of use and low cost, ELISA is widely used for the detection of cancer pathogens, and other disease related proteins (Jia *et al.*, 2009). ELISA has been used to detect and quantify markers of dementia in different matrices but mostly in CSF (Wang *et al.,* 2016*;* Alves *et al.,* 2014; Sparks *et al.,* 2012; Jia *et al.*, 2009; Sjögren *et al.*, 2001) and one of the key aims of this research project is to attempt detection of some of these markers in serum which is a much less invasive bodily fluid to obtain. However due to the low levels of some protein markers in early stages of Alzheimer's disease and other diseases, it is not possible to detect them in serum by ELISA, which is why it is important to develop new techniques that can detect biomarkers at the onset of diseases (Humpel, 2011). Also, standard ELISA techniques such as sandwich ELISAs are time consuming and multistage, making it impossible to get real time measurements, therefore limiting the application of such a technique in clinical use (Jia *et al.*, 2009).

The measurement of tau protein has been reported using a variety of different methods including electrochemical biosensors, mass spectrometry and surface plasmon resonance (Lifke *et al.*, 2019, Pérez-Ruiz *et al.*, 2018,Wang *et al.*, 2017, Barthélemy *et al.*, 2016, Esteves-Villanueva, Trzeciakiewicz and Martic, 2014). Measurements have also generally been done using ELISAs which in some cases have reportedly measured total tau protein levels in a variety of matrices such as CSF, plasma, serum, saliva and buffers (Table 2..2) (Pekeles *et al.*, 2018, Zetterberg *et al.*, 2013, Pérez-Ruiz *et al.*, 2018, Sparks *et al.*, 2012, Jia *et al.*, 2009)

Commercial tau ELISAs are mostly sandwich assays which use monoclonal capture antibody immobilised on a plastic plate surface of a treated ELISA plate. Antigen in the form of standards and unknown samples are then applied to the plate and tau protein binds to the capture antibody. The bound tau is then detected by a primary anti-tau antibody which is subsequently bound by a horseradish peroxidase conjugated to an appropriate secondary antibody. The addition of an enzyme substrate enables the colorimetric detection of bound tau (Acker *et al.*, 2013, Olczak *et al.*, 2017).

There are examples of commercially available enzyme-linked immunosorbent assays (ELISAs) for quantification of protein tau include kits from Thermofisher, Innotest and Invitrogen. However, they are costly and can be unreliable as they are not sensitive enough to quantify protein tau in plasma and serum samples (Pérez-Ruiz *et al.*, 2018) in low concentration, possibly due to matrix effects of samples containing large amounts of proteins and lipids which can interfere with protein detection. Levels of tau in CSF, serum and plasma are generally low during the pre-symptomatic stage of AD typically below the detection limit of commercial ELISAs. However some studies have reported enhanced ELISA methods for measurement of tau in these different matrices, methods such as magnetic capturing and digital detection (Pérez-Ruiz *et al.*, 2018 ,Ono *et al.*, 2014, Rissin *et al.*, 2010) bienzyme-substrate recycling (Hu *et al.*, 2002) , and biotin-tyramide amplification detection (Luk *et al.*, 2009 , Stegurová *et al.*, 2014). These studies have reported detection levels of tau at attomolar, femtomolar and picomolar concentrations but have all failed to provide sufficient information for reproducibility studies.

A 2013 ELISA study carried out by Zetterberg and Co-workers reported significantly raised levels of tau in plasma of AD patients compared with both controls and mild cognitively impaired (MCI). However, there was no correlation between tau levels in plasma and CSF, suggesting that steady-state concentrations of tau in these two body fluids are differentially regulated. Some tau ELISAs have shown that plasma tau levels are elevated in

AD but with overlapping ranges across diagnostic groups, this overlap diminishes the utility of plasma tau as a diagnostic test. Implying that further studies are needed to evaluate plasma tau as a first-in-line screening tool for AD (Blennow, 2017 ; Zetterberg *et al.*, 2013).

The majority of commercially available tau ELISAs are mostly developed and optimized for the detection of tau in CSF (Table 2.1); it is noteworthy that these commercial kits as well as reported in house ELISA show variation in their LoDs and assay ranges (Tables 2.1 and 2.2). As a result many studies have employed their own in-house ELISAs for the measurement of tau (Lifke *et al.*, 2019; Pérez-Ruiz *et al.*, 2018; Wang *et al.*, 2017; Acker *et al.*, 2013; Sparks *et al.*, 2012). As mentioned in Section 1.4.1, tau protein is a microtubule-associated protein which is present in biological fluids in up to six isoforms which vary according to alternative spliced variants. Most in-house ELISAs are mainly based on those commercially available, however, they use different tau isoforms as calibrators, thus making it difficult to compare ELISA protocols directly (Pérez-Ruiz *et al.*, 2018; Acker *et al.*, 2013). For example, in a study carried out by Pérez-Ruiz *et al.*, (2018) using purified 2N4R tau as the calibrator, an attempt to benchmark the in-house ELISA with a commercial kit (Total tau ELISA, Euroimmun, Germany) as reference ELISA which used a shorter recombinant peptide as calibrator resulted in noticeable inconsistencies between the values estimated by both assays. This implied that the values estimated from the in-house ELISA were relative to the 2N4R tau and the ones calculated from the reference ELISA were relative to the synthetic peptide, which hampered fair comparison of both assays. A similar experience has been reported by Acker *et al* (2013).

Although tau as a core CSF biomarker has been well-validated clinically, a problem has been the variability in measurements between clinical laboratories, and over time between batches of reagent (Lifke *et al.*, 2019; Mattsson *et al.*, 2013; del Campo *et al.*, 2015; Blennow, 2017). This problem stems from differences in analytical procedures for the manual ELISA methods between laboratories and from variability in reagent quality and manufacturing procedures for the kits (del Campo *et al.*, 2015; Algeciras-Schimnich *et al.*, 2013; Mattsson *et al.*, 2013). It is for the above reasons that this study has employed the use of its own in-house ELISA method of quantifying tau protein.

Here we have developed an ELISA to specifically detect the most representative full-length tau 2N4R isoform using 39E10, a monoclonal antibody which was raised against full-length human tau and targets amino acid sequence 189 – 195 on full length tau, an epitope common to all isoforms of tau. The 39E10 antibody was also used for the biosensor, therefore the ELISA measurements can be used to directly compare with the biosensor measurements.

As seen in chapter three, the biosensor is able to detect levels of tau down to the 10^{-2} pM range. Therefore, in order to compare levels achieved with ELISA, endeavoured to design the ELISA to achieve as low LoD as possible so that useful comparisons could be made.

Biosensor signals are prone to electromagnetic interferences such as cable shields and lengths, applied frequency, effects of wind and temperature on the ionic concentration of analyte/electrolyte under test and poor connection between electrodes and improper electrolyte contact with electrodes (Wang, 2006; Grieshaber *et al.*, 2008; Karunakaran, Rajkumar and Bhargava, 2015) . However, levels determined by ELISA are not influenced by these factors.

Therefore, the purpose of this study is to develop an ELISA to confirm that changes in tau concentrations between individuals, as determined by the biosensor, are due to specific changes in tau concentration and not due to other variables which might cause electromagnetic interference such as those mentioned above

Table 2.1: Levels of tau in CSF using commercial ELISAs

Commercial ELISA kit	LOD	Range (pg/ml)	Matrix	Reference
Tau (Total) Human ELISA Kit From Invitrogen	<10	31-2000	CSF	Thermofisher scientific, accessed 31, January 2020, https://www.thermofisher.com/elisa/product/Tau-Total-Human-ELISA-Kit/KHB0041
Human Total-Tau ELISA Kit from Euroimmun	44.2	85-1,300	CSF	Biocompare, accessed 31 January 2020 https://www.biocompare.com/25138-Assay-Kit/14854323-Human-Total-Tau-ELISA-Kit
INNOTEST hTAU Ag from Furjibio	34	50 - 2500	CSF	Furjibio, accessed 31 January 2020 https://www.fujirebio.com/en/products-solutions/innotestr-htau-ag
Human Tau ELISA Kit from abcam	3.3	31.3-2000	Plasma CSF Serum supernatant	Abcam, accessed 31 January 2020 https://www.abcam.com/human-tau-elisa-kit-ab210972.html
Human Tau proteins ELISA kit from Cusabio	3.9	15.6 - 1000	Plasma CSF Serum	Cusabio, accessed 31 January 2020 https://www.cusabio.com/ELISA-Kit/Human-Tau-proteins-ELISA-kit-88976.html
Human Tau (Total) ELISA from BiovVendor	<12	31.2-2,000	CSF	BioVendor, accessed 31 January 2020 https://www.biovendor.com/human-tau-total-elisa
Tau (Total)	3.2	17.2-	CSF	Biocompare, accessed 31 January 2020

ELISA from IBL - America		1,100		https://www.biocompare.com/25138-Assay-Kit/12529423-Tau-Total-ELISA
Tau ELISA Assay Kit from Eagle biosciences	5.2	31.25-2000	serum, plasma, CSF	Eagle bioscience, accessed 31 January 2020 https://eaglebio.com/product/tau-elisa-assay-kit/
Human Tau ELISA Kit from Biorbyt	29	78.1-5000	Cell lysates Tissue homogenates	Biorbyt, accessed 31 January 2020 https://www.biorbyt.com/human-tau-elisa-kit-orb551544.html
Human Tau proteins ELISA Kit from Biomatik	3.9	15.6 - 1000	Plasma Serum CSF	Biomatik, accessed 31 January 2020 https://www.biomatik.com/elisa-kits/human-tau-proteins-elisa-kit-cat-ekc35714/

Table 2.2: **Reported tau levels in different matrices of healthy individuals**

Matrix	Range in healthy individuals (pg/ml) (Mean and SD)	reference
CSF	372.0 ± 114.2	(Kawarabayashi *et al*., 2020)
CSF	295.5 ± 90.01	(Kawarabayashi *et al*., 2020)
CSF	380 ± 120	(Mori *et al*., 1995)
CSF	507 ± 254	(Zetterberg *et al*., 2013)
CSF	263 ± 164	(M. Sjögren *et al.*, 2001)
CSF	215 ± 77	(Hu *et al.*, 2002)
CSF	150 ± 50	(Blennow *et al.*, 1995)
CSF	310 ± 108	(Mattsson *et al*., 2016)
Plasma	8.80 ± 10.1	(Zetterberg *et al*., 2013)
Plasma	2.74 ± 0.76	(Fossati *et al*., 2019)
Plasma	819.5 ± 294.4	(Sparks *et al*., 2012)
Plasma	2.58 ± 1.19	(Mattsson *et al*., 2016)
Plasma	5.58 ± 2.51	(Mattsson *et al*., 2016)
Serum	86.89 ± 67.60	(Li et al., 2020)
serum	496 ± 89	(Mirzaii-Dizgah, Mirzaii-Dizgah and Mirzaii-Dizgah, 2020)
Saliva	57.1 ± 3.8	(Mirzaii-Dizgah, Mirzaii-Dizgah and Mirzaii-Dizgah, 2020)
*Saliva	9.6	(Ashton *et al*., 2018),(Shi *et al*., 2011)

2.3. Mass spectrometry

Mass spectrometry (MS) is currently among the most popular and powerful analytical techniques for the identification and characterization of proteins (Liu, Qing and Deng, 2014). This technique involves the breakdown of organic compounds into ionic fragments in a gas phase. Following the subsequent separation of the ions on the basis of their different masses, MS allows the identification of compounds based on their mass to charge ratio. This technique is highly specific and sensitive such that each fragment of a particular mass is detected sequentially with time (Reed, 2007; Liu *et al.,* 2014).

Mass spectrometry instruments consist of three main components which are the ion source, the mass analyzer, and the detector. The ion source converts the sample molecules into ions, and the mass analyzer then applies electromagnetic fields which sort out the ions according to their masses. The detector then detects the separated ions and provides data to calculate the abundance of each ion present (Reed 2007). Electrospray ionisation (ESI) and matrix-assisted laser desorption ionisation (MALDI) are two ionization techniques that were introduced in the 1990s, and since then they have been the preferred routine methods for the analysis of peptides and proteins. These techniques have the advantage of very high sensitivity and also allowing the molecules to stay reasonably intact during the ionisation process. Both MALDI MS and ESI MS have been successfully used to identify, characterise and quantify markers of Alzheimer's disease (Barth *et al.,* 2016; Liu *et al.,* 2014; Portelius *et al.,* 2008). Some of the disadvantages of the mass spectrometry are that they are quite expensive, large instruments and require very high skill to operate them.

2.4   Western blot analysis

Western blot analysis also known as immunoblotting or protein blotting is a core technique in cell and molecular biology. Western blotting is used to detect the presence of a specific protein in a complex mixture extracted from cells (Moore,B.C, 2009). The procedure of Western blotting procedure relies upon three key elements to accomplish this task (Fig.2.3): the separation of protein mixtures according to size using gel electrophoresis; the efficient transfer of separated proteins to a solid support; and the specific detection of a target protein by matched antibodies (Mahmood and Yang, 2012). Artificial antibodies are created that react with a specific target protein. The sample to be tested is prepared and combined with these antibodies on a membrane if the target protein is present, after a gel electrophoresis step this will result in a stained band on the Western blot. Once detected, the

target protein is visualized as a band on a blotting membrane, X-ray film, or an imaging system (Moore, B.C, 2009).
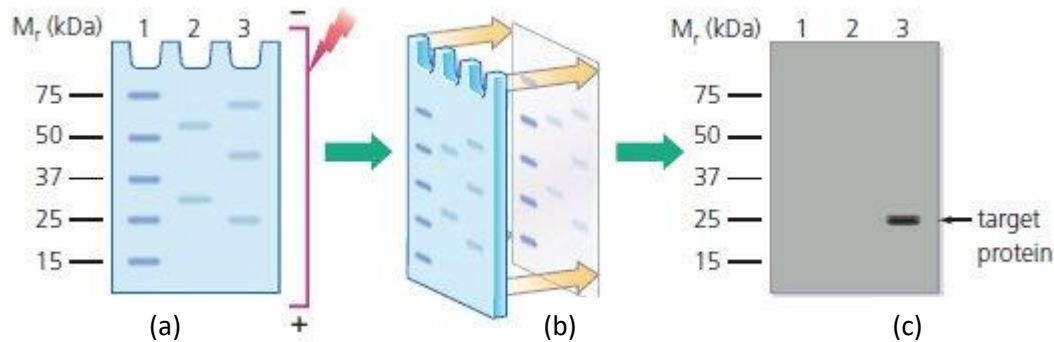
Figure 2.3: **Schematic representation of Western blot technique.** (a) represents the separation of protein mixtures by electrophoresis, (b) represents transfer to a blotting membrane and (c) represents the detection of target protein, which only becomes visible in the final stage as a band similar to that shown in lane 3. Lane 1: Prestained molecular weight standards (Protein ladder). Lanes 2&3: Protein mixtures (Moore, B.C. 2009) .

Western blots are widely used across a range of scientific and clinical disciplines. Their ability to clearly show the presence of a specific protein both by size and via antibody binding makes them well-suited for evaluating levels of protein expression in cells, and for monitoring fractions during protein purification (Moore, B.C. 2009).

They are also helpful in comparing expression of a target protein from various tissues, or seeing how a particular protein responds to disease or drug treatment (Kang *et al.*, 2014). Western blot is typically considered to be semi-quantitative, as it only provides a relative comparison of protein levels, but not an absolute measure of quantity for a specific target protein in a particular experiment and therefore cannot be used to attach a precise concentration to a particular sample. ELISAs are more suitable for this purpose and generally more sensitive.

Western blotting is disadvantageous in that it is non-quantitative and time consuming. Although very straightforward, WB requires great expertise to get good results.

2.5. Biosensors

A biosensor is an analytical device incorporating a biological material in an intimate contact with a suitable transducer that converts the biochemical signal into quantifiable electric signal (Sharma, Sehgal and Kumar, 2003). The biosensor consists of three basic components (Fig 2.4); the biological/recognition system often called a biorecpetor, a

transducer, and detector / microelectronics (Karunakaran, Rajkumar and Bhargava, 2015). The signal that is produced is proportional to the concentration of the specific analyte, or group of analytes under investigation. The target analyte binds to the analyte recognition element e.g., an antibody, which is immobilized on the transducer surface. The transducer converts this biochemical reaction to a readable signal. This resulting electrical signal is detected and processed to give user friendly results that are easy to analyse and interpret. Many different biomaterials (Table 2.3) and transducer elements can be used in biosensing, however, in the construction of a suitable biosensor for the detection of a particular substance, the biomaterial used should be highly specific to the analyte of interest.
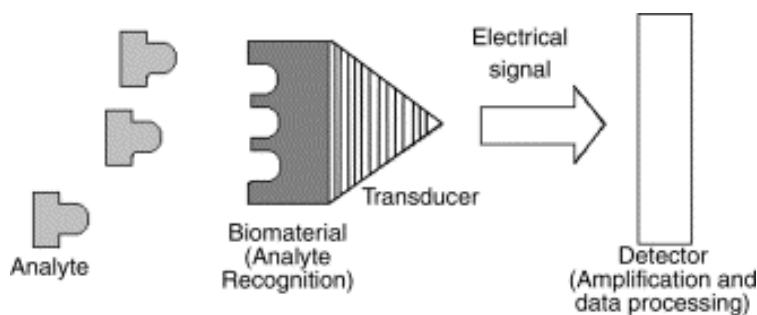
Figure 2.4: **Schematic representation of biosensor**. Source: (Sharma, Sehgal and Kumar, 2003).

The analyte (antigen) binds to biomaterial (antibody). This biological interaction produces a biochemical signal which by way of the transducer is converted to an electrical signal. The electrical signal is then detected (Ameri *et al.*, 2020)**.**
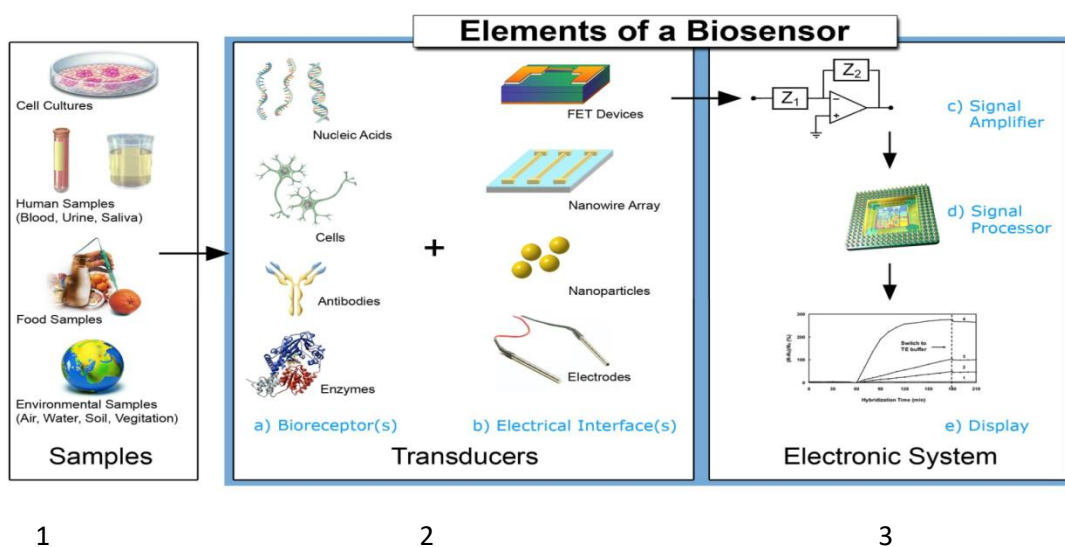
Figure 2.5: **Elements of a biosensor** (Grieshaber *et al.*, 2008), different biological samples (including body fluids, food samples, cell cultures and environmental samples) from which

analytes can be measured as indicated in 1, 2a shows bioreceptors including aptamers (Mishra, Sharma and Mishra, 2018) that can specifically bind to the analyte, while 2b shows transducer elements on which specific biological events form an interface to generate a biochemical signal which can be amplified and converted by signal amplifier to an electronic signal as shown in 3c. This electronic signal is then processed by a detector circuit (3d) and by means of computer software the processed data is converted to a meaningful physical parameter (3e) describing the process under investigation.

There are many associated advantages of using biosensor technology as a sensitive detection method. They are very specific since the analyte recognition molecule can distinguish between the analyte under investigation as well as similar molecules, and real-time measurements are obtained within a short time period. They also offer high sensitivity and selectivity even when a complex or turbid sample matrix is used (Kissinger, 2005; Wang *et al.*, 2017). Biosensors are fairly easy to construct as both the transducer and the region for selective chemistry are situated on a single platform.

Biosensors have been applied in disease monitoring, drug discovery and detection of various molecules including heavy metal ions or fluid biomarkers corresponding to a disease stage (Aloisi *et al.*, 2019). Furthermore, the biosensor technology has the possibility of being introduced as point of care equipment allowing on-the-spot analyses outside the laboratory (by the bedside), without the need to add on any reagents except the sample to be tested (Kissinger, 2005)**.** The biological component of a biosensor can be classified into two main groups; catalytic and non-catalytic (Sharma, Sehgal and Kumar, 2003; Ameri *et al.*, 2020).

The catalytic group includes enzymes, microorganisms, and tissues, while the non-catalytic group consists of antibodies, receptors, lectins, and nucleic acids (Sharma *et al*., 2003; Karunakaran *et al.*, 2015). Catalytic sensors detect the change in the concentration of a component resulting from the catalysed reaction, to produce a signal. In non-catalytic sensors the binding event that occurs between the receptor and analyte of interest produces the signal (Kissinger, 2005). The biosensor being developed in this project is based on an antibody-antigen reaction.

2.5.1 Types of biosensors

There are several types of biosensors, based on the nature of the bioreceptor/biological recognition element and the transducer that is used, as shown in Table 2.3. Examples of some common transducers incorporated into biosensors include optical (colorimetric, fluorescence, luminescence interferometry), mass charge (piezoelectric,/acoustic wave), thermometric, electrochemical (potentiometry, conductometry,

impedimetry, amperometry, voltammetry), calorimetric (thermistors) or magnetic in nature (Karunakaran, Rajkumar and Bhargava, 2015). This section describes these different transducers, the associated detection methods, and the advantages and disadvantages of each

Table 2.3: **Different types of biological recognition elements and signal transducers employed in biosensor development.**

Bioreceptors	References	Transducers
Antibody-antigen interaction • Based on the specific and high affinity antibody-antigen binding interactions	(Kassanos *et al.*, 2008), (Karunakaran, Rajkumar and Bhargava, 2015), (Wang *et al.*, 2016) (Karunakaran, Rajkumar and Bhargava, 2015), (Liu *et al.*, 2012)	Optical Mass charge Thermometric Electrochemical
Nucleic acid interactions • Detection of specific DNA sequences by hybridisation		
Enzymatic interactions • Conversion of analyte into sensor detectable product • Detection of an analyte that acts as enzyme inhibitor or activator • Evaluation of the modification of enzyme properties upon interaction with the analyte •	(Karunakaran, Rajkumar and Bhargava, 2015), (Lenigk *et al.*, 2000), (DeLoache *et al.*, 2015), (Yang *et al.*, 2014). (Su *et al.*, 2011), (D'Souza, 2001), (Ng *et al.*, 2010)	
Cellular interactions (microorganisms) • Mammalian cells, but could also be bacterial cells • Act as Primary		

transducers for
signal generation
- Secondary
transducer converts
signal by electrical
or optical means

**Biomimetric materials
(synthetic bioreceptors)**

- Genetically
engineered
molecules (e.g.,
single chain
antibody
fragments)
- Artificial
membranes
- Molecular
imprinted polymers

(Rushworth *et al.*, 2014),
(Karunakaran, Rajkumar and
Bhargava, 2015),(Yang *et al.*,
2016)

Table 2.4: Types of biosensors and the advantages and disadvantages associated with them

Types of transfer	Advantages	Disadvantages
Optical Biosensors	- High quality fibers and optoelectronic are available at affordable prices - Rapid - Optical signal not affected by electrical or magnetic interference - Possibility of obtaining more information within a range - Samples can be tested simultaneously at different wavelengths without interference from one another - Both direct and indirect detection possible - Small, flexible, fast, and safe, as no electrical device interacts with the	- In case of SPR systems, it would be too costly - Instrument accuracy and sensitivity easily affected. - Conformational change due to labelling (Fan *et al.*, 2008)

	body (Fan *et al.*, 2008)	
Mass charge biosensors (Piezoelectric biosensors)	• Label-free detection • Potential to provide quantitative and qualitative analysis • Highly sensitive (piezoelectric • Reusable with no obvious degradation in performance • Inexpensive, easy-to-use and rapid response • insensitive to electromagnetic fields and radiation, enabling measurements under harsh conditions (Tombelli, Minunni and Mascini, 2005; Vives, 2008))	• Limited applicability: environments factors make it difficult to establish the relationship between added mass and change in resonant frequency (Mohanty, 2015) • Difficult to detect low molecular-weight analytes on basis of mass addition alone (Knudsen *et al.*, 2006)
Thermometric biosensors	• Long term stability • Cheap • No disturbances in measurements by varying optical or ionic sample characteristics • Multiple applications (Ramanathan and Danielsson, 2001)	• Complicated thermostating • Weak sensitivity/nonspecific heating effects (Ramanathan and Danielsson, 2001)
Electrochemical biosensors	• Easy miniaturisation • Good detection limits, even with small analyte volumes • Can be used in turbid biofluids. • Inexpensive • Simple and sensitive • Robust (Grieshaber *et al*., 2008; wang *et al*., 2016)	• Lack of surface architectures, contributing to decreased sensitivity (Grieshaber *et al.,* 2008)

2.5.1.1   Optical biosensors

Optical biosensors are powerful tools for detection and analysis in fields such as biomedical research, healthcare, pharmaceuticals, and environmental monitoring. Two types of optical detection systems exist; fluorescence-based (Kunzelmann, Solscheid and Webb, 2014) and label-free detection (Campbell and McCloskey, 2002). In fluorescence based detection, either the bio recognition molecule (e.g. an antibody), or the analyte of interest (antigen) is labelled with a fluorescent tag (e.g. dyes such as ethidium bromide, fluorescein and green fluorescent protein). On detection, the intensity of the fluorescent signal indicates antibody-analyte binding (Damborský, Švitel and Katrlík, 2016). Despite the fact that this method is very sensitive, one major drawback is that the labelling process may result in a conformational change thus interfering with the function of the biomolecules by affecting binding of antibody to analyte (Fan *et al.*, 2008).

Detection methods for label free techniques include Refractive Index (RI) detection, optical absorption detection, and Raman spectroscopic detection. Some of the main research areas in optical sensor development include surface plasmon resonance (SPR) based biosensors, optical waveguide based biosensors, and optical fibre based biosensors (Fan *et al.*, 2008) .

 Fluorescent based optical biosensors have been reported to offer promising analytical outcomes for various biological analytes including tau protein. There was however some limitations such as low water solubility and stability experienced in the recent decades in terms of using fluorescent probes. Recent studies have employed the use of proteins and enzymes for biological targets to control these shortcomings (Kunzelmann, Solscheid and Webb, 2014)

The surface plasmon resonance (SPR) biosensors are optical sensors emerging rapidly through the past decades and have been shown to be highly sensitive tools to measure the target molecules either qualitatively or quantitatively (Damborský, Švitel and Katrlík, 2016). SPR is the fundamental principle of many colour-based biosensor applications and lab-on-a chip sensors. In SPR biosensors for biomolecular interaction analysis, one of the biomolecules is immobilised on a metal surface, and the other partner is added in excess over that surface. SPR spectroscopy is then used to measure the changes in refractive index that occurs at the metal surface when the two biomolecules interact (Bergström & Mandenius 2011; Karunakaran et al. 2015). SPR devices make use of electron bombardment or application of incident light beam to a sample, and at a specific wavelength and beam-angle, resonance occurs (resonance is the tendency of a system to oscillate at larger amplitude at

some frequencies than at others). Resonance causes excitation of surface electromagnetic waves, known as surface plasmon polaritons.

These waves move along the metal/dielectric interface, where the interface could be between a gold surface and an aqueous solution. The movement of these waves through this interface causes a change, and therefore, any change at the interface (e.g. building a biofilm on the gold surface) will be detected due to change in characteristics (Figure 2.6) (Nguyen *et al.*, 2015). SPR has been used for characterising proteins, where the protein layer is adsorbed on the solid surface. This method gives the possibility of obtaining information on the orientation, distortion, and efficiency of immobilisation procedures as well as the interaction between molecules of interest (Cross *et al.*, 2003). SPR has also been used in the development of a hand-held biosensor to detect ricin (a protein toxin) as well as other biological agents , for example amyloid-β (Aβ) fibril formation and interaction monitored by SPR have been documented (Stravalaci *et al.*, 2011).
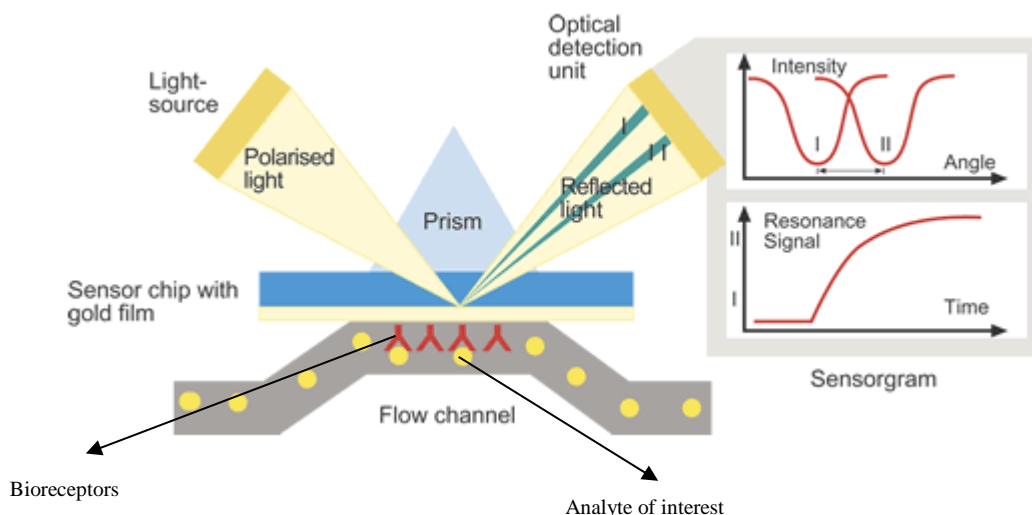
Figure 2.6: **Schematic representation of SPR** (The University of Arizona, 2019).

The gold surface creates a resonator for the incoming light. Light is directed at and reflected from the side of the surface not in contact with sample, and SPR causes a reduction in the reflected light intensity at a specific combination of angle and wavelength. One binding partner (antibody) is immobilized on the surface of a sensor chip in a flow cell, and the other binding partner (antigen) flows over the surface of the sensor chip interacts with the immobilized molecules. This biomolecular binding event causes changes in the refractive index at the surface layer, which are detected as changes in the SPR signal.

While most SPR biosensors are able to detect tau protein at levels of nanomolar concentration, immuno-based SPR biosensors have been developed which can amplify the detection signal and allow tau detection at picomolar concentrations (Špringer *et al.*, 2020). Direct and sandwich-based methods have been used in the development of SPR immunosensor for tau detection both in buffer and artificial CSF at nanomolar range. Since the introduction of metallic nanostructure, gold NPs-DNA conjugates have been implemented in DNA sandwich-like detection strategies to effectively amplify SPR signal (Zanoli, D'Agata and Spoto, 2012; Mariani *et al.*, 2015). Furthermore, the enhancing properties of Multi-Walled Carbon Nanotubes (MWCNTs) have been investigated by adding MWCNTs to an immuno-based sandwich format analysis to enhance tau protein detection (Lee *et al.*, 2011). Although being largely studied in biosensing (Jacobs, Peairs and Venton, 2010), this type of nanostructure is less employed in SPR (Lee *et al.*, 2011). Inspired by the above method, Lisi *et al.*, 2017 coupled a secondary monoclonal antibody (mAb2) to MWCNTs (MWCNTsmAb2) by means of a sandwich strategy, taking into account that tau clinical levels are significant at pM range. These nanostructured amplifiers were successfully exploited for signal amplification, obtaining a gain of more than two orders of magnitude compared to the unlabelled strategy (Lisi *et al.*, 2017). Conclusively, Lisi et al. 2017 reported the preliminary and encouraging results on the use of MWCNTs-antibody conjugation for the improvement of the analytical performances of SPR sensing for the detection of tau in the picomolar range, which may open new roads for innovative and sensitive SPR-based methods.

An SPR biosensor using DNA aptamer/antibody assay for Tau381 (also known as 1N3R one of the six isoforms of tau) detection in human serum (Tao *et al.*, 2019) and plasma (Kim, Wark and Lee, 2016) samples had detection limits of 0.7 pM and 10 fM respectively. Kim and team performed a sandwich method, where tau antibody was added after attachment of tau to the aptamers on the surface of a SPR chip for better signal enhancement. However, some unexpected signals were also generated from non-specific binding of molecules such as proteins and DNA to the gold surface that concealed the main signal from target analyte (Kim, Wark and Lee, 2016). Masson et al. (2016) have suggested that recording the signals prior to attachment of aptamers or other recognition elements is an authentic way to increase the specificity of outcomes (Masson *et al.*, 2006). Another SPR platform for tau protein detection was developed using multimode optical fibers with a 40 nm-thick gold-covered core to immobilize antibodies against tau proteins on the surface of the sensor. This biosensor preserved tau detection in blood samples based on immunoreaction (Vu Nu *et al.*, 2018).

Raman scattering is a phenomenon whereby photons are scattered inelastically by matter. Raman scattering also known as Raman effect is the basis of Surface-enhanced Raman spectroscopy (SERS), a molecular detection technique that enhances the Raman scattering when the target is absorbed on the surface of a rough metal or by nanostructures such as plasmonic-magnetic silica nanotubes (Chen *et al.*, 2019). The electromagnetic field around nanostructure and nanomaterials enhances the Raman spectroscopy signals significantly. SERS based biosensors have shown to be very sensitive and promising for detection of analytes with low concentrations in solutions (Yuan *et al.*, 2017). A SERS biosensor for tau protein was developed with a detection limit less than 25 fM. This technique used functionalized magnetic silica nanoparticles and monoclonal anti-tau as capturing agents; these are capable of attaching to tau protein inside the samples and functionalized gold nanoparticles with polyclonal anti-tau acting as the SERS surface. Gold nanoparticles were activated by a EDC/NHS polyclonal anti-tau layer attached to their surface and 5,5-dithiobis (2- dinitrobenzoic acid) (DTNB) was used to shield the gold nanoparticle surface of nanoparticles as well as a Raman reporter. The use of polyclonal anti-tau as the bioreceptor increased the intensity of signal in samples with low concentration of tau protein. Interaction of anti-tau with tau protein in solution resulted in aggregation of nanoparticles producing a sharp peak at SERS spectrum due to the coverage of DTNB. Based on concentration of tau within the sample, peak height could vary (Zengin, Tamer and Caykara, 2013).

Optical biosensors incorporating a label have been widely used in the detection of biological molecules, as measurement is easier due to the occurrence of a colour reaction. Besides bringing about a conformational change, tagging a molecule with a fluorescent tag can also lead to the blocking of an important active site. Furthermore, with time, the excitation/emission efficiency of the fluorophore is affected, and also, exposing the fluorophore to light, by photo bleaching, affects quantitative measurements, such that assays can be read only once. Factors such as quenching and self-quenching are also thought to render fluorescent tags less efficient (Fan *et al.*, 2008). Labelling molecules, being a time consuming and expensive process would make it difficult to manufacture cost effective biosensors for commercialisation purposes. Research into Label-free optical biosensors such as SPR is still ongoing. However, label free optical biosensors can also have drawbacks, and it has been reported that in the case of SPR there is a sensitivity issue to specific signals, as well as undesirable tendencies towards non-specific signals (Fan *et al.*, 2008). While research is ongoing in the optical field, it is important that other types of biosensors are considered.

2.5.1.2 Mass sensitive biosensors (Piezoelectric biosensors)

Mass sensitive biosensors detect small mass changes caused by binding reactions occurring on the surface of small piezoelectric crystals. Applying a specific electrical signal to crystals, results in them vibrating at a specific frequency. The frequency of that oscillation is dependent on the electrical signal frequency and the mass of the crystal, such that upon binding of the target analyte, the mass of the crystal will increase, changing the oscillation frequency. This change in oscillation frequency can then be measured electrically and used to determine the mass of bound analyte to the crystal (Porcelli and Filho, 2018). The oscillation frequency is inversely proportional to mass concentration of target analyte bound to the receptor-coated surface. This correlation can provide an estimate of the ligand surface coverage and be useful in determining kinetic binding constants. Primarily, a piezoelectric biosensor is constructed by immobilizing a receptor (antibody, nucleic acid, mimetic receptor, etc.) onto the surface of a piezoelectric quartz crystal (PQC) and monitoring the frequency changes due to the binding of target molecules or ligand (antigen, nucleic acid or protein, etc.). The frequency of oscillations decreases on ligand binding and can be used to quantitatively estimate the ligand concentration, whereas the real-time monitoring of these changes can be used to calculate the kinetic binding constants (Pohanka, 2018)

Piezoelectric devices offer the advantages of being portable, simple to use, inexpensive to manufacture, while also being suitable for real-time monitoring of biological reactions such as antibody-antigens and are highly sensitive and specific. Nanoparticles in piezoelectric biosensors are a promising method to further amplify the signal (Pohanka, 2018). Quartz crystal microbalance (QCM) has shown to be a potential material for developing sensor platforms with an easy and cost-effective procedure that provides real time assays in short time. The QCM relies on a quartz crystal that undergoes different current-induced oscillations according to mass loading on the surface or changes of the viscosity or density of the media surrounding the sensor. The oscillation frequency is inversely proportional to interface phenomena. Hence, in these platforms, biochemical interactions can be directly displayed in real time and without any labels, allowing for simple detection of key biomarkers using integrated chemistries, e.g., thiol chemistry coupled to amino coupling for receptor attachment, and several assay formats (Li *et al.*, 2018). These biosensors are used for sensing various chemicals and biomolecules with high sensitivity. An oscillation at a particular frequency will be generated through applying a voltage on QCM which is the basis for the operation of piezoelectric biosensors (Vashist and Vashist, 2011). Moreover, piezoelectric immunosensors are developed that use QCM for transduction and two specific

monoclonal antibodies with different epitope recognition sites for capturing tau proteins in buffer and CSF sample. Primary monoclonal antibody is initially immobilized on the surface of QCM. Subsequently, to perform sandwich-based assay and enhance selectivity, secondary antibody is added to the test environment. Changes in frequency are observed after surface interactions (Li *et al.*, 2018). In this platform, the primary mAb (mAb1) recognizes the proline rich region (amino acids 189–195) of tau protein and is used as a capturing receptor for its direct detection by QCM measurements. Once bound to the analyte, it leaves the target protein free for further binding to a secondary mAb (mAb2) to improve the selectivity and detection limit of the bioassay. Finally, the analytical performances of the direct detection (by means of mAb1 recognition) and the sandwich-based assay (via mAb1/tau/mAb2 recognition) were directly compared. A modification of the classical sandwich strategy was performed by substituting the mAb2 with tubulin, as an alternative natural recognition element (Li *et al.*, 2018). High specificity and affinity of this recognition and its aimed stoichiometry played a major part in the appropriate usage of tubulin as a secondary binder for tau protein (Ackmann, Wiech and Mandelkow, 2000). Ackmann et al. (2000) evaluated a $K_D = 75 \pm 30$ nM and a stoichiometry of 0.20 (defined by factor n = [tau]bound / [MT]) for tau protein in 5 – 500 nM, which is exactly where they focused on detecting tau in CSF (Ackmann, Wiech and Mandelkow, 2000). For detecting the appropriate operating conditions, various buffers were employed to test tau–tubulin binding (mAb1 as primary receptor). Initially, tubulin was dissolved in the PB buffer, in which biomolecular interactions usually take place. No secondary signal was reported due to tubulin dimers binding to tau (5 ± 2 Hz, n = 3); this finding was consistent in CSF. Subsequently, it was revealed that other buffers PIPES, PEM and MES containing Mg^{2+} salts and GTP (guanosine 5′-triphosphate) lead to tubulin polymerization (Choudhury *et al.*, 2013; Kadavath *et al.*, 2015). It has been found that important unspecific binding in MES buffer occurs when CSF was spiked with 100 mg L−1 human serum albumin (HAS), likely due to unspecific interactions between tubulin and HSA in solution. PEM however, was reported with an insignificant interference and it was further elected for tau–tubulin interaction analyses (Li *et al.*, 2018). Finally, compared to the natural secondary antibody-based approach, tau– tubulin has demonstrated a wider functional range coupled to a signal improvement, dose–response trend at lower tau concentration, than is usually investigated and closer to the physiological levels in the reference matrix for protein tau biomarker (Li *et al.*, 2018). These findings expand the present limitations in application of tubulin as an alternative receptor for tau protein,

considering its highly promising polymerization and reversible interaction with this key AD hallmark (Li *et al.*, 2018).

Generally, non-specific binding on these sensors has also been highlighted as a limiting factor to their sensitivity and specificity when testing with real samples (Knudsen *et al.*, 2006) . It has previously been shown that piezoelectric devices have the ability to detect medically important analytes (S.Tombelli, 2012). Another advantage of these devices is their good temperature stability. However, they require specific design concept, as the mechanical nature of the sensing mechanism can cause the enclosure of the biosensor as well as sample handling systems to interfere with the sensing mechanical motion, thus affecting sensor performance (Mohanty, 2015)

2.5.1.3 Thermometric / Thermal biosensors

Thermometric biosensors measure the absorption or evolution of heat during a biochemical reaction such that the amount of heat absorbed or evolved is proportional to the product formed as a result of the biochemical reaction (Karunakaran, Rajkumar and Bhargava, 2015). In thermometric devices, heat is measured using thermistors, also referred to as enzyme thermistors, and in such devices, the heat measured is a result of the reaction between immobilised enzyme molecules with a suitable substrate (Ramanathan and Danielsson, 2001). Applications of Thermistors include enzyme activity (metabolites such as ethanol, glucose, and lactate have been determined by thermometric devices immobilised with alcohol oxidase, glucose oxidase, and lactate oxidase respectively), clinical monitoring (blood glucose has been successfully measured), process monitoring (monitoring the fermentation process of penicillin G, lactate, sucrose, and glucose), and in environmental settings, measuring heavy metal ions such as Hg^{2+}, Cu^{2+}, and Ag^+ based on their activity to inhibit urease (Ramanathan and Danielsson, 2001)

This type of biosensor has attracted less attention in the miniaturisation field due to weak sensitivity. However, one of their main advantages is their stability. Since in thermistors there is no chemical contact between the transducer and the sample, they have very good long-term stability. Thermistors are also cheap, and measurements are not disturbed by varying optical or ionic sample characteristics (Ramanathan and Danielsson, 2001). However, development of thermistors has been hindered due to their poor sensitivity, and very little research in that area has been presented for the past few years.

2.5.1.4 Electrochemical biosensors

Electrochemical biosensors are molecular sensing devices which intimately couple biological recognition elements such as antibodies, enzymes, or DNA probes such as short ssDNA or ssRNA (Ellington and Szostak, 1990; Tuerk and Gold, 1990) to an electrode transducer. Electrochemical biosensors can be grouped in two classes: biocatalytic and affinity sensors. In biocatalytic platforms, an enzyme acts as a sensing element and an electric signal is produced via a specific catalytic reaction whereas in affinity types, antibodies or nucleic acids are detecting elements (Grieshaber *et al.*, 2008).

Generally, electrochemical biosensors rely exclusively on the measurements of currents and/or voltage to detect binding between the recognition element and target molecules including bacteria, parasite, virus, protein and nucleic acid. Electrochemical biosensors can be subdivided into categories depending on the transducer and measurement implored. They can be divided into DC and AC techniques, where DC techniques include, potentiometric, amperometric and voltametric transducers, and the AC technique can be impedimetric.

In potentiometric measurements, the potential difference between either an indicator and a reference electrode, or two reference electrodes is determined by a voltmeter when there is no significant current flowing through them (Thévenot *et al.*, 2001). The potential difference measured is due to the oxidation and reduction of the species in the sample solution rather than their concentration (Kassanos *et al.*, 2008). The transducer may be an ion-selective electrode (ISE) based on thin films or selective membranes as recognition elements (Thévenot *et al.*, 2001) and the analytical information is obtained when the ISE converts the bio recognition process into a potential signal (Wang, 2006). The most commonly used potentiometric ISE based biosensors are the pH electrodes, and one example of its use is in glucose biosensors (Ocvirk, Buck and DuVall, 2017), where glucose oxidase is immobilised on the surface of the pH electrode. Although glucose has no influence on pH in the working medium, the enzymatic reaction that results in the formation of gluconate, causes acidification leading to a change in pH (Yang *et al.*, 2014).

Amperometric biosensors are based on the measurement of current that results from the electrochemical oxidation or reduction of an electroactive species. This type of measurement is taken by maintaining a constant amplitude voltage at a platinum, gold or carbon based working electrode, or an array of electrodes with respect to a reference electrode (Thévenot *et al.*, 2001; Grimnes and Martinsen, 2015). The application of a fixed potential causes the analyte in the sample to react and a current to pass through the sample.

Voltammetry involves the application of a time dependent potential to an electrochemical cell, and measuring the resulting current as a function of the applied potential (Grieshaber *et al.*, 2008). In voltammetry, different potentials are applied by sweeping through a range of voltages, and as different species react at different potentials, the concentration of different species would be determined in the same experiment, therefore making it unnecessary to separate the different species and then conducting several experiments (Kassanos, Demosthenous and Bayford, 2008). Cyclic voltammetry is a common version of voltammetry, and in this method, the voltage is swept, but at a predetermined voltage level this sweep is reversed ending the cycle at the starting voltage (Li and Miao, 2013). The main aim of biosensor development is to provide small devices that can be used as Point-of-Care testing equipment. The development of these types of devices would mean that they could be operated by semi-skilled operators. Electrochemical biosensors have reached commercialisation stage and are currently being used worldwide. As mentioned above, one of the most popular commercially available electrochemical biosensors is the blood glucose sensor, also known as glucometers or blood glucose monitors, based on screen printed enzyme electrodes, coupled to pocket size amperometric meters (Wang, 2006).

The glucose biosensors have also been further developed so that other key metabolites such as urea, creatinine, lactate, uric acid, cholesterol, and ketones could be detected, and in some cases these mini-devices can actually detect multiple analytes at the same time Electrochemical biosensors have gained popularity and success due to their specificity, speed, portability, and low cost (Thévenot *et al.*, 2001; Hammond *et al.*, 2016). As demonstrated by the blood glucose biosensors, they also allow testing to occur anywhere and at any time, as compared to conventional testing methods, where all the testing would have to be done in the laboratory, while also employing and training appropriate staff (phlebotomists, biochemists, and laboratory managers) to obtain and process the samples. The main advantage of this development is that measurements can be taken instantly and results obtained immediately, with as little as 0.3 μl samples, compared to other laboratory testing where about 1 ml sample is required, and results (unless tests have been ordered as urgent) would be available to the clinician/patient after several days, and depending on the tests, maybe longer to reach the patient.

It has been reported that the effectiveness of the detection process in electrochemical biosensing can be enhanced by using aptamers rather than antibodies due to their cheaper mass production, higher rate of chemical stability, structural modification, affinity, specificity, and electrodes fixation density.. Aptamers are short, single-stranded DNA or

RNA (ssDNA or ssRNA) molecules that can selectively bind to a specific target, including proteins, peptides, carbohydrates, small molecules, toxins, and even live cells (Lakhin, Tarantul and Gening, 2013). However the cost of developing aptamers on a small scale was its draw back, hence, it wasn't suitable for this research. In addition, aptamer chemistry was not well developed until the end of this research, in comparison to the antibody chemistry which is well established. Consequently, the antibody approach was decided upon. Aptamers have become a hot topic in electrochemical sensing and clinical testing (Zhu *et al.*, 2012).

Dan Tao et al. developed a label-free electrochemical aptasensor for detection of Tau381 in human serum with a detection limit of 0.70 pM (Tao *et al.*, 2019). To construct the sensing element, a specific aptamer against Tau381 was immobilized on a gold nanoparticle component of a nanocomposite comprised of carboxyl graphene/gold/thionine NPs (CG/TH/ AuNPs) conjugated on a glassy-carbon electrode (GCE) surface. Due to its electrochemical reversibility and rapid electron transfer, thionine (TH) was used as redox agent (Zheng *et al.*, 2014). After the interaction between aptamer and Tau381, TH generated an electrochemical signal which was measured with differential pulse voltammetry (DPV).

Several reaction sites and adequate space for electrocatalytic active substances are provided by MWCNTs, considering the surface topological defects and large specific surface area. Some of the major MWCNTs drawbacks during clinical applications include low dissolving rate and high accumulation tendency (Rio-Echevarria *et al.*, 2019). Nevertheless, carbon nanotubes are well dispersed in water, under influence of ultrasound, by another type of carbon nanomaterial, named graphene oxide (GO) (Tung *et al.*, 2011), due to the synergy between them. For improving the low conductivity of GO, some of its oxygen-based groups are reduced thereby forming rGO (reduced graphene oxide) (Sok and Fragoso, 2019). Additionally, rGO contributes to the higher electrode modification potential of MWCNTs-rGO nanocomposite compared to MWCNTs-GO ones.

Possessing a high adsorption rate, biocompatibility and film-forming potential, chitosan (CS) can immobilize specific antibody and fix modified materials on the electrode (Sok and Fragoso, 2019). Furthermore, AuNPs are commonly added to biomolecules (antigen or antibody) to modify and amplify signal due to their high physicochemical stability, conductivity and biocompatibility, along with large specific surface (Ramalingam, 2019). In one study, MWCNTs-rGO-CS nanocomposites were utilized to modify the gold electrode conductivity. Tau-441 protein was also modified with AuNPs in terms of signal amplification. A 3-electrode system, $[Fe(CN)_6]_3^-$ and $[Fe(CN)_6]_4^-$, served as the redox probe and provided the basis of this study (Carlin and Martic-Milne, 2018) DPV (differential pulse

voltammetry) was performed to analyze the tau-441 protein and the specific antibody interaction, which was indicated by the sensing signal and controlled by the formation of tau-441 protein- antibody complex. The complex formation and together with electron transfer led to signal alternations. The electrochemical biosensor response was linear at the 0.5–80 fM. with LOD (limit of detection) of 0.46 fM, represented by DPV at 100–500 mV range. A total 42 serum analyses were successfully done by the biosensor for healthy samples, patients with mild cognitive impairment and dementia (Li *et al.*, 2020). The process of detection of tau-441 protein needs to be highly sensitive, since the blood brain barrier (BBB) leaves only an insignificant amount of tau-441 protein in the blood. Another approach for electrochemical biosensing of tau protein was implemented by immobilizing anti-tau on the surface of gold electrodes to provide a biorecognition element following tau441 interaction with anti-tau molecules. Moreover, the electrochemical impedance spectroscopy has been employed to screen the interaction of antigen-antibody. A subsequent decline in charge-transfer resistance is noted due to the attachment of tau441 to Ab-Au (Wang *et al.*, 2017). According to the review by Mohanty, (2015). In electrochemical sensing, gold electrodes can be directly immobilised with thiol modified compounds, which is contrary to the case of piezoelectric biosensors, where surface modification of the gold electrode is more complicated due to more complex immobilisation chemistries. Compared to other types of biosensors (non-electrochemical transducers) and looking at the advantages and disadvantages of each (Table 1.6), the development of electrochemical biosensors seems more promising, and would be more readily accepted/approved in the biosensor market.

2.6 Detection of tau Using tetrapolar EIS: Biochemistry and theory
2.6.1 Biochemistry

2.6.1.1 Proteins

Generally, proteins play an important role in most biological processes taking place in living organisms and they have very diverse functions. The largest proportions of proteins constitute of enzymes and are responsible for catalysing most of the chemical reactions in biological systems. Some proteins are responsible for transmission of specific stimuli as well as transporting molecules and ions to other locations in the body of an organism (Stryer, 1995). Examples include haemoglobin which transports oxygen in blood and myoglobin that transports oxygen to the muscles. Some other proteins are responsible for mechanical

support, such as Tau protein to microtubules while others provide high tensile strength to the bone and skin through the presence of collagen and for coordinated motion, as they play an important role in muscle contraction. In addition to the abovementioned functions, proteins play a crucial role in the immune system in the form of antibodies which help to fight foreign substances (Berg et al., 2012, Stryer 1995) by specifically binding these foreign substances also known as antigens in a stable manner.

2.6.1.2 Antibodies

Antibodies are soluble glycoproteins produced by plasma cells particularly B lymphocytes, which belong to the immunoglobulin supergene family of proteins involved in the immune system. Antibody synthesis is stimulated by the entry of foreign molecule (antigen) into the mammalian system and the antibody produced usually has a specific affinity for the antigen that stimulates its synthesis. This specific affinity is for a specific region of the antigen called the epitope. The antigen could be another protein, polysaccharides, nucleic acids, viruses or microorganisms. There are five different types of antibodies, IgA, IgD, IgE, IgG and IgM, where Ig stands for immunoglobulin (Stryer, 1995). IgG is the most common form found in serum (Campbell et al., 2005) and is the form most commonly used in immunosensors, as it binds with the highest affinity to its antigen compared to other forms. The antibody comprises of three main parts. Two which are responsible for antigen binding known as Fab, where F stands for fragment and ab for antigen-binding. The third is called Fc, since it crystallizes (hence the c in Fc) and does not bind with antigens (Campbell et al., 2005). It however, binds to specific proteins and cell receptors (Stryer, 1995). IgG consists of one Y-shaped unit which is made up of two types of polypeptide chains and contains in total two of each type. Therefore, two of these are identical and are known as heavy chains (H) and the other two are also identical and are known as light chains (L). The Fab consists of the entire L chain and part of the H chain and the Fc consists of the rest of both H chains. The tip of the L and H chains of the Fab parts are extremely variable, and this is usually the site where antigens bind to antibodies (Berg, Tymoczko and Stryer, 2012). The high variability of this region allows for the very diverse antigen recognition. Antibody-antigen binding allows the organism to recognise an antigen and attack it. Binding can also lead to target neutralization, by not allowing an antigen to function properly (Stryer, 1995). Through noncovalent bonding, antibodies can strongly bind selectively and specifically to a very wide range of biomolecules, cells, viruses and chemicals. Detection and monitoring of the level of presence of antibodies is a very useful

diagnostic tool as this gives information regarding the health of a patient. For example, IgG is found elevated in some forms of hepatitis (Olsen et al., 2006; Schemmerer et al., 2017). Antibodies are also extensively used in clinical laboratories for the detection of antigens and as tags with fluorescent-labelling in a number of different applications, such as ELISA (Knutson et al., 2016; Li et al., 2017; Stephen, Gunasekaran and Anitharaj, 2018).

2.6.2 Biosensing and immobilization strategies

From Section 2.6 the nature by which biomolecular detection occurs has been established. However, for biosensor application, this needs to somehow be coupled unto the electronic transducer. This is done by direct immobilization of the biomolecules on the transducer surface. As in all affinity-based biosensor technologies and standard immunoassays (ELISA), the performance of EIS biosensors is directly dependent on the properties and methods of immobilization of the biomolecular layers on the sensor's surface (Grieshaber et al., 2008; Karunakaran et al., 2015). The quality of the immobilization procedure dictates the stability, sensitivity, response time, reactivity and reproducibility of the sensor (Franks et al., 2005). The molecular probe has to be irreversibly attached on the solid support, and the surface coverage needs to be controllable. This is to avoid insufficient coverage (pin-hole effect) of the electrode surface following the probe-immobilization procedure, which could hinder the sensors response due to limited binding sites (Love et al., 2005; Daniels and Pourmand, 2007). Furthermore, the pin-hole effect could lead to non-specific adsorption of non-targeted molecules that might be present in the test sample, to the electrode surface resulting in magnified results (Daniels and Pourmand, 2007). Apart from the coverage of the electrode surface, another important aspect is the immobilization of the target molecule in the right orientation at an optimum density such that it retains its original functionality (Luppa, Sokoll and Chan, 2001). Finding a suitable ligand for a specific target biomolecule can also be a problem (Daniels and Pourmand, 2007).

The simplest and fasted way of immobilization of antibodies on substrates is by direct adsorption. This, however, is very unreliable, as the adsorption of antibodies on the surface of the substrate in the right orientation, a very important aspect of biosensing, cannot be guaranteed (Rusmini, Zhong and Feijen, 2007). Direct covalent coupling (using e.g., thiols, amines) which is another method for biomolecular immobilization provides stronger and stable attachment of proteins to a substrate although still possibly in a random manner. Furthermore, the regions which can covalently bind to the support may be associated with the Fab regions of the antibodies. This can result to inactivation of the immune reaction

properties of the antibodies and hence loss of the natural activity of the biomolecule (Rusmini, Zhong and Feijen, 2007). Another very commonly used method is based on the exploitation of the avidin-biotin and the streptavidin-biotin systems. These systems are relatively simple and effective, forming very strong, stable and irreversible bond (Rusmini, Zhong and Feijen, 2007). However, use of these systems makes this technique very expensive and also the fact that biotinylation of antibodies can occur at random places resulting in wrong orientation of the antibodies (Rusmini, Zhong and Feijen, 2007).

The introduction of SAMs in the field of biosensors has significantly improved the performance of impedance biosensors (Luppa, Sokoll and Chan, 2001; Love et al., 2005). This approach was adopted for the connection of the biosensor presented in this research.

2.6.2.1 Self-assembled monolayers

Self-assembled monolayers (SAM) are layers of a single molecule on a substrate formed by self-organisation of molecules in an ordered manner by chemisorption on a solid surface (Arya et al., 2007). Also known as a cross linker, SAM consists of three main parts; the surface active head group that binds strongly to the solid surface, an alkyl group that gives stability to the assembly by van der Waals interactions and a functional group that plays an important role in coupling the biomolecules to the monolayer (see fig 2.7). SAMs have the ability to form stable uniform surface structure which helps in the orientation and controlled immobilisation of biomolecules.
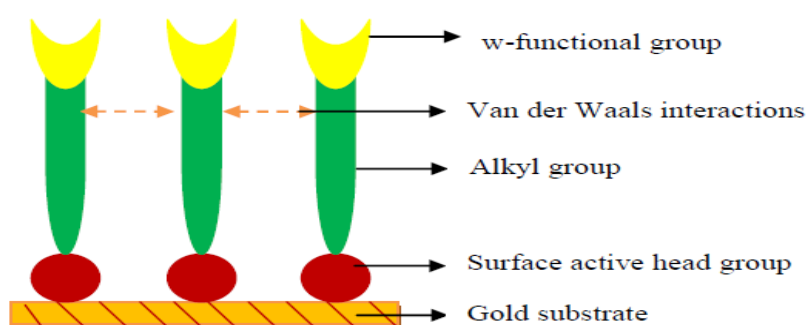
Figure 2.7: Schematic representation of Self Assembled molecules (SAMs).

The surface active group binds to the gold substrate via chemisorption, and the alkyl group gives stability to the assembly of the monolayer by van der Waals forces. The functional group (w) binds to biomolecules such as antibodies.

SAM cross linkers usually contain at least two reactive groups which can react with a number of groups, such as sulfhydryls, carboxyls, carboxylic acids, carbohydrates and amines, and

create chemical covalent bonds. Proteins, including antibodies have many of these functional groups and can therefore be readily conjugated using cross-linking agents. Some other applications of SAMs have been in the study of protein structure and function, preparation of immunogens, immunotoxins, and other conjugated protein reagents. Cross-linkers can be divided into two main categories depending on the number and similarity of the reactive groups:

1) Homobifunctional cross linkers e.g., 3, 3'-dithiobis [sulfosuccinimidylpropionate] (DTSSP) having two identical reactive groups (Fig. 2.8a) and,

2) Heterobifunctional cross linkers e.g., sulfosuccinimidyl 6-[3'-(2-pyridyldithio) propionamido] hexanoate (sulfo-LC-SPDP) with two different reactive ends (Fig 2.8b).

a)

DTSSP
M.W. 608.51
Spacer Arm 12.0 Å

b)

Sulfo-LC-SPDP
M.W. 527.57
Spacer Arm 15.6 Å
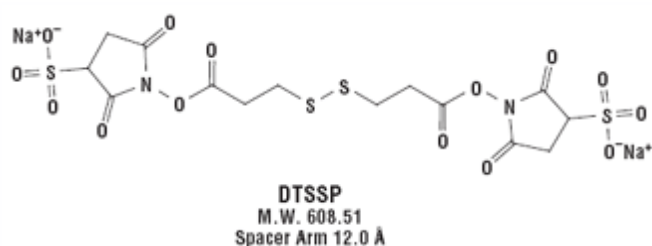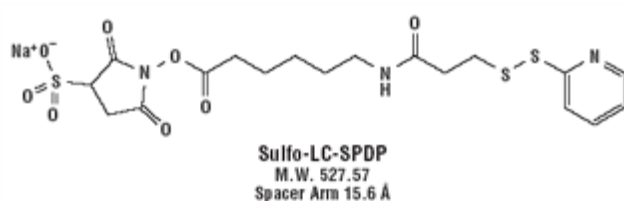
Figure 2.8: **Example of homobifunctional and heterobifunctional cross linkers** (a): DTSSP (3, 3´-Dithiobis[sulfosuccinimidylpropionate]) is a homobifunctional cross linker. There are two identical groups joined together by a disulphide bond. (b) sulfosuccinimidyl 6-[3'-(2-pyridyldithio) propionamido] hexanoate (sulfo-LC-SPDP) has two different reactive groups.

Different molecules self-assemble on different substrates. The most commonly used SAMs in the field of impedimetric biosensors are disulphides, sulphides or thiol molecules, which assemble on gold, copper, silver, palladium and platinum. The formation of the SAM and its characteristics, directly depend on the metal used as well as its quality. For example, alkane-thiol monolayers formed on gold substrates are very densely packed and are very well ordered in contrast to those formed on silver (Love *et al.*, 2005). For the purpose of this work,

gold is the substrate of choice for the formation of monolayers because of its reasonably inert properties and also formation of a very stable linkage with thiol group. Some examples of thiol linkers and their structures are shown on Table 2.5.

Table 2.5: Example of thiol cross linkers, their chemical name, type, and structures.

Chemical name	Homo/Hetero -bifunctional	structure
Bis(β-[4-azidosalicylamido]ethyl) disulphide	Homo-bifunctional	
Dithiobis(succinimidylpropionate) (DTSP)	Homo-bifunctional	
NHS-SS-Diazirine	Hetero-bifunctional	
N-Succinimidyl 3-(2-pyridyldithio) propionate	Hetero-bifunctional	
Sulfosuccinimidyl(perfluoroazidobenzamido)ethyl 1,3'-dithiopropionate	Hetero-bifunctional	

For the purpose of this research, dithiobis [succinimidyl propionate] (DTSP) / 3,3´-dithiobis [sulfosuccinimidylpropionate] (DTSP) was used as a cross-linker for SAM assembly. DTSP is a cleavable homobifunctional linker (see structure of DTSP in Table 2.9). It is composed of an amine-reactive N-hydroxysuccinimide (NHS) ester at each end of an 8-

carbon spacer arm. NHS esters react with primary amines at pH 7-9 to form stable amide bonds. Proteins, including antibodies, generally have several primary amines in the side chain of lysine residues and the N-terminus of each polypeptide is available as targets for NHS-ester crosslinking reagents (Thermo scientific, Pierce proteins research products, 2009).
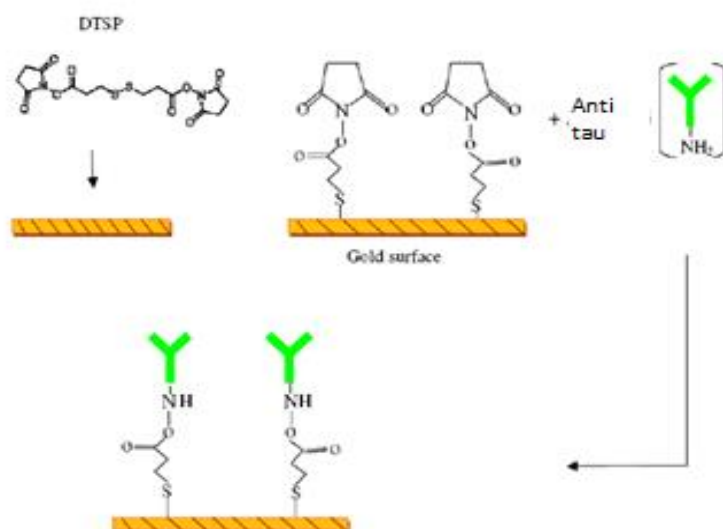
Figure 2.9: **Illustration of how DTSP binds to a gold surface.**

DTSP cleaves and adsorbs to the gold surface leaving the NHS groups free for proteins to bind to. In order to develop a biosensor, a vital step is to immobilize the antibody on a solid substrate (Fowler, Stuart and Wong, 2007) without significantly reducing binding activity, as compared to soluble antibodies. Such reduced binding ability is due to steric hindrance of the molecules in the solid-phase surface compared to that in solution. However, it has been suggested that the random orientation of antibodies on the solid-phase surface might be a further reason for their reduced binding activity (Oh *et al.*, 2004). Chemical immobilization of antibodies through thiol layers also has shortcomings and the sensitivity of the biosensor can be affected. One factor affecting the sensitivity is the structure of the antibody. If the Fab fragments of the antibodies are hidden, less antibody-antigen binding sites would be exposed. Such random orientation of antibodies can also lead to the loss of biological activity (Rusmini, Zhong and Feijen, 2007) The best way to immobilize antibodies would be by exposing the Fab fragments to facilitate binding, an important step in the development of a biosensor. Another way of possibly enhancing the sensitivity of the

antibody-based assay would be by minimizing the distance between the transducer surface and the immobilized film of protein, while giving the monolayer a two-dimensional structure (Oh *et al.,* 2004). To overcome this problem so that antibodies could be immobilized in an oriented manner, several methods have been proposed, such as the use of protein G, the thiolation of antibodies and use of Fab fragments.

SAMs can be developed by simply immersing a clean metal substrate into a solution containing the necessary dissolved chemical at room temperature. and can be combined with F_c receptor proteins, such as protein A and G, which are described in the following section.

2.6.6.2 Protein A and G

Protein G is a bacterial cell wall protein from group G streptococci, and is produced as a recombinant in *E.Coli* for research use. While, native protein G has two immunoglobulin binding sites, as well as albumin and cell surface binding sites, in recombinant protein G the albumin and cell surface binding sites have been eliminated to ensure the maximum specific IgG binding capacity (Thermo Scientific, Pierce Proteins Research Products, 2010). Protein G specifically interacts with the Fc portion of antibodies (Neubert *et al.*, 2002) leaving the paratope to face the opposite side of the protein-G immobilized solid support (Fig 2.10).

(A)
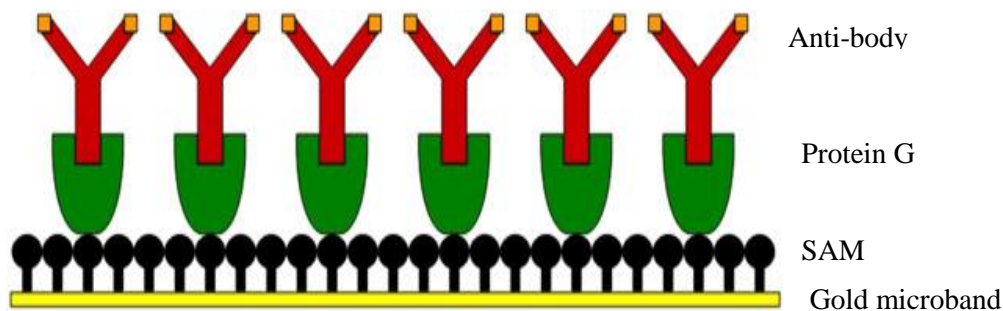
(B)
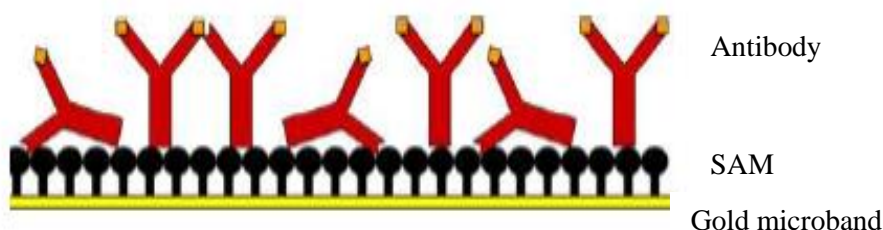
Figure 2.10: Antibody immobilisation with and without Protein G. (A) Antibodies immobilized with the protein G layer. From bottom to top: the golden substrate, SAM layer,

protein G layer and antibodies (B) Antibodies immobilized without the protein G layer illustrating its reduced detection ability (Neubert *et al.*, 2002).

The use of protein G as an approach to orientate the immobilization of the antibody layer has been reported by different groups, with the outcome being of mixed conclusion (Kassanos *et al.,* 2008, Neubert *et al.,* 2002, Oh *et al.,* 2004). In the study by Neubert et al. (2002), an affinity capture MALDI mass spectrometry methodology was developed by covalently immobilising recombinant protein G onto gold discs for the purpose of orientating an IgG such that their Fab domains pointed away from the target surface for the test antigen hCG β core fragment (hCGβ*cf*) to bind to. This method of immobilising antibodies via a protein G layer resulted in an increase in MALDI signal as compared to the use of randomly immobilised antibodies. In the study by Oh et al. (2004), a surface plasmon resonance (SPR) based immunosensor using self-assembled Protein G was developed for the detection of *Salmonella typhimurium*. The effect of protein G on the interaction between antibody and antigen was investigated by comparing the shift degree of SPR angle by the binding interaction.

It was noticed that the shift degree of SPR angle in case of immobilised antibody on solid surface using protein G was larger than that of the SPR angle in case of directly immobilised antibody on solid surface without protein G, suggesting that the use of protein G leads to better immobilisation of antibodies and better detection of the antigen of interest. Kassanos et al. (2008) compared two antibody immobilisation methods in the development of an electrochemical biosensor for the hormone hCG. The first method involved the direct immobilisation of antibodies on the SAM whereas the second method involved the immobilisation on antibodies on a protein G layer, coupled to the SAM. Unlike the previous studies, it was reported that the biosensor constructed without protein G was equally as successful at detecting hCG.

Bacterial cell-surface protein A (from *Staphylococcus aureus*), protein G (from *Streptococcus strain G148*), recombinant forms of these and recombinant protein A/G, can be covalently bound to SAMs (Mayes, 2002). These proteins have a high affinity for and can only bind to the F_c non-antigenic regions of antibodies, thus ensuring that the F_{ab} regions are available to bind with antigens. Due to their capability of binding to the F_c region of immunoglobulins from many species, protein A and G have found extensive use in the purification of antibodies and as universal labels for immunometric assays (when conjugated with an enzyme or fluorescein). A very interesting property of these proteins is that the protein A and G-antibody reaction is reversible, which can be exploited for regenerating or

altering the surface functionality of a sensor (Mayes, 2002). In contrast to breaking the bonding of an antibody with its antigen, this can be performed quite easily (using mild acidic buffers) without affecting or damaging other layers or the solid support.

The field of immunosensor probe-immobilization strategies is an active research area and great effort is put into understanding and improving the immobilization strategies, reducing non-specific binding and optimizing probe density and orientation and the scientific community does not seem to have concentrated on one specific capture probe immobilization strategy (Daniels and Pourmand, 2007).

2.6.3 Electrochemical impedance spectroscopy

Electrochemical impedance spectroscopy (EIS) is an experimental method for characterizing electrochemical systems (Ates, 2011) such as in corrosion, electrodeposition, batteries and fuel cells. EIS is a well-developed branch of alternating current (AC) techniques that describes the response of a circuit to an alternating current or voltage as a function of frequency. Impedance (Z) is a measure of the degree to which an electric circuit resists the flow of electrons or current when a voltage is applied across its terminals. One advantage of EIS over other bio-sensing methods is that it allows label-free and real-time detection of biomolecules by relying on the measurement of small changes in the transducer-electrolyte interface impedance in order to detect and quantify probe-analyte interactions (Manickam *et al.*, 2012). Although some of the instrumentation for performing EIS techniques are complex, bulky and expensive bench-top systems which typically only have a single or a few measurement channels, this technique offers the possibility of miniaturization into a Point-of-Care device.

2.6.3.1 Electrochemical impedance measurement and interpretation
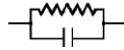
Electrochemical impedance measurements are made using a small AC voltage or current (Suni, 2008). The response of the measurement can be modelled using a combination of resistors, capacitors, inductors by means of an equivalent circuit. Depending on how the electronic components of the system are configured, both the magnitude and the phase shift of the current can be determined (Park, 2003). Impedance is expressed as a complex number, where the in-phase current response determines the real component (resistance) of the impedance, while the out-of-phase current response determines the imaginary components (capacitance and inductance collectively known as reactance) (Suni, 2008).

The overall equation describing impedance which is the sum of the individual effects of impedance of the different components (Table 2.6) of the circuit is given by:

Z= R + jX,   (1)

where the real part of the impedance is the resistance R, the imaginary part of the impedance is the reactance X, and $j = \sqrt{-1}$. Reactance is a measure of the opposition of capacitance and inductance to current. This can be explained graphically as shown (Fig 2.12).

Table 2.6: Showing the different circuit components with their different and combined impedance equations

Circuit Element	symbol	Impedance equation
Resistor	—www—	$Z = R + 0j$ $j = \sqrt{-1}$
Capacitor	—||—	$Z = 0 - j / \omega C$ $\omega = 2\pi f$
Inductor	—mm—	$Z = 0 + j\omega L$ $\omega = 2\pi f$
Simple RC circuit	—www—||—	$Z = \dfrac{R}{1+\omega^2 C^2 R^2} - \dfrac{j\omega CR^2}{1+\omega^2 C^2 R^2}$

Where:

ω= angular frequency in rad/s = $2\pi f$, f = is the frequency in Hz

C = capacitance in farads

L = inductance in henries (H)

Impedance is very similar to resistance, however impedance varies with frequency (because of capacitive and inductive effects) whereas resistance is frequency independent (Grieshaber *et al.*, 2008). The impedance (Z), having a magnitude and phase, is expressed as a vector quantity.
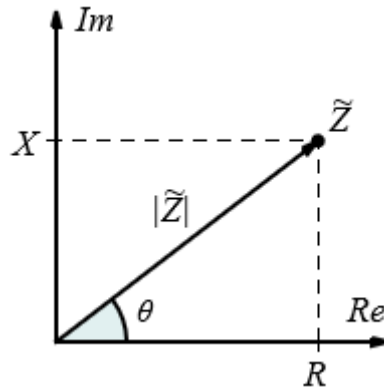
Figure 2.11: Graphical representation of impedance.

The X axis represents the resistance (R), also referred to as the real component of the impedance and the Y axis represents the reactance (X), also referred to as the imaginary component. The resistance and reactance are then added up as vectors to give the impedance vector Z. The magnitude (|Z|), the length of the vector, can be expressed as

$$|Z| = Sqrt\ (X^2 + R^2), \qquad (2)$$

and the phase angle can be defined by:

$$\tan \Theta = X/R \qquad (3)$$

Affinity-based biosensing is a common electrochemical system used to estimate the concentration of an analyte in an aqueous sample (Manickam *et al.*, 2012). As discussed in chapter one, biosensors make use of biological recognition elements (also known as probes) such as DNA oligonucleotides and antibodies, which can selectively bind to the analyte (Grieshaber *et al.*, 2008) as shown in (Fig. 2.12).
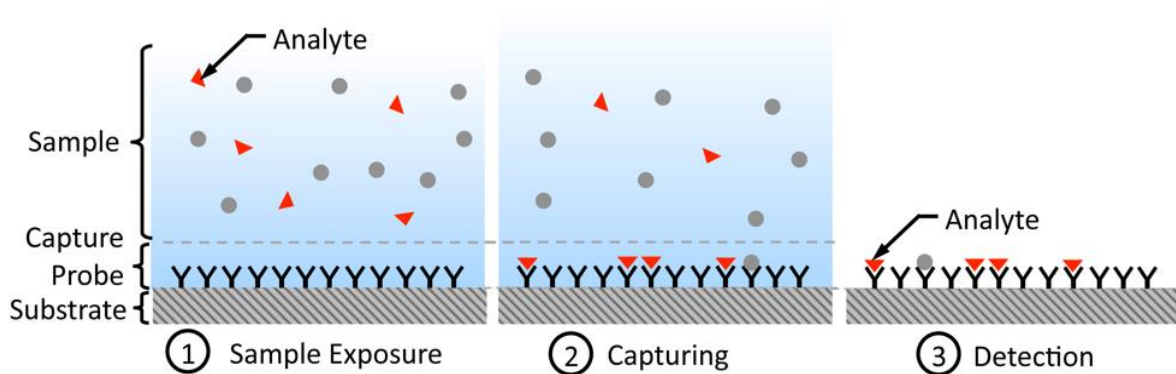
Figure 2.12: **Schematic representation of biosensing steps**. Source: (Manickam *et al.*, 2012).

First, the capturing probe molecules are immobilized on a solid surface typically electrodes in the case of EIS. Next the probes are exposed to a sample containing the analyte of interest that can freely diffuse and attach to the probes. Finally, for detection, the number of captured analytes attached to the probes is estimated from the impedance (Manickam *et al.*, 2012).

Understanding of the electrode/electrolyte interface is of crucial importance in impedimetric biosensing applications. Due to the reduced size of the electrodes to μm and nm, the effect of this interface on the measured impedance becomes more significant. The real and imaginary parts of the impedance are geometrically defined, the smaller the dimensions, the larger the real and imaginary parts of the impedance and detection is performed by monitoring changes to this interface. At the electrode-electrolyte interface shown on Fig. 2.13, a electric double layer is created resulting from the rearrangement of charged electrons in the metal electrode and ions in the electrolyte. The double layer is a very important parameter in EIS studies. A frequency response analyser (FRA) can be used to impose the AC signal which results in an electric field-induced disturbance of the charges across the dielectric double layer. The AC voltage and current response by the system is analysed by the FRA to determine the resistive, capacitive and inductive behaviour of the system at a particular frequency. The electrical field induced disturbance initiates physicochemical processes in the system which have different characteristic time constants exhibited at different frequencies; for example electron transfer at high frequency and mass transfer at low frequency (Suni, 2008).   Impedance spectroscopy when applied over a broad range of frequencies can be used to characterise the various physiochemical processes of the electrochemical system and quantify the impedance associated with them. Subsequently, an equivalent circuit model for the electrode-electrolyte interface such as a simple Randles circuit, which relates various circuit elements to the different electrochemical phenomena can be employed to understand EIS biosensing as shown on Fig. 2.13 (Manickam *et al.*, 2012).
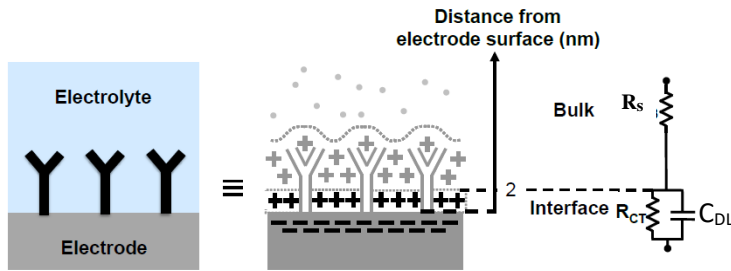
Figure 2.13: **Shows the simple Randles equivalent circuit used to model the electrode-electrolyte interfaces**. Source: (Daniels and Pourmand, 2007)

It consists of the bulk resistance of the solution R_s in series with the impedance of the electrode-electrolyte interface. The interface impedance consists of the charge transfer resistance (Rct) in parallel with the capacitance of the double layer (C_{DL}).

The charge transfer resistance (Rct) is attributed to the electrostatic interactions of ions in the solution with the electrons in the electrodes, which produced a current. A net charge is relocated from the electrode to the electrolyte or vice-versa (Manickam *et al.*, 2012). The double layer capacitance (C_{DL}) is attributed to the spatial distribution of ions formed in the proximity of the electrode-electrolyte interface. As mentioned above, EIS takes advantage of the changes in the interface impedance with the attachment of the analytes to the probes. Changes in interphase impedance can result from attachment of large target molecules onto an immobilized probe which reduces the capacitance C_{dl}, due to the increase in the thickness of the double layer and reduction in the dielectric constant (εr) near the interface (e.g., εr of water is about 81, whereas εr of organic molecules is around 2–3). Also, the formation of larger molecular complexes formed can block the flow of current through the interface, leading to an increase in Rct (Daniels and Pourmand, 2007). Finally, the impedance can also change due to changes in the charge density near the electrode surface, which can be caused by the ionization of both probe and analyte molecules. It is important to realize that the different independent electrical parameters can be used for EIS analysis. For example, in the immunoassay system by Wang et al. (2017) and Rushworth et al. (2014), Rct changes significantly with the concentration of captured antigen. On the other hand, Mirsky et al. (1997) used changes in capacitance with antigen-antibody bindings for EIS bio-sensing.

2.6.3.2 Representation of impedance data

Equivalent Circuit (EC) modelling is usually used to obtain valuable data for EIS analysis, as it allows meaningful properties of the electrochemical system to be extracted. ECs consist of electric components such as resistors (R), capacitors (C), and inductors (L), which are used to model the system under investigation. Different equivalent circuits can be used to model EIS data, the most commonly used is the Randles circuit. EIS data can be represented in two different ways, either showing the phase and magnitude plots as on the Bode plots or on a complex plane known as on the Nyquist or Cole-Cole plot.

2.6.3.2.1 Complex plane plot

In the complex plane plot also known as a Nyquist or Cole-Cole plot, the impedance imaginary component (Z"), which indicates the capacitive behaviour, is plotted against the impedance real component (Z') at each excitation frequency, such that each point on the plot represents the impedance at one particular frequency. This type of plot has the advantage of allowing easy visualisation of the effect of ohmic resistance, Rs, which is the impedance at high frequencies, and the polarization resistance or charge transfer resistance.
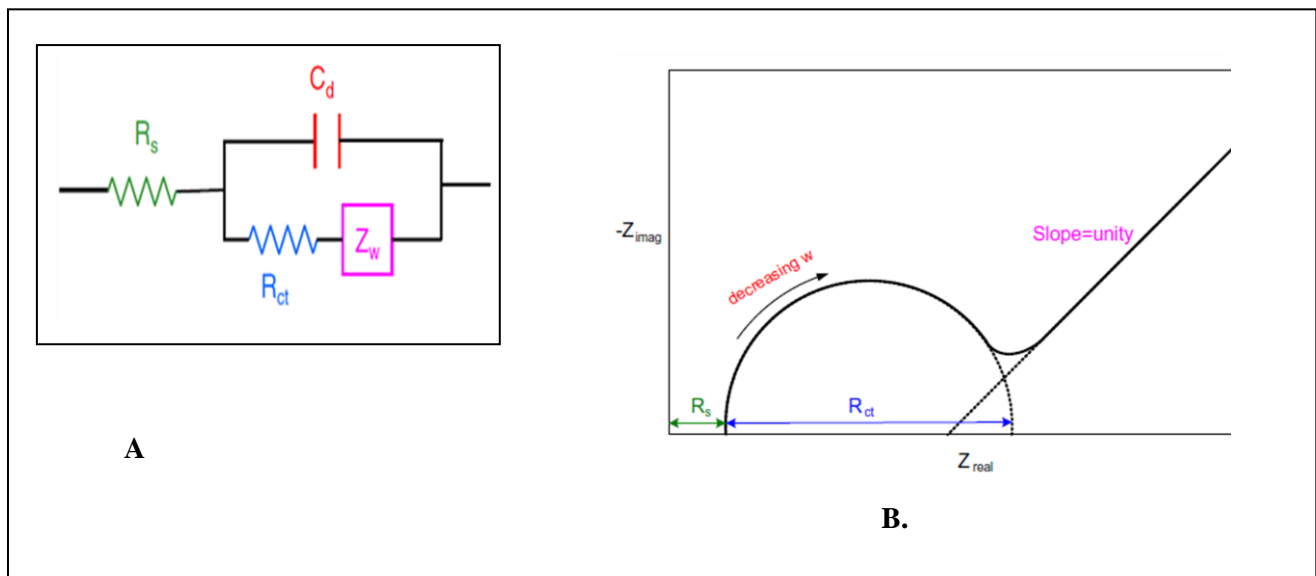
Figure 2.14: **Represents the simple Randles circuit for a simple electrochemical system.**
Source: (Park, 2003)

This equivalent circuit yields the Nyquist plot shown in Fig. 2.14A-B, Rct is the charge-transfer resistance, which is inversely proportional to the rate of electron transfer; C_{dl} or C_d also referred to as Cp (constant phase element (CPE), an equivalent model of double-layer capacitance) is the double-layer capacitance; R_s is the solution- phase resistance; and Z_w is the Warburg impedance, which arises from mass-transfer limitations at low frequency,

where the system acts as an open or short circuit and capacitance becomes infinite. The semi-circle represents frequencies (ω) which increase from right to left in order to obtain the best results from the impedance data (Park, 2003).

2.6.3.2.2 Bode plot

Bode plots allow the absolute impedance |Z| (or the real and imaginary components of the impedance) to be examined, as well as the phase shift, θ, of the impedance as a function of frequency. In Bode plots, the logarithm of frequency is used to allow a wide range of frequencies to be plotted on the same graph, whilst treating each decade equally. The magnitude, |Z|, can also be plotted on a logarithmic scale so that a wide impedance range can be plotted on the same set of axes.
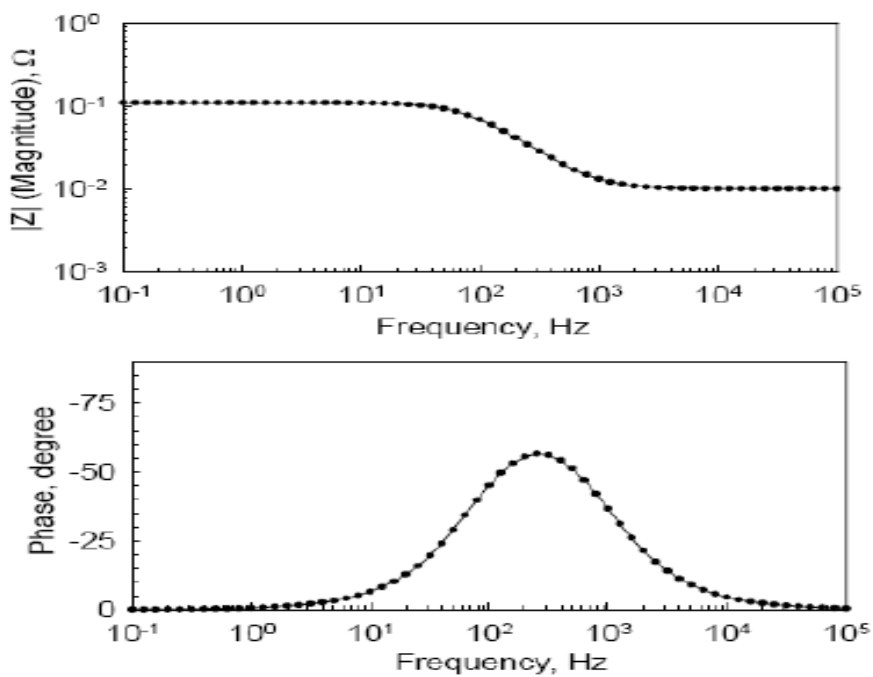
Figure 2.15: **Bode plot demonstrating the magnitude of the frequency response gain, and a Bode phase plot, expressing the frequency response phase shift**. Source: (Park, 2003).

Unlike the Nyquist plot, the Bode plot explicitly shows frequency information. The degree to which an electrical circuit permits the flow of current through it is defined as the admittance (Y) which is the opposite of impedance represented as

$Y = 1/Z$ (4)

The expression for the overall admittance (Y) (magnitude and phase) of the electrode-electrolyte system is given by

$$|Y(j\omega)| = \frac{1}{R_{ct}+R_s}\frac{\sqrt{1+(\omega C_{dl}R_{ct})^2}}{\sqrt{1+(\omega C_{dl}\frac{R_{ct}R_s}{R_{ct}+R_s})^2}} \tag{5}$$

$$\theta(j\omega) = -tan^{-1}\left(\omega C_{dl}\frac{R_s R_{ct}}{R_s+R_{ct}}\right) + tan^{-1}(\omega C_{dl}R_{ct}) \tag{6}$$

2.6.4 Electrodes and Electrode systems

The transducer element is a vital part in developing a biosensor, as it enhances sensitivity (Lisdat and Schäfer, 2008). Different electrode systems, namely monopolar, dipolar, tripolar, and tetrapolar exist. In monopolar systems, two electrodes are present, but one of the electrodes known as the working electrode is dominant, with the other one being neutral. In a dipolar system (Fig 2.16), there are two electrodes that are similar and contribute in the same way as each other (Ma, Su and Nathan, 2015a). One electrode behaves as the counter electrode (CE), injecting current to the cell, while the other electrode, known as the working electrode (WE), allows the injected current to be measured. Two electrode techniques are usually used for impedance measurement of high impedance materials or systems, where the parasitic cable impedance and the electrode/electrolyte contact impedance maybe considered negligible.
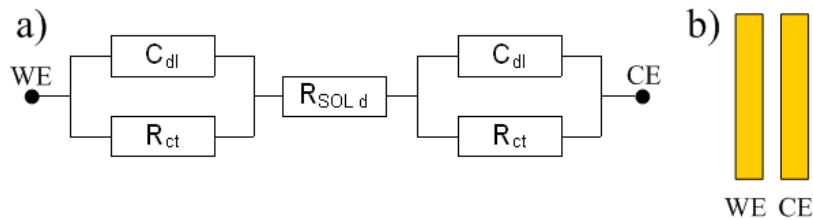
Figure 2.16. a) Two electrode system equivalent circuit model. b) An example of two parallel coplanar gold electrodes acting as the working (WE) and counter electrodes (CE).

Tripolar otherwise known as three-terminal impedance measurement technique, similarly to the two electrode technique, the full cell potential measured includes the voltage drop caused by the WE cable and therefore, this technique is also prone to errors especially when measuring low impedance cells (Brad and Falkuner, 2001). The impedance of the connection cables can be of the same order of magnitude or even larger than the impedance of a low impedance cell under investigation. This may result into making it extremely difficult to differentiate between the two impedances or even ending up measuring the impedance of the cable instead of the system under analysis and thus leading to large errors.

The four terminal techniques also known as tetrapolar system (Fig 2.18) eliminates these problems, making sure that the impedance measured is that across the cell and not that

of the WE and CE cables. This together with accurate measurement of the current through the cell enables the accurate measurement of very low frequencies. In such a four-terminal system, current is applied and measured between separate pairs of electrodes. The measuring electrodes need to be connected to a very high input impedance measurement system so that no current flows through them (Kassanos, 2021). In the previously sections one electrode/electrolyte interface was considered. However, each current carrying electrode will have an electric double-layer and hence an equivalent circuit associated with it. In the four-terminal measurement, no current flows through the voltage measurement electrodes to the cables, thus minimising the effects of polarization (inhibition of the passage of potential determining ions through phase boundary i.e. the electrolyte double layer) (Kassanos *et al.,* 2008; Ma *et al.,* 2015)
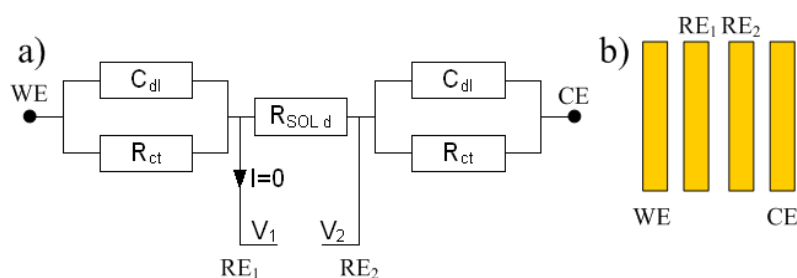
Figure 2.17. a) The four electrode measurement system equivalent circuit model (adapted from Kassanos 2021) An example of four parallel coplanar gold electrodes acting as the working (WE) counter (CE) and voltage measurement reference electrodes (RE).

Investigations of biological materials due to their electrical properties have been carried out for several years now, using conventional electrodes, but more recently, focus is being put on microelectrodes (Rahman, Lo and Bhansali, 2006). Microelectrodes offer more advantages over the conventional electrodes as they have a very small Voltage (I-R drop), making it possible to take impedance measurements of samples such as biological fluids and specimens which have high resistivity. Microelectrodes are also better to use as they allow small currents to be applied, meaning that they are less destructive to the sample under investigation, which is very much desirable in biological samples, and in *vivo* measurements (Rahman, Lo and Bhansali, 2006). This project involves the use of microelectrodes, in an attempt to develop a miniaturised device for sensing biomarkers of Alzheimer's disease.

Microelectrodes are so called, as they have dimensions of tens of micrometers or less, down to submicrometer range (Stulík *et al.*, 2000) and they exist in different forms such as microdisks, microband and interdigitated array. Figure 2.18 shows the basic types of microelectrodes and their arrays.
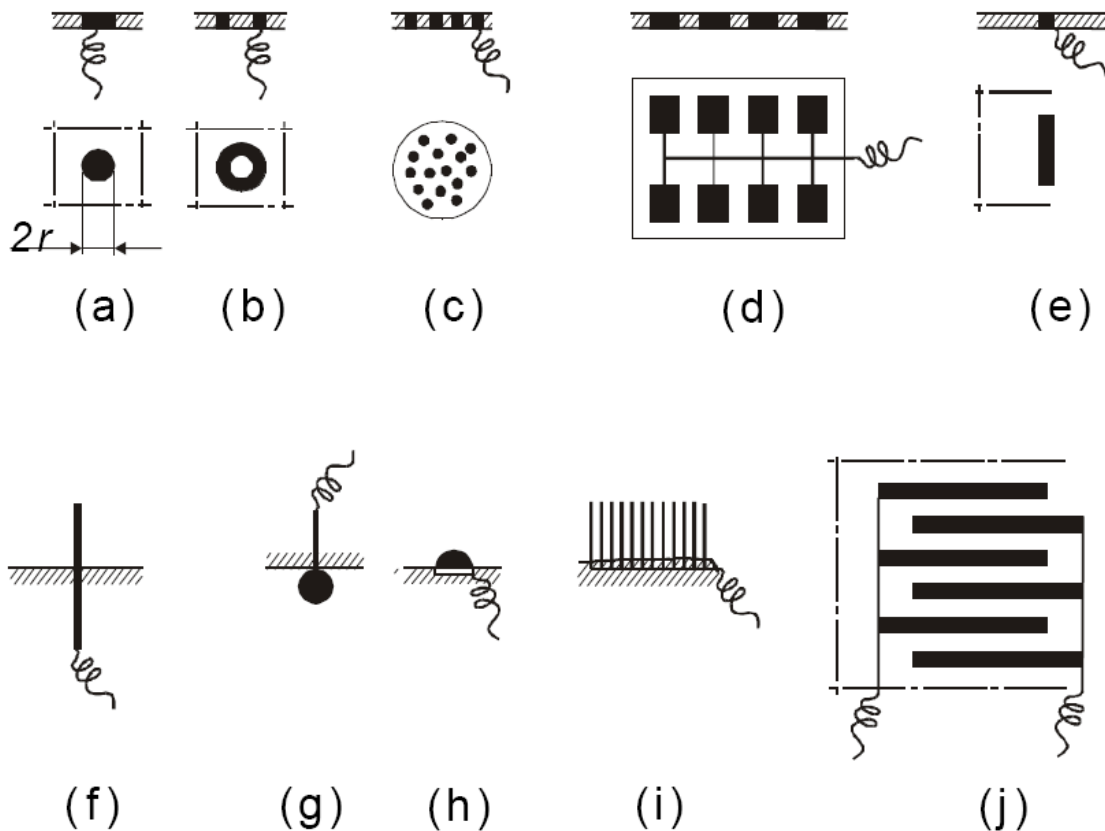
Figure 2.18: Most important geometries of microelectrodes and microelectrode arrays. Where (a) microdisk; (b) microring; (c) microdisk array (a composite electrode); (d) lithographically produced microband array; (e) microband; (f) single fibre (microcylinder); (g) microsphere; (h) microhemisphere; (i) fibre array; (j) set of 2 electrodes (Stulík *et al.*, 2000)

This project has used commercially available gold microband electrodes (Tetrapolar system). These electrodes have been used previously for initial bio-sensing application experiments by Kassanos et al. (2008). Despite the fact that four electrode systems are advantageous over others, there are important factors that need to be considered to enhance sensitivity, one of which is the surface area of those electrodes that carry current, as a large surface area lowers the electrode surface impedance (Hediger , 2002)

Increasing the surface area so that there is an increase in the number of attached probes on the surface of the sensor has also been an attempt at increasing the sensitivity (Daniels and Pourmand, 2007). The building up of the probe on the surface of the sensor leads to the detection of the antigen of interest at a certain region above the electrode surface plane, while still maintaining a close distance (Kassanos, Demosthenous and Bayford, 2008). The distance from the electrode surface, at which the biological detection occurs can be affected by the distance between the band electrodes, as illustrated in Fig. 2.19a, showing the measuring depth at different electrode spacing. However, the measuring depth is not much dependent on the electrode dimensions, as shown in 2.19b, where the electrodes are of different dimensions, with the electrode centre distances being equal (Grimnes and Martinsen, 2015).
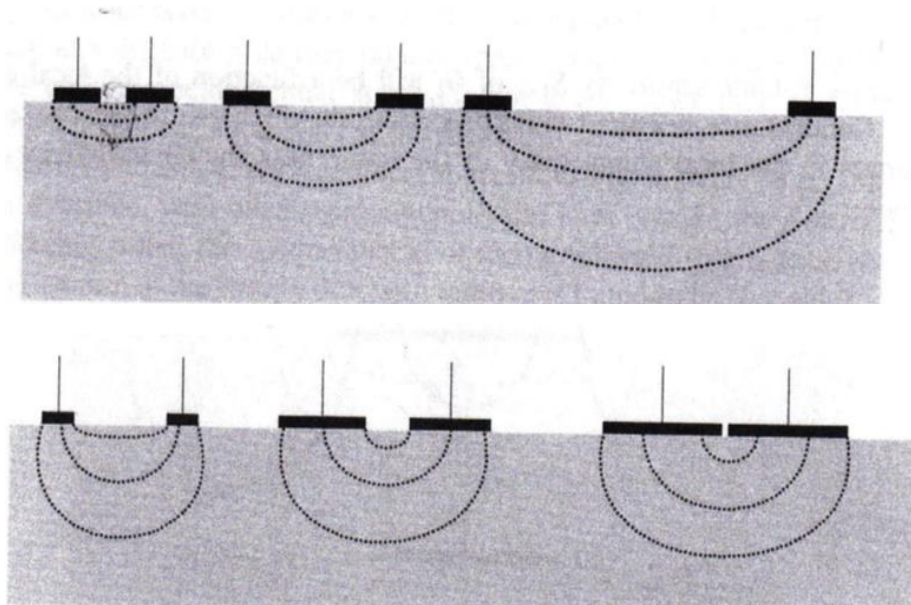
Figure 2.19: **Different electrode sizes and spacing**, a) shows that the distance between microbands affects the measuring depth. Left to right, as the gap between electrodes gets bigger, the measuring depth increases. (b) The dimension of the electrodes does not affect the measuring depth. Left to right, as the electrodes get wider, the measuring depth stays the same (Hema, 2010)

This information on the electrode dimensions and gap between electrodes indicate that the suitability of the electrodes currently being used should be considered and modified for the specific purpose of biosensor development. This would be of upmost importance, as constructing a biosensor involves building up different biological layers on the surface of electrodes, and depending on the dimensions of those layers, and electrode gap, dimension and the measuring depth could be affected, thus omitting the sensitive region on the

biosensor, where the important biological interactions between the antibodies and antigen is occurring.

2.6.5 Electrode materials

Electrochemical analysis depends on the reaction on an electrode surface. The working electrode material or substrate can strongly influence the efficiency of the reactions being performed, implying that the properties of electrode substrates are of great significance for successful electrochemical analysis (Li and Miao, 2013). Such properties to be considered include electrical conductivity, mechanical properties, toxicity, availability and cost. Since different electrode substrates have different biocompatibility, physical and chemical properties, a biomolecule usually exhibits extremely different electrochemical performance on different electrode substrates. It is therefore of crucial importance to choose the appropriate electrode substrate for successful electrochemical analysis. Many electrode substrates such as noble metals including gold, silver, latinum , mercury, as well as carbon and semi conductive materials such as graphene, graphene oxide and carbon nanotubes (CNTs) have been exploited as electrode materials in electrochemical bio-sensing (Li and Miao, 2013). However, factors such as toxicity , susceptibility to oxidation and lack of sufficient information on immobilization protocols limits the application of some materials as electrode substrates used for the analysis of biologic species (Daniels & Pourmand 2007; Stacey, 2015; Ou *et al.,* 2016). Table 2.7 gives some of the advantages and disadvantages of different electrode substrates.

Table 2.7: Some electrode substrates with their advantages and disadvantages in electrochemistry.

Substrate	Advantages	Disadvantages
Graphene	- High mechanical strength - lower impedance uniform response across frequencies, and fewer chemical reactions with tissue - Low cost - Large surface area - Good thermal conductivity	- Contains defects which can affect conductivity - Being just one atomic layer thick, its durability is concerning - the electrochemistry is unknown - its biocompatibility has not been rigorously tested - Difficulty in preparation
Silver electrodes	- Second most studied substrate to gold - Great conductivity - Forms high quality self-assembled monolayers (SAMs) with simpler structure	- Readily oxidises in air - Toxic to cells
Gold	- It is straight forward to prepare thin films of gold by physical vapor deposition, sputtering, or electrodeposition. - Capable of forming good insulating self-assembled monolayer (SAM) layer - Historically the most studied substrate. Thin films of gold have been used in a number of existing spectroscopies and analytical	- Expensive - Forms a more complex SAM structure - Metal contains larger grain molecules making which could make the surface less smooth

Substrate	Advantages	Disadvantages
	techniques, including SPR spectroscopy.	
	• Gold is non-toxic to cells and tissues. The bond formed with thiols is quite stable lasting days to weeks when in contact with complex media of cells and tissues.	
	• Easy to pattern by a combination of lithographic tools (micromachining) and chemical etchants	
	• Gold is inert; it does not react with most chemicals. Gold has very strong affinity for thiols and does not undergo any unusual reactions with them. Also because of the high affirnity of thiols for gold, they have the ability to displace any adventitious materials on the surface of gold	
Nickel	• Good electrical conductor • Excellent material for electroless deposition	• Exhibit toxicity • Bonding to thiol groups not completely understood
Copper	• Good electrical conductor	• Highly susceptible to oxidation

The application of electrochemical impedance spectroscopy (EIS) in electrochemical immunosensors on Au electrodes has been extensively used for biosensing of proteins to include apoliprotein (Zhang *et al.*, 2007), carcinoembryonic antigen (Tang *et al.*, 2007), interferon (Bart *et al.*, 2005), *E. coli* (Yang, Li and Erf, 2004) among others. Detection of tau-tau interactions by means of EIS, using immobilized tau441 on Au surface, has been previously demonstrated by Jose O. Esteves-Villanueva, Trzeciakiewicz and Martic, (2014). Martić, Beheshti, Rains, *et al.*, (2012) and Ahmadi *et al.*, (2017) employed the use of cyclic voltammetry and square-wave voltammetry to study the detection of ferrocene-phosphorylated tau410 protein isoform on Au surfaces. The use of EIS in studying the binding of this phosphorylated isoform of tau (phosphorylated tau410) to Pin1 protein has been reported (Martić, Beheshti, Kraatz, *et al.*, 2012). Tau interactions with heparin, transferrin, and ferritin have been monitored by EIS for full-length tau441 protein (Trzeciakiewicz *et al.*, 2015; Jahshan, Esteves-Villanueva and Martic-Milne, 2016) . Recently, an immunosensor, based on the detection of non-phosphorylated full-length tau441 protein directly, using anti-tau antibodies immobilized on a polycrystalline Au surface (Ab-Au) was reported. The tau441 protein binding to Ab-Au was determined by EIS. The EIS response was evaluated as a function of anti-tau antibody type, and the optimal anti-tau antibody for the electrochemical assay was determined (Carlin and Martic-Milne, 2018)

Current biosensing detection techniques are now highly benefiting from the incorporation of nanomaterials into biosensors, which has put an end to former problems of conventional biosensors (e.g., sensitivity and selectivity) by means of modification of biorecognition layers. However, the expense and duration of processing, as well as sensitivity and selectivity, still have to be improved throughout future investigations. With the arrival of various nanomaterials and their specific properties, biosensing methods have remarkably improved (Zhang, Guo and Cui, 2009). Various types of nanomaterials such as gold nanoparticles (Li, Schluesener and Xu, 2010), magnetic nanoparticles (Haun *et al.*, 2010) ,quantum dots (Ma, Li and Zhang, 2018) and carbon nanotubes (Yang *et al.*, 2015) have been added to biosensors and due to their unique chemical and physical characteristics, vast changes in identification of biomolecules have been made (Holzinger, Goff and Cosnier, 2014). Biosensors have shown to be a favourable method for early detection of AD biomarkers within the cerebrospinal fluid (CSF) (Li *et al.*, 2016). As reported in section **Error! Reference source not found.**, total tau protein and phosphorylated tau (P-tau) are known as promising CSF biomarkers for early diagnosis of AD, therefore with adequate knowledge from the structure of these biomarkers, highly sensitive and specific biosensors

could be created (Blennow, 2005; Shui *et al.*, 2018). Raised levels of tau protein inside CSF samples indicates neurodegenerative disorders and axonal damages which makes it a target biomarker to screen for AD progression (Humpel, 2011).

For the purpose of this work, gold is the substrate of choice as it is very stable and stays in its solid neutral state, over a wide range of potential as well as pH levels. Also, there are a number of surface immobilization protocols available for attachment of biomolecules onto a gold surface ((Lai *et al.*, 2006; Arya *et al.*, 2010; Rushworth *et al.*, 2014). These protocols take advantage of the strong thiol bond, *i.e.*, gold-sulphur bond.

3.   Detection of tau using Tetrapolar EIS: application

3.1. Summary

The method used for developing the biosensor and the concentrations and volumes used for the initial steps of SAM, protein G used in the construction of the biosensor are adapted from work reported by Neubert et al., 2002 and Kassanos et al., 2008. Further experiments are new investigations in the construction of a biosensor for Tau. The EIS experimental set up, methods and results all of which are further subdivided into subsections. The chapter closes with conclusions drawn from the results obtained. The experimental set up describes the laboratory setting and the physical and chemical components involve in the construction and testing of the biosensor. The methods section gives an idea of how the biosensor was constructed and is broken down into 3 main sub-sections (coupling chemistry, sensitivity and specificity confirmed by Western blotting). Within each method subsection, the experimental method for individual investigations is described.

3.2. Materials and methods

3.2.1 Biochemical and biological materials

The 3,3´-Dithiobis[sulfosuccinimidylpropionate] (DTSSP), protein G, phosphate buffered saline *(*PBS) and sulphuric acid were purchased from Thermo Fisher Scientific (UK). Ethanolamine, bovine serum albumin (BSA), skimmed milk powder, 3,3',5,5'-tetramethylbenzidine liquid substrate and Tween20 were obtained from Sigma-Aldrich (UK). Anti-tau antibody (39E10) and human full-length tau441 were from Cambridge Bioscience (UK). Human serum taken from confirmed normal individuals was purchased from BBI Solutions, UK. Human cerebrospinal fluid (CSF) was kindly donated to us by Professor Henrik Zetterberg UK dementia research institute at UCL.

3.2.2 Electrodes

The electrodes used were commercially available electrodes purchased from Windsor Scientific Ltd. (Slough, UK). There were four gold microbands fabricated using standard microelectronic technology on a p-doped silicon substrate of a 350μm thickness (Fig. 3.1c). In more detail, on top of the substrate there was a substrate oxynitride passivation layer of 200nm thickness. Subsequently, there were four titanium (Ti) strips with dimensions 2mm×10μm×10nm (length × width × thickness) each, used as an adhesion layer, on top of

which the four gold microbands were deposited, each being 2mmx10μmx250nm in size. On top there was a final organic polymer passivation layer of 1.8μm thickness, leaving an open window of 1mmx1mm exposing 1mm of the length of each gold microband electrode. This determined the active area of the device (Fig 3.1Ci). The distance between each neighbouring microband was 10μm, the same as their width. All microbands were coplanar and parallel to each other. A not-to-scale figure is shown in Fig. 3.1Cii. The electrodes were purchased mounted on a printed circuit board (PCB) with 8mm width and 25mm length (Fig. 3.C). The PCB had four gold-plated pins used to connect the PCB to a PCB connector specially designed for these electrodes shown in Fig. 3.1a. The connector was used to connect each microband to the appropriate BNC socket of the impedance analyser (Figure 3.1b). The first electrode was treated as the working electrode (WE), at which the generator output of the impedance analyser was connected. The fourth electrode was used as the counter electrode (CE) and was connected to the current input BNC socket of the instrument. The second and third electrodes were used as the reference electrodes (RE) and were connected to the V1 Hi and V1 Lo BNCs of the instrument, respectively.

3.2.3 Impedance analyser

A Solartron Impedance/Gain-Phase Analyser 1260 model (Solartron Analytical, Farnborough, UK) was used in the lab to conduct impedance measurements on the biosensors. The analyser was connected to a PC and the data collected using the Smart software that was supplied by the manufacturer. The biosensor was connected through a set of four connectors and cables to the other side of the analyser via a shielding box. Figure 3.1b illustrates the experimental set up. The purpose of the box was to provide shielding to the electrodes to protect the measurements from external electromagnetic noise.
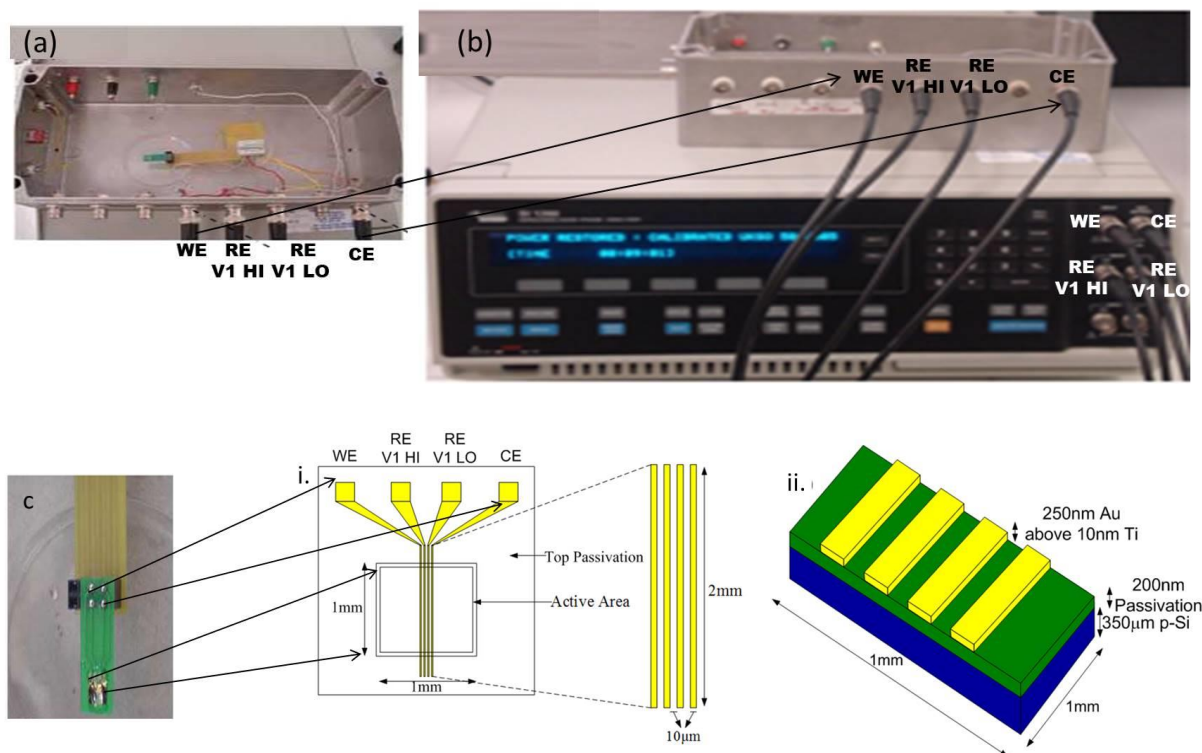
Figure 3.1: Experimental Setup (Kassanos, Demosthenous and Bayford, 2008), (a) shows the sensor connected in the shielding box to prevent electromagnetic interference with measurements; (b) the impedance analyser connected to the shielding box; (c) close up of the sensor and schematic diagrams of the microband electrodes purchased: in (i) the active area of the sensor, i.e. the non-passivated region, is within the square region of 1mmx1mm dimensions. Also shown in (i) are the connections to the impedance analyser. (ii) Not-to-scale representation of the active region of the sensor, not showing the final passivation around it for clarity purposes.

Key:
WE= Working Electrodes
RE V1 HI= Reference Electrodes
RE V1 LO = Reference Electrodes
CE = Counter Electrodes

The Smart software combined with the 1260 analyser forms an advanced electrochemical measurement system which allowed impedance measurement to be taken. An AC signal of 5mV based on literature was applied between the working and counter electrodes. Other signal amplitudes were not applied as from previous studies by (Kassanos *et al.,* 2008), where it was noticed that when AC signals of 5 mV, 10 mV, and 15 mV were applied, the EIS data shared a very similar trend between them, indicating that the bio-impedance of the sensor was unaffected by a change in signal amplitude. For measurement purposes, signals were applied in a wide frequency range between a minimum of 10 Hz and a maximum of 1 MHz but data was plotted and reported between 40 Hz and 40 KHz as this spectrum provided the best

representation of the data. Full range measurements (Appendix 1) appeared noisy at the extremes.

3.3 General procedure for construction of the biosensor

3.3.1. Preparation of the sensor surface

The gold microbands were washed with 5 ml of pure ethanol followed by 5 ml of de-ionized water and 5 ml of PBS to remove any impurities from the surface of the sensor after which it was allowed to dry at room temperature. Since this work made use of full antibodies which cannot be directly immobilised on the gold surface, a SAM was developed on the active area surface of the device. This was achieved by introducing 10 µl of 10 mM DTSP in deionised water, a cleavable homobifunctional linker that anchors on gold surfaces by the dissociative chemisorption of its disulphide group. The cross-linker was left to incubate on the gold surface at room temperature for 1 hour, after which the biosensor was flood washed with de-ionised water, followed by phosphate buffered saline (PBS X1, pH 7.2). Potassium hexacyanoferrate (II) and potassium hexacyanoferrate (III) ($K_4Fe (CN)_6$/$K_3Fe(CN)_6$) (1:1 v/v ratio) was used as redox probe to increase conductivity and also improve the electron transfer rate. This conducting solution was used to acquire all impedance readings.

3.3.2. Immobilisation of protein G

A layer of recombinant protein G was then added. This step allowed protein G to form a layer on the SAM through the interaction between the sulfo-NHS ester and amino groups and on the opposite side would bind to the Fc portion of the antibodies, exposing the antigen binding site to which the antigens would later bind. After incubation with recombinant protein G for 45mins, the biosensor and therefore excess protein G was washed with deionised water followed by PBS. Ethanolamine was used to further saturate any unreacted sulfo-NHS ester group in DTSSP after protein G binding before addition of immunoglobulin G (IgG) antibody (anti-tau/anti-amyloid oligomer).

3.3.3. Immobilisation of the antibodies

Antibody was added and left to incubate on the surface of the sensor for 1 hour. The incubation allowed the antibodies to be captured via their Fc region by the previously immobilised protein G layer. The sensor and therefore excess free antibody was then washed away with deionised water and PBS, completing the construction of the biosensor which was then ready to be tested with the antigen. All biosensors were always incubated in a humidified environment to prevent the evaporation of reagents.

Figure 3.2: **Humidified chamber into which biosensors were incubated at every stage in their construction.**

Water was filled under the yellow part and a sponge was added to soak the liquid and maintain the humid environment.

3.3.4   Equivalent Circuit Modelling

The experimental data were fitted to a simple electrical equivalent circuit in ZVIEW data fitting software. Detailed description of the equivalent circuit and circuit elements (constant phase element (CPE) and Warburg element) may be found in (Section 2.8.2.1).

3.4. Optimization procedure

3.4.1   Investigating the coupling of DTSSP as a SAM layer and protein G on the gold electrode surface

Neubert et al. (2002) and Kassanos et al. (2008) developed a similar sensor using a gold substrate, DTSSP and protein G for the detection of hcG beta. SAM and protein G were coupled to the sensor as described in Section 3.3.1 and Section 3.3.2 respectively.

3.4.2. Optimizing antibody concentration

After coupling of the protein G layer and taking impedance readings, the sensor was washed with 5ml deionised water and 5 ml PBS. The sensor was incubated with 10 µl of

solution of anti-tau in PBS at room temperature (the antigen concentration 1 μg/ml, 10 μg/ml, 100 μg/ml and 125 μg/ml) for 45 minutes each to determine the antibody concentration that saturates protein G layer. The sensor was then washed with 5ml deionised water and 5ml of PBS to get rid of any excess or unbound antibody. After each wash, the impedance reading was taken between 10 Hz and 1MHz at 5 mV. Experiments were repeated atleast three times.

3.4.3. Verification and confirmation of construction of sensor build up.

As mentioned in Section 3.3.1, at each stage of biosensor assembly, impedance measurements were conducted in 10mM, $K_4Fe(CN)_6/K_3Fe(CN)_6$ (1:1 v/v ratio) in PBS pH 7 using SMART software on a Solatron impedance /gain-phase analyser 1260 model by applying a sinusoidal signal of 5mV amplitude between the working and counter electrodes (Figure 3.). This signal was applied across a frequency spectrum ranging from 10 Hz to 1 MHz to produce EIS measurements. EIS parameters Rs (Solution resistance), Rct (charge-transfer resistance or interfacial resistance) and Cp (constant phase element, an equivalent model of double layer capacitance) were generated by fitting the data into the Randles equivalent circuit model using Zview software.

The constructed sensor was confirmed performing cyclic voltammetry. Each layer in the sensor build up after incubation was cycled in 10 mM K4Fe $(CN)_6$/K3Fe $(CN)_6$ (1:1 v/v ratio) in PBS pH 7 between -0.4 V and +0.8 V at a potential of 100 mVs^{-1} and the resulting voltagrams were overlapped. Experiments were repeated 3 times.

Each used electrode was regenerated by cycling the electrode in 2 M sulfuric acid at 100 mVs^{-1} between -0.1 V and +1.74 V.

3.4.4. Verification of the sensitivity of the sensor

The fully built sensor was then subjected to different successive concentrations of 10 μl tau (10^{-2}, 1, 10^2, 10^4, and 10^5) pM for the Tau biosensor and allowed to react for 25 mins at room temperature. Each experiment was repeated at least three times. After each reaction, the biosensor was flood washed with 5 ml of de-ionized water followed by 5 ml of PBS before the impedance was recorded in 10 mM K4Fe $(CN)_6$/K3Fe $(CN)_6$ (1:1 ratio) in PBS pH 7 as described above. EIS parameters R_s (solution resistance), Rct (charge-transfer resistance or interfacial resistance) and Cp (constant phase element, an equivalent model of double-layer capacitance) were generated by fitting the data to the Randles equivalent circuit model using Zview software.

3.4.5. Verification of the specificity of the built sensor

Two fully built sensors were tested for specificity by subjecting one to successive concentrations of BSA (10^{-2}, 1, 10^2, 10^4, and 10^5) pM and the other to successive dilutions of human serum (1:1000, 1:500, 1:20, 1:10, 1:1) and allowed to react for 25 mins. After each reaction the electrode was flood washed and impedance readings taken as described in Section 3.2.3. Experiments were repeated at least three times

3.4.6. Confirmation of specificity and sensitivity of the biosensor

The ability of the biosensor to specifically detect tau was evaluated by subjecting a built sensor to human serum spiked with different concentrations of tau (10^{-2}, 1, 10^2, 10^4, and 10^5) pM and allowed to react for 25 mins. EIS readings were taken after each incubation as described in Section3.2.3.

3.5 Results and Discussion

3.5.1 Coupling chemistry

The biosensor for detection of tau and amyloid oligomer was constructed in a stepwise manner, including coating, incubation and washing steps. The small surface area of the active area made it possible to use very small incubation volumes. The formation of SAM and coupling of protein G were not monitored directly but was confirmed through final antigen capture verified by EIS and confirmed by cyclic voltammetry. The assembly of each layer of the biosensor surface was confirmed by EIS measurements. Impedance measurements were performed at each stage of the layer-by-layer assembly in 10 mM K_4Fe $(CN)_6$/$K_3Fe(CN)_6$ (1:1 ratio) in PBS pH 7 over a frequency range of 10 Hz to 1 MHz; however, as mentioned earlier in this report only data within the range of 40 Hz to 40 kHz is reported as this spectrum gave the best representation of the data viz. semi-circular shapes which can be fitted into a Randles equivalent circuit, a useful tool in interpreting EIS data which accounts for the resistive and capacitive processes at different frequencies. The EIS data from a representative biosensor was presented as Nyquist plots (Fig. 3.3A). Fitting the data presented in Fig. 3.3A to the Randles equivalent circuit model, demonstrated that the interfacial charge-transfer resistance (Rct) changed after each layer was deposited on the gold sensor surface (Fig. 3.3B), namely bare gold, DTSSP or SAM, protein G, ethanolamine and anti-tau antibody, indicating the successful construction of the biosensor.
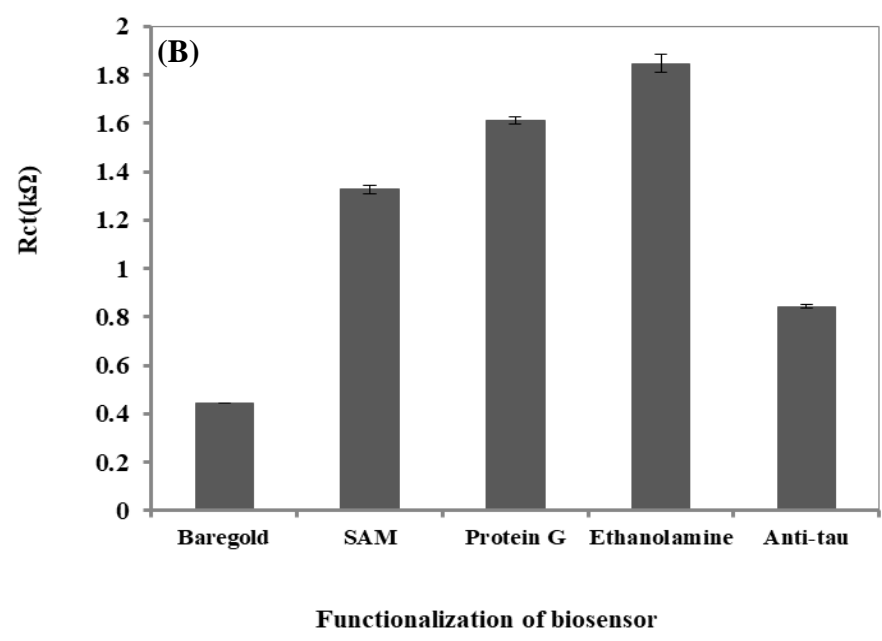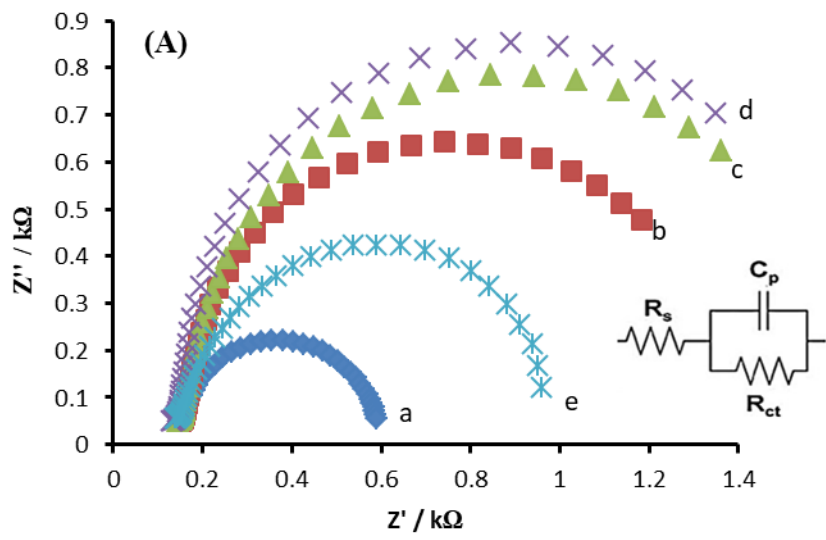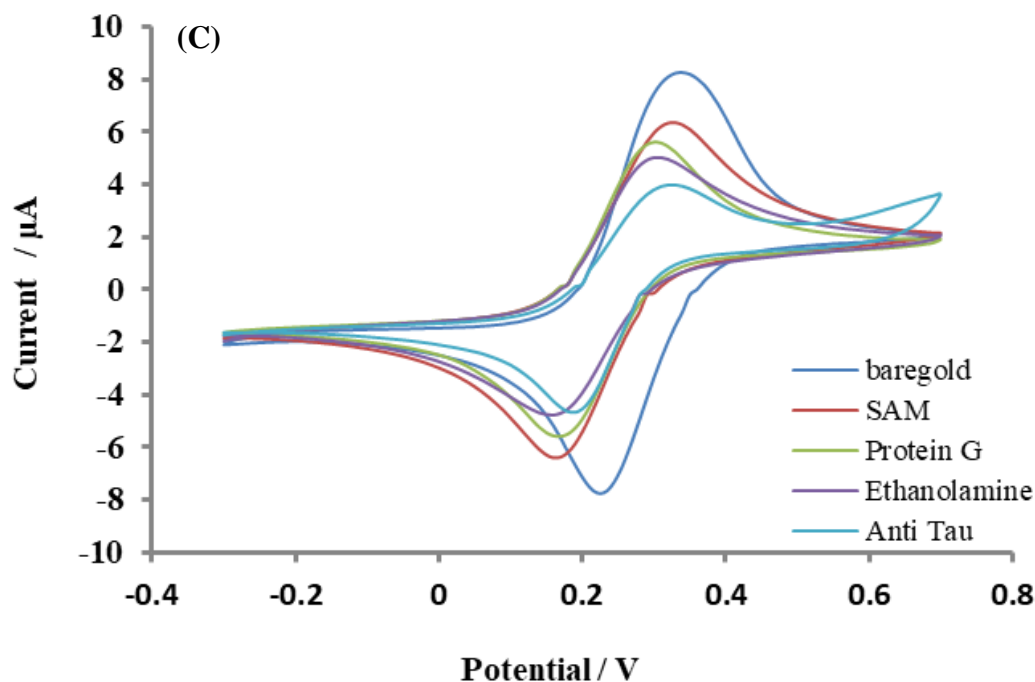
Figure 3.3: **Construction and assembly of the biosensor** (Wang *et al.*, 2017). (A) is the layer-by-layer development of the biosensor verified by electrochemical impedance spectroscopy (EIS). The imaginary component of impedance (Z″) was plotted against the real component of impedance (Z′) in Nyquist plots. Impedance data were recorded after each stage of construction: (a) bare gold, (b) DTSSP or SAM, (c) protein G, (d) ethanolamine and (e) anti-tau antibody, in 10 mM $K_4Fe\,(CN)_6/K_3Fe\,(CN)_6$ (1:1 v/v ratio) in PBS pH 7 over a frequency range from 40 Hz-40 kHz. Insert shows the Randles equivalent circuit model which was used to fit the data. R_s=solution resistance, Rct=charge-transfer resistance and Cp=constant phase element. (B) The interfacial charge-transfer resistance (Rct) variance across the functionalization steps, presented as mean ± SEM, n=3 (number of replicates) (C) Representation of the characterization of layer-by-layer construction of the biosensor verified by cyclic voltammetry (CV) as described in Section 3.4.3.

EIS is one of the most powerful electroanalytical techniques frequently used in characterizing materials and surface interfaces (Carneiro et al. 2017). The advantage of EIS over other electrochemical techniques is that it requires only a small AC voltage signal , which makes it possible to analyse biological molecules in an unaltered state by providing responses as simplified current-potential characteristics (Carneiro *et al.*, 2017). The impedance spectra include a semicircle portion and linear portion, which can be used to describe the interface properties of the electrode for each immobilized step. In this work, only the semi-circle portion is reported for a clearer view of the results. The portion of the semicircle at higher frequencies corresponds to the electron-transfer resistance (R_S and Rct) which controls the electron transfer kinetics of the redox process at the electrode interface. A significant change in the impedance spectra can be observed after each modification of the

gold electrode with DTSSP, protein G, ethanolamine, and anti tau in comparison with the bare gold electrode as shown on Fig. 3.3A. The SAM of DTSSP formed a layer that blocked the surface of the gold electrode increasing the charge-transfer resistance and consequently a semi-circle in the impedance spectra was observed. Upon addition of the protein G layer and blocking with ethanolamine, the diameter of the semicircle is significantly enlarged due to the generation of an insulating protein layer on the modified electrode surface which hindered the electron transfer. These results also proved that the protein G and ethanolamine were successfully immobilized on the modified electrode surface. Upon addition of the anti-tau unto the gold/ SAM/ protein G/ ethanolamine modified layer, a significant contrasting decrease in electron transfer resistance was observed as displayed by a significant decrease in the diameter of the semi-circle, It has been reported that highly charged molecules, with high conductivity improve the electron transfer rate (Correia dos Santos *et al.*, 2003; Guan *et al.*, 2019), hence this could be resulting from the effect of the strong positive charge on anti-tau. The pattern of variation of the different layers in the construction of the biosensor is consistent with the results attained by cyclic voltammetry (Fig. 3.3C).

3.5.2   Optimization of antibody concentration

It is important to coat the sensor surface with sufficient amount of antibody that will produce a maximum sensor response. Too small an amount of antibody to coat the sensor surface will result in a diminished sensor response and so will too much antibody, as an excessive surface density of antibody can result in diminished antigen-binding efficiency (Spitznagel and Clark, 1993). To determine the optimal antibody concentration for immobilization, the sensor was coated with different concentrations of monoclonal antibody. This resulted in the sensor exhibiting different antibody densities on their surface. After incubation with the antigen, impedance measurements were presented as Nyquist plots where the imaginary component of impedance (Z'') was plotted against the real component of impedance (Z') as shown on Fig. 3.4.
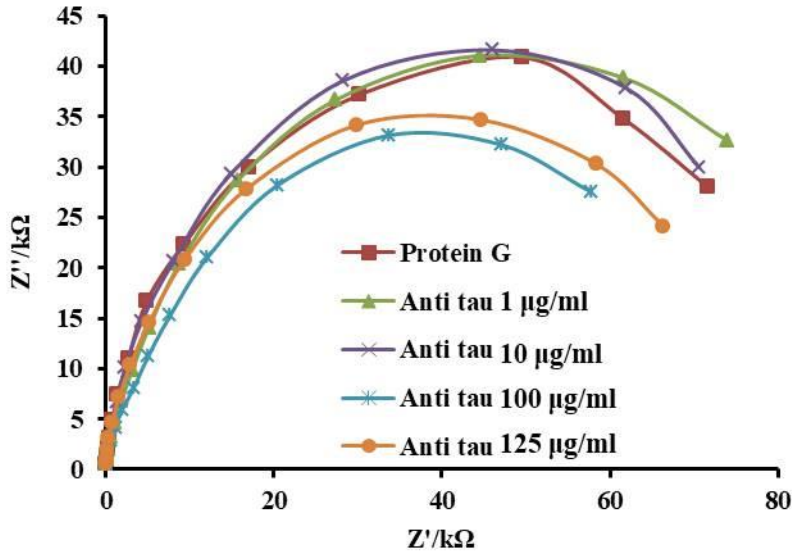
Figure 3.4: EIS analysis of the biosensor upon cumulative incubations with anti tau concentrations (ug/ml) (1, 10, 100, 125) in PBS., followed by rinsing with dH2O and PBS, in 10 mM K4Fe(CN)6/K3Fe(CN)6 (1:1 ratio) in PBS pH 7 over a frequency range from 10Hz1MHz. Impedance measurements were presented as Nyquist plots where the imaginary component of impedance (Z″) was plotted against the real component of impedance (Z′)

One-way analysis of variance with post hoc analysis between protein G alone and anti tau concentrations (1, 10, 100, 125 μg/ml) showed that there was no significant difference (P>0.05) in signal response between the protein G and antitau concentrations of 1 and 10 μg/ml, but a significant difference (P< 0.05) was seen with antitau concentrations of 100 and 125μg/ml. However, the post hoc analysis further revealed no signiant difference (P>0.05) between 100 and 125μg/ml concentrations of antitau. Therefore, the antibody concentration of 100 μg/ml was seen as the concentration that saturated the sensor surface and yielded the maximum impedance response.

3.5.3   Sensitivity and specificity

3.5.3.1 Detection of different concentrations of tau

The EIS data from a representative sensor is presented as Nyquist plots in Figure 3.5. EIS parameters as shown in Table 3.1, Rs (solution resistance), Rct (charge-transfer resistance or interfacial resistance) and Cp (constant phase element, an equivalent model of double-layer capacitance) were generated by fitting the data to the Randles equivalent circuit model using Zview software. Rct was chosen as the parameter to evaluate the binding of tau to the biosensors in the experiments as the system is based on the Faradic impedance, measured in the presence of redox mediators (Rushworth *et al.*, 2014). Rct values increased upon addition of increasing concentrations of tau (from 10^{-2} to 10^5 pM), as demonstrated by

the increasing height and diameter of the semi-circular Nyquist traces (Figure 3.5), which correspond to increased capacitance and resistance of the sensor surface respectively.
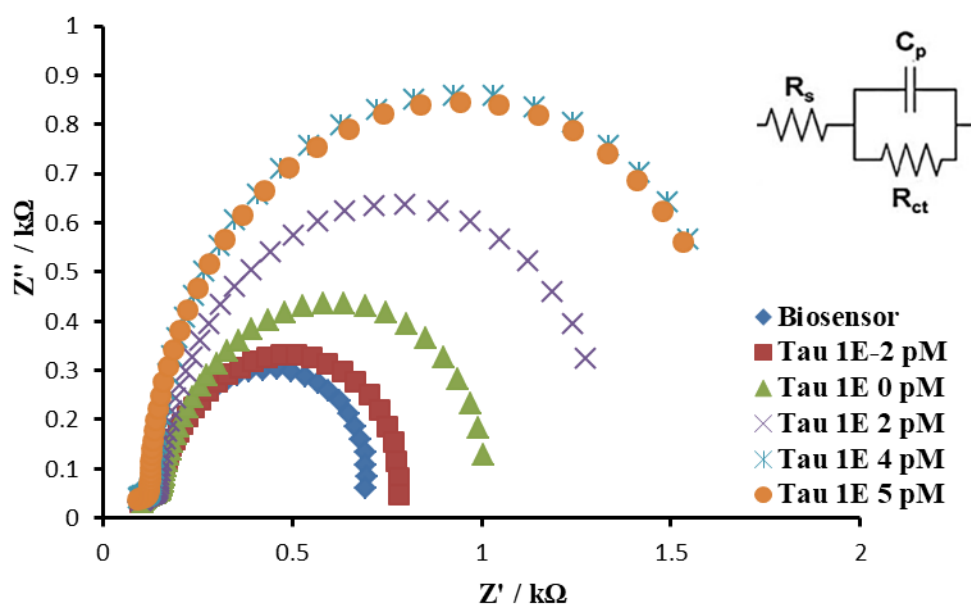
Figure 3.5: **Biosensor response to different concentrations of tau as measured by EIS**. EIS analysis of the biosensor upon cumulative incubations with tau (concentrations from 10^{-2} to 10^5 M) in PBS followed by rinsing with dH_2O and PBS, in 10 mM $K_4Fe(CN)_6/K_3Fe(CN)_6$ (1:1 ratio) in PBS pH 7 over a frequency range from 10Hz-1MHz. Impedance measurements were presented as Nyquist plots where the imaginary component of impedance (Z″) was plotted against the real component of impedance (Z′). Inset shows a Randles equivalent circuit model used to fit the data, where Rs=solution resistance, Rct=charge-transfer resistance and Cp=constant phase element.

There was a trend of increasing interfacial resistance after tau bond to the biosensor as represented by increasing diameter of the semi-circle with increasing concentration of tau from 10^{-2} to 10^4 pM; no further change was seen with increasing concentration of tau upto (10^5pM). This implies that the interfacial surface was saturated with tau. The limit of detection (LOD) calculated according to IUPAC (International Union of Pure and Applied Chemistry) was 0.2 pM (McNaught and Wilkinson, 1997)

Table 3.1: **EIS parameters obtained from fitting the Nyquist plots shown in Figure 3..5 to the Randles circuit model (Alternative presentation of data with standard error in Appendix 3)**

Electrode	Rs (Ω)	Error	Cp (F)	Error	Rct(Ω)	Error
Biosensor	130.6	1.9303	1.60E-07	2.87E-09	592.3	14.328
tau 10^{-2} pM	139.2	2.0078	1.60E-07	2.82E-09	647.1	16.93
tau 1 pM	150	2.153	1.57E-07	2.64E-09	844.1	24.463
tau 10^2 pM	142.8	1.7558	1.55E-07	1.95E-09	1266	39.359
tau 10^{-4} pM	125.6	1.4714	1.29E-07	1.26E-09	1789	53.002
tau 10-5 pM	119	1.1154	1.23E-07	9.28E-10	1739	37.808

3.5.3.2 Specificity of the biosensor

The specificity of the sensor was tested by incubations with bovine serum albumin (BSA), a commonly used plasma protein standard. Albumin is reportedly the most abundant protein component in serum and CSF. The EIS data from a representative sensor is presented as Nyquist plots in Figure 3.6.
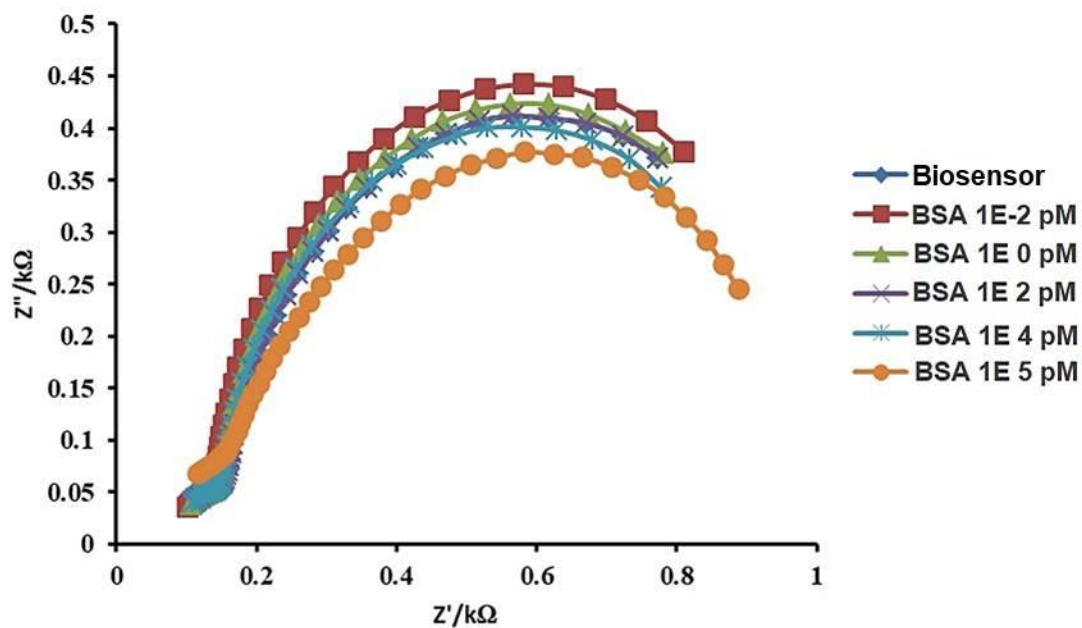
Figure 3.6: **Biosensor response to different concentrations of BSA as measured by EIS.** EIS analysis of the biosensor upon cumulative incubations with BSA (concentrations from

10^{-2} to 10^5) pM in PBS followed by rinsing with dH$_2$O and PBS, in 10 mM K$_4$Fe(CN)$_6$/K$_3$Fe(CN)$_6$ (1:1 ratio) in PBS pH 7 over a frequency range from 10Hz-1MHz. Impedance measurements were presented as Nyquist plots where the imaginary component of impedance (Z'') was plotted against the real component of impedance (Z').

From data shown in Appendix 4, the difference in detection by the sensor of the different concentrations of BSA ($P > 0.05$), n= 3, one-way analysis of variance revealed that there was no significant difference in the changes observed with increasing concentrations of BSA from 10^{-2} to 10^5 pM. This implied that the biosensor is unresponsive to BSA incubation over the range of concentrations from 10^{-2} to 10^5 pM.

To further confirm the unresponsiveness of the sensor to BSA, the percentage change in interfacial charge resistance of the different BSA concentrations measured are compared with reference to the percentage change of the interfacial charge resistance of the lowest concentration of tau (10^{-2} pM) detected by the sensor. Less than 1% change in Rct at 10^5 pM (See Appendix 4 for data set) of BSA was observed compared to more than 46% change in Rct at 10^{-2} pM of tau (see Appendix 3 for data set) as shown on Figure 3.7.
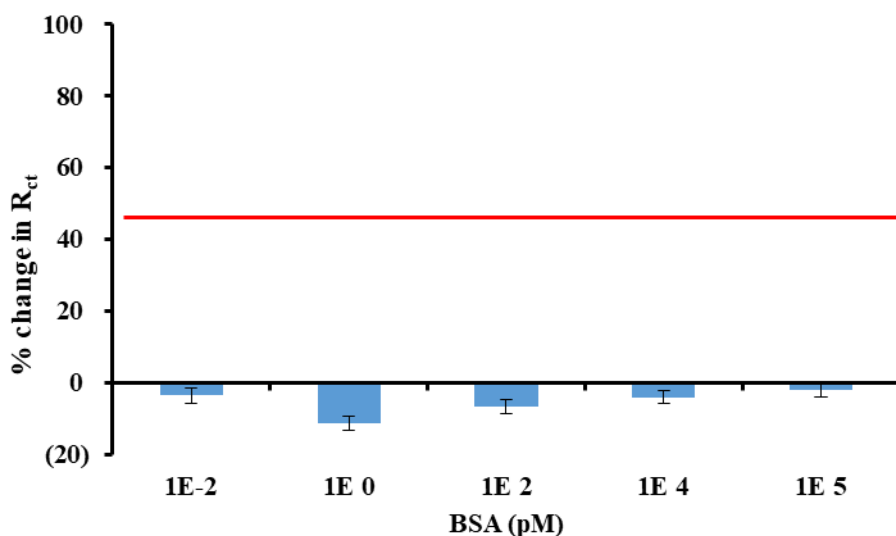
Figure 3.7: Influence of increasing concentrations of bovine serum albumin (BSA) on the Rct of the biosensor response in PBS compared to Rct value of the lowest concentration of tau.

Less than 1% change in Rct at 10^5 pM of BSA comparing to more than 46% change in Rct at 10^{-2} pM of tau. The horizontal line shows the specific response to 10^{-2} pM of tau. Data is ploted as mean ± SEM for n =3

3.5.4 Calibration curves for tau biosensor

The semi-circle spectra from tau biosensor like in Fig. 3.5 and incubation of the sensor with BSA like in Figure 3.7 were fitted into a Randles equivalent circuit model and the Rct values were generated. The Average Rct values from three independent experiments (See Appendix 3 and 4) were calculated and ploted against the concentrations of tau and BSA (10^{-2} to 10^{5}) pM as shown on Figure 3.8 to generate a standard curve for quantification of tau

The Biosensor response to tau was further quantified by normalising the Rct values from the impedance data (Appendix 3). The normalisation equation used was

$$\frac{Rct - Rct0}{Rct0} \qquad (1)$$

Where Rct0 represents the Rct value of full biosensor with anti-tau antibody deposition.
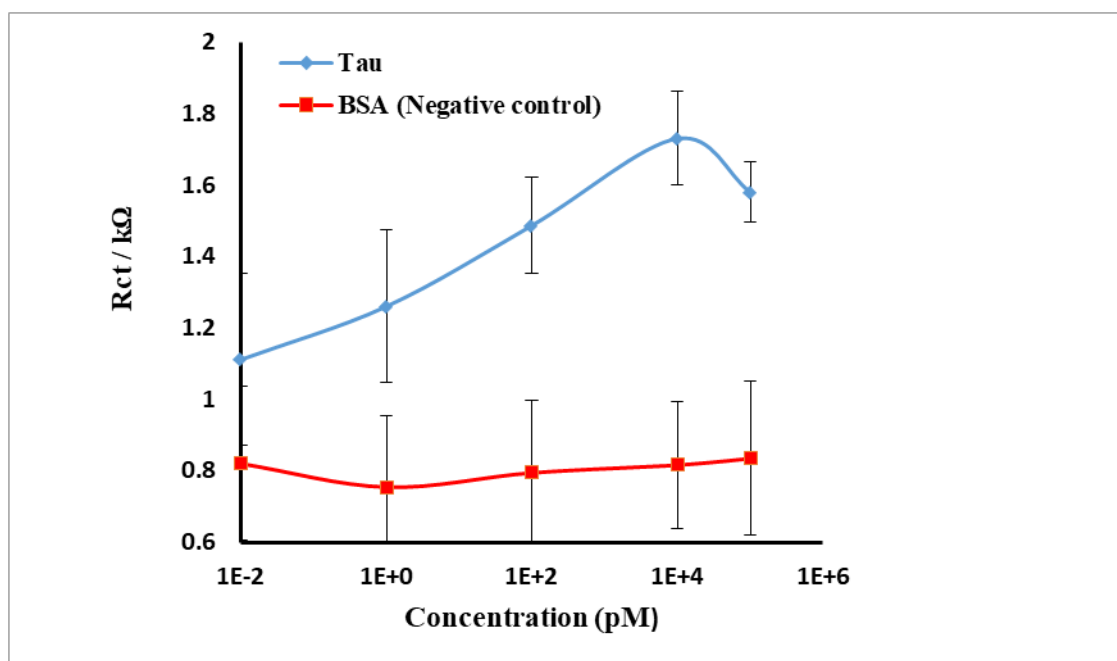
Figure 3.8: Calibration curves of tau binding to biosensor.

The response of biosensor after cumulative incubation with different concentrations of tau or BSA in PBS containing 10 mM $K_4Fe(CN)_6/K_3Fe(CN)_6$ (1:1 ratio) pH 7 was determined by EIS. The charge-transfer resistance (Rct) values of the anti-tau antibody interfaces following incubation with tau or BSA were determined by fitting the data to the Randles circuit model using Zview software. These Rct values were compared statistically for tau and BSA using a two tails t-test assuming unequal variances, *P<0.05. Data is ploted as mean ± SEM for n= 3 (number of replicates).
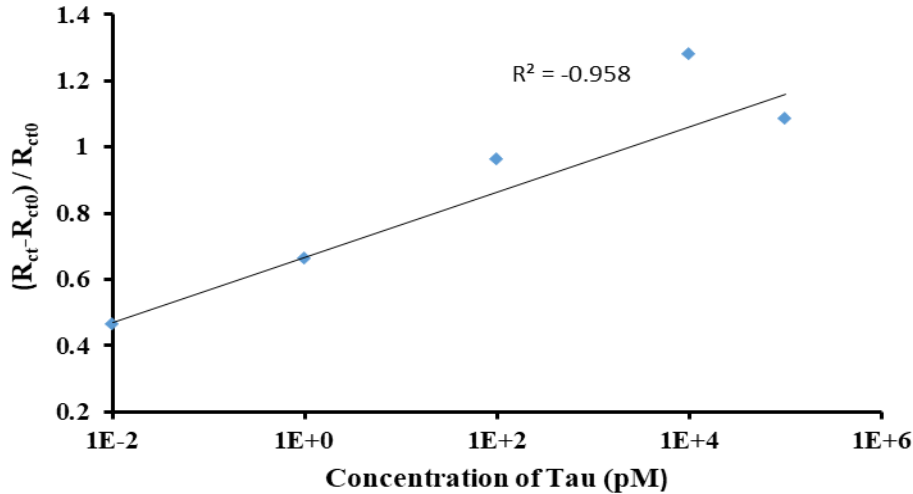
Figure 3.9: shows normalised data, a plot of percentage of Rct change of equilibrated biosensor (Rct0) after incubation with increasing concentrations of tau.

From Fig. 3.8 and Fig. 3.9, there was a trend of increasing interfacial resistance after tau binding to the biosensor, while no significant response was detected following BSA incubation (Fig 3.6 and Fig 3.8). The Rct value for tau binding reached a plateau with no further increase at the tau concentration of 10^4 pM which meant the biosensor interfacial surface was saturated. (Fig. 3.9)

3.5.5 Confirmation of specificity and sensitivity of biosensor using human serum (HS) spiked with tau

Furthermore investigations looked at the ability of the biosensor to detect tau in human serum (HS) to confirm the sensitivity and selectivity of the tau biosensor as described in Section 3.4.6. The trend of the biosensor response to tau in HS in Nyquist plots (Fig. 3.10A) was similar to that in Fig. 3.5. displayed for tau only, indicating that the biosensor is sensitive and specific enough to recognize tau down to a concentration of 0.01 pM (10^{-2} pM) in HS. The sensor was unresponsive to human serum at a range of dilutions in PBS implying that components of serum do not interfer with tau measurements (Fig. 3.10B). Although the percentage of Rct change versus full biosensor (Rct0) was lower than that for tau only, the relative increase (3 fold) was similar between the tau concentration range of 10^{-2} and 10^4 pM for tau only (0.6-1.6) (Fig. 3.10) and tau in a dilution of 1:1 HS (0.08-0.29) (Fig.3.10C), indicating that HS did not affect the specificity and sensitivity of the tau assay. The low change of Rct may be due to the small size of the electrode and non-specific interference of human serum to the biosensor.

(a)
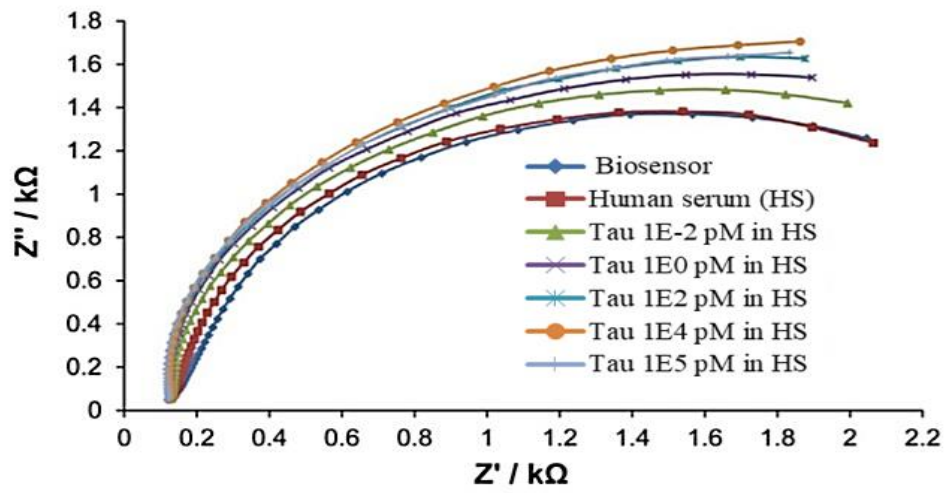
(b)
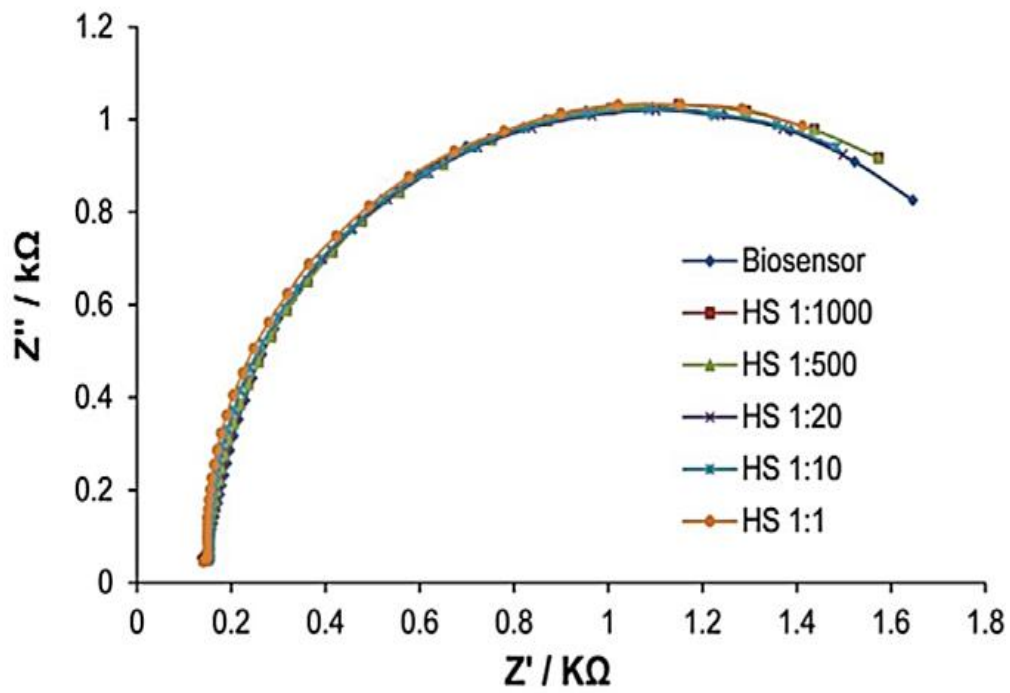
(c)
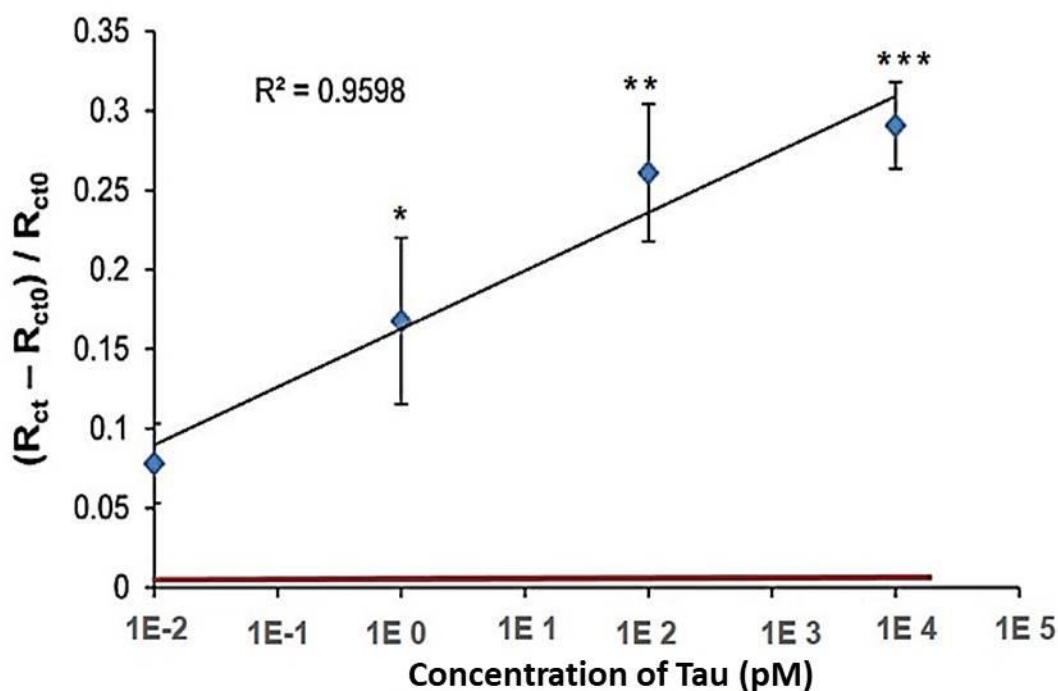
Figure 3.10: **Biosensor response to (A) different concentrations of tau spiked in human serum (HS) and (B) HS in PBS with different dilution factors, as measured by EIS.** EIS analysis of biosensor upon cumulative incubations with tau (concentrations from 10^{-2} to 10^{5} M) spiked in HS followed by rinsing with dH_2O and PBS, in 10 mM $K_4Fe(CN)_6/K_3Fe(CN)_6$ (1:1 ratio) in PBS pH 7 over a frequency range from 40 Hz-40 kHz. Impedance measurements were presented as Nyquist plots where the imaginary component of impedance (Z'') was plotted against the real component of impedance (Z'). (C) Calibration curves of tau in HS binding to biosensor.

The percentage of Rct change versus full biosensor (Rct0) after cumulative incubation with different concentrations of tau in HS was plot as mean $\pm$ SEM for n= 3 (number of replicates). The charge-transfer resistance (Rct) values of the anti-tau antibody interfaces following incubation with tau were determined by fitting the data to the Randles circuit model using Zview software. These Rct values were compared statistically for tau and HS only using two tails t-test assuming unequal variances, $*p<0.05$, $**p<0.005$, $***p<0.001$ respectively. The horizontal red line shows the biosensor response to HS only.

3.6   Discussion

The appropriate coupling of biomolecules on the surface of biosensors is crucial for their successful construction to detect target molecules. The biosensor developed in this project is on gold microband electrodes, using antibodies (anti-tau 39E10) for the specific capture of

full-length tau (tau441). The first step in the construction of this biosensor involves the coupling of crosslinker to form a SAM layer; this is an important step, as direct immobilisation of antibodies on a gold surface does not guarantee adequate binding, which could result in an unsuccessful biosensor. The first part of the set of experiments in this project looked at the use of DTSSP SAM as a cross-linker between the tau antibody and the gold surface. This was then modified to accommodate an extra layer of protein G on the SAM surface to enhance the antibody orientation. The SAM attached to the gold surface by means of a thiol bond exposing the amine reactive sulfo-NHS ester which bound protein G (Fig. 3.3A). Subsequently, the unreacted NHS sites were blocked with ethanolamine. Anti-tau antibodies were immobilized via N-terminal to produce Ab-Au surfaces. The formation of the SAM/ SAM-pr G/ SAM-pr G - eth/ layer on the gold surface was not monitored directly, but their suitability to be used for this application was assessed through the antigen capture reaction that was recorded through the change in impedance. However, the addition of anti-tau to the modified gold surface did not result in the expected increase in impedance (Fig. 3.3A). As explained previously, impedance is equal to the resistance in a circuit. In this biosensor, the biofilm on the electrode surface is believed to act as a resistor, hence impeding the flow of ions between electrodes upon injecting a voltage, leading to an increase in impedance on the addition of each layer. The addition of anti-tau lead to a drop in impedance rather than an increase, suggesting that this extra layer might have facilitated the flow of ions rather than impeding it. Another explanation could be that not enough antibodies were bound on the surface, but this is contradicted by the impedance response on testing the sensor with tau, which implies that this result might be due to the strong antibody-antigen interaction, and not simply the addition of a layer on the surface of the sensor.

Cyclic Voltammetry (CV) was used to verify the surface modification steps for the preparation of the Ab-Au surface section 3.4.3. CV confirmed the successful surface modification; Fig. 3.3C shows CV of the bare gold electrode with the characteristic oxidation/reduction peaks for the $[Fe(CN)_6]^{3-/4-}$ redox probe. The successful modification of the Au surface resulted in the reduced electron transfer kinetics associated with the $[Fe(CN)_6]^{3-/4-}$ redox probe and decreased current in CV. The final Ab-Au surface was characterized with a low current due to the successful surface modifications which effectively insulated the electrode surface and reduced the interfacial electron transfer between the $[Fe(CN)_6]^{3-/4-}$ redox and electrode surface. Thus, both CV and EIS indicate the successful surface modification and immobilization of anti-tau antibody on the Au surface (Ab-Au). The increase in interfacial Rct observed in EIS, due to surface modification, was also evidenced

as a dramatic loss of current in CV. Hence, the current (in CV) associated with $[Fe(CN)_6]^{3-/4-}$ redox probe was reduced due to the surface functionalization of the Au electrode.

Experiments carried out on the specificity and sensitivity (Sections 3.4.4 4) of the biosensors constructed with antibodies immobilised on the SAM layer was the next focus of this project. Monitoring of binding of tau441 protein was accomplished by incubating Ab-Au surfaces in tau441 protein in solution, and subsequently measuring EIS. Figure 3.8 shows that as the concentration of tau increased from 10^{-2} to 10^4 pM, there was an increase in the impedance ratio, but a further increase in tau concentration resulted in a slight drop in impedance. This graph indicated that the maximum concentration of tau that could be detected for these biosensors was 10^4 pM. The drop in impedance at high tau concentration in this case can be considered negliglible. It is expected that as the antibodies get saturated, no further antigen will bind, thus resulting in the impedance change remaining constant, and forming a plateau as can be considered to be the case with this sensor. The calculated LOD of the unmodified sensor at 0.2 pM compared to other biosensors for tau protein is lower, for example in the study by Tao *et al.,* 2019 reported LoD for the aptasensor for tau at 0.7 pm, a value over three times higher than that reported in this project.

The selectivity of the electrochemical biosensor was tested with the bovine serum albumin (BSA) (Fig.3.6), a plasma protein standard, which may be found at high concentrations in biological liquid, such as plasma. In addition, albumin is the most abundant protein in the complex biological matrix, such as cerebrospinal fluid (CSF) and serum. After incubation of the constructed sensor with BSA concentrations (10^{-2}, 1, 10^{-2}, 10^4, and 10^5) pM, an insignificant change in impedance was observed with increasing concentration of BSA. This data indicates that the electrochemical biosensor was selective for tau441 over BSA, which is an important feature of future biosensors with application in complex biological fluids like plasma, serum or CSF. To further test and confirm selectivity, Fig. 3.10A shows the constructed sensor in the presence of tau spiked in HS and Fig 3.10B shows the constructed sensor in the presence of a range of dilutions of HS without tau. The sensor exposed to HS alone exhibited no major impedance change but the other sensor was responsive to tau spiked in HS, however with lower Rct values compared to tau in PBS and this may be due to interference by HS or the small size of the electrode. This project involved the construction of biosensors on commercially available gold electrodes of a tetrapolar configuration. The design of the electrodes in this system could have contributed to some of the variations noticed. According to Grimnes and Martinsen, (2015), the gap between the

electrodes can affect impedance measurement, as the wider the gap, the deeper the measuring depth. The sensitive region of the biosensor is also governed by physical arrangement of electrodes as well as their geometry. The electrodes used in this study being bought off the shelf, are not optimal for the specific purpose of tau detection. Fabrication of better electrode designs offering the maximum sensitivity in the region of antibody-antigen interaction has been explored and currently there is progress with such electrodes at the research group at Middlesex university as part of another project. Designing these electrodes requires the use of specialised software that would take into consideration the dimensions of the biomolecules to be immobilised on the surface of the biosensor to determine the appropriate electrode dimensions and spacing required.

The surface of one of the gold microband electrodes being of 1mm length within the active area, and $10\mu m$ (0.01mm) width gives a total surface area of 0.01mm2 or $10,000nm^2$. The estimated height of an antibody is 15nm, width 4nm, and thickness of 3.5 nm, suggesting that enough antibodies should be bound on the surface of the electrode. However steric hindrance might be a problem, as well as random orientation of the antibodies, such that despite being immobilised they would not be binding effectively to the antigen. The large standard errors on Fig.3.8 and Fig. 3.10 indicate variation between similarly constructed biosensors suggesting that reproducibility and stability are a major problem in their construction. Possibly because the electrodes were regenerated and reused, the surface of the electrodes may have had residues on them from not being properly cleaned. Also, the conditions under which the electrodes were stored in the laboratory after regeneration could not be trusted to maintain the purity of the cleaned electrode surface. However, as the sensors were washed after each set, the impedance profile seem to get more stable, maintaining that stability.

Due to a limited number of electrodes and as a result of no more of these electrodes being fabricated by the company, further work was not done to obtain data to perform specificity and sensitivity analysis by testing CSF samples, an outcome that would have suggested the degree of selectivity and sensitivity for this sensor as well as possible enhancements. Since the ultimate aim of this work is to fabricate biosensors that could be commercialised, the best way to move forward with this work is to use new electrodes (in the process of being fabricated and tested at Middlesex University). By doing so, the biochemistry techniques used on the biosensor's surface would be much more reliable and could be easily controlled and investigated.

Chapter 4

Design And Development of ELISA For Measuring Tau And Confirmation of Tau Detection By Western Blotting

4.   Summary

In this Chapter, the ELISA laboratory based method that was developed to determine the interaction between tau antibody (39E10) and full length tau (2N4R), employed by the antibody and protein pair used for EIS in the previous chapter is described to compare with the results from the novel biosensor. In addition the effect of the different reagents; capture antibody, detector antibody and substrate used for colour generation, were investigated for optimal detection and quantification of tau in different matrices: phosphate buffer saline (PBS), 5% human serum(HS) and cerebrospinal fluid (CSF). The assay range of the ELISA was determined to be 1pM to 10^5 pM and the limit of detection (LOD) 10^4 pM for tau in PBS and 5% human serum. In Addition to the ELISA assay, Western blot analysis was used to confirm the detection of full-length Tau in PBS and 5% Human serum as further described this Chapter. The final section of this chapter compares the ELISA laboratory based method with the tetrapolar EIS point of care method as well as the results achieved by both methods.

4.1 Introduction

In this project an ELISA was developed to specifically detect the most representative full-length tau 2N4R isoform using 39E10, a monoclonal antibody which was raised against full-length human tau and targets amino acid sequence 189 – 195 on full length tau, an epitope common to all isoforms of tau. As seen in chapter three, the biosensor is able to detect levels of tau down to the 10^{-2} pM range. Therefore, in order to compare levels achieved with ELISA, this project endeavoured to design the ELISA to achieve as low LoD as possible so that useful comparisons could be made.

Biosensor signals are prone to electromagnetic interferences such as cable shields and lengths, applied frequency, effects of temperature on the ionic concentration of analyte /electrolyte under test and poor connection between electrodes and improper electrolyte contact with electrodes (Wang, 2006; Grieshaber *et al.*, 2008; Karunakaran, Rajkumar and Bhargava, 2015) . However, levels determined by ELISA are not influenced by these factors.

Therefore, the purpose of this study is to develop an ELISA to confirm that changes in tau concentrations between individuals, as determined by the biosensor, are due to specific

changes in tau concentration and not due to other variables which might cause electromagnetic interference such as those mentioned above

The aims of this chapter are:

- To use 39E10, the antibody used to develop the bioreceptor component of biosensor, as capture antibody for the development of a sandwich ELISA assay to detect full-length tau (also known as 2N4R the most representative isoform of tau protein) protein levels in different matrices such as PBS, human serum and cerebrospinal fluid.
- Use Western Blot analysis to confirm detection of full length tau.
- Compare ELISA and EIS methods and results

4.2   Materials and Methods

4.2.1   Materials

All solutions were prepared using deionised water purified with milli-Q 50 ultrapure water system (Millipore,UK). Blocking buffer with stabiliser was purchased from Rockland UK. 100% methanol, phosphate buffer saline (PBS) was supplied by Thermos Fisher scientific UK. Semi-skimmed milk, Nunc 96 well plates, tween20 and 3,3′,5,5′-Tetramethylbenzidine (TMB) Liquid Substrate were obtained from Sigma Aldrich UK. Human serum from normal individuals was purchased from BBI Solutions UK. Tau antibody (39E10), human tau 441 were purchased from Biolegend. Streptavidin HRP conjugate, goat anti-mouse conjugated HRP and mouse biotinylated tau antibody were supplied by Abcam. For Western blotting, 10X running buffer, enhanced chemiluminescent (ECL) substrate, Trans-blot Tubor transfer system, transfer pack mini size, Premade gels, 2X laemmli sample buffer and protein ladder were purchased from Biorad. 2M sulphuric acid was made in the Lab. Absorbance readings were obtained using a microplate reader from BMG-LABTECH. Chemiluminescence was acquired using Licor odyssey Fc detection system from Licor bioscience Ltd UK. CSF samples were kindly donated by Professor Henrik Zetterberg UK dementia research institute at UCL.

4.1.2   General Sandwich ELISA method.

Nunc 96 well plates were coated with various concentrations of capture antibody (39E10) in carbonate / bicarbonate buffer (pH 9.6), covered with an adhesive plastic and incubated overnight at 4°C. The coating solution was removed and the plate washed three times with 200 μl phosphate buffer saline (PBS) containing 0.1% tween20 (0.1%PBST).

Excess solution from the washes was removed by blotting the plate on paper towel. Any remaining protein-binding sites in the coated wells were blocked by incubating with 200 µl blocking buffer in each well for 2 hours at room temperature after which the plate was washed as mentioned above. 100 µl of diluted samples of tau were added to each well in duplicates and incubated for 1 hour. This step was followed by a washing as described above. 100 µl of diluted biotinylated tau antibody was added to each well and incubated for 2 hours at room temperature followed by further washing to remove any unbound biotinylated antibody. 100 µl of Streptavidin HRP was then added to each well and allowed to react for 1hour at room temperature. After further washing, 100 µl of TMB was added to the wells for 30mins in the dark to allow colour development. Further colour development was stopped by the addition of 50µl 2M sulphuric acid. Using a microplate reader, absorbance of the wells was captured at a wavelength of 450nm. All reagent concentrations / dilutions were made up in blocking buffer. A standard curve was prepared from the serial dilutions with concentration on the X axis (log scale) vs absorbance on the Y axis (linear).

KEY:

Capture antibody	TMB (3,3', 5,5' Tetramethylbenzidine) Substrate
Biotinylated Tau antibody	Non-specific binding block
Tau protein	TMB precipitate
Streptavidin HRP(Horseradish peroxidase) conjugated	
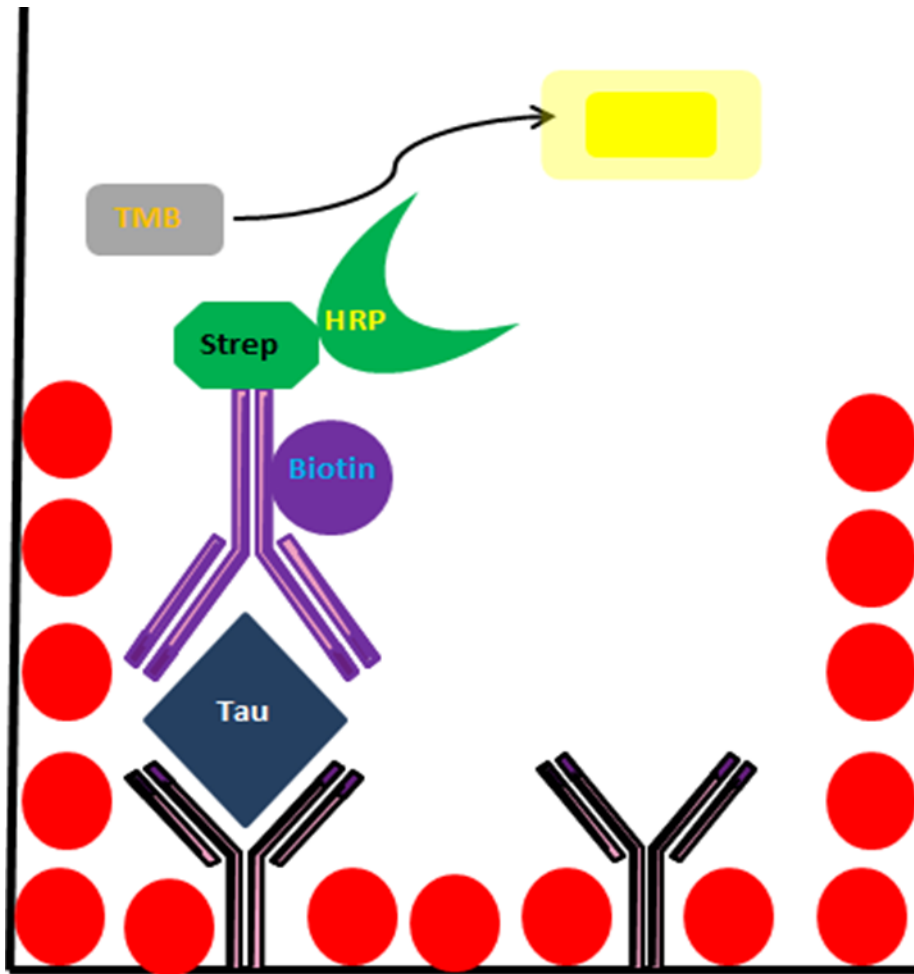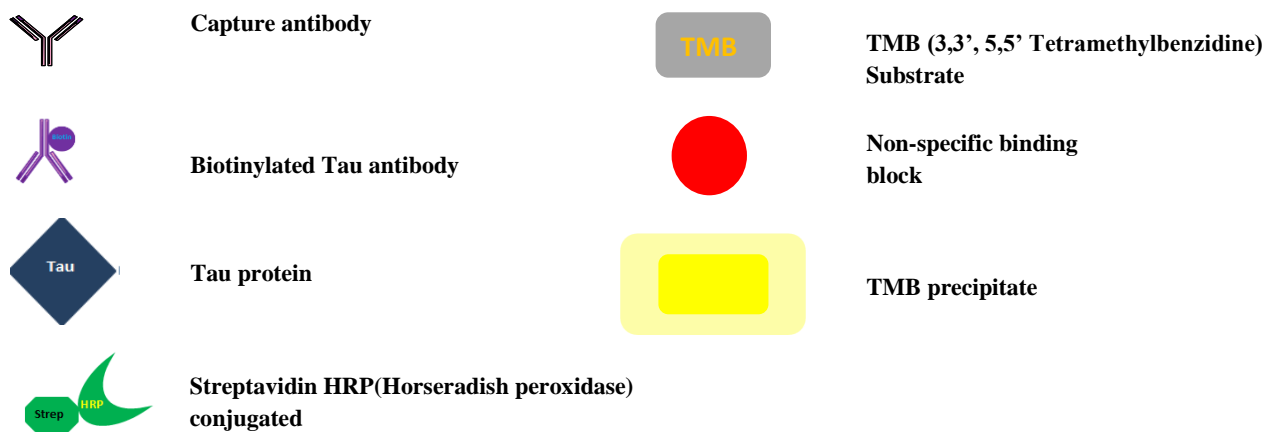
Figure 4.1 Illustration of in-house sandwich ELISA assay for the detection of tau.

The TMB substrate is oxidised by hydrogen peroxide in the presence of HRP on the enzyme-labelled streptavidin and a coloured product (signal) is formed which is read by a plate reader. The signal is directly proportional to the amount of Tau present and unknown samples can be interpolated through use of the standard curve measurements.

4.1.2.1 Optimization of Capture Antibody (39E10)

The effect of capture antibody (CA) (39E10) concentration on the assay was investigated by coating plates with 0μg/ml, 0.25μg/ml, 0.5μg/ml, 1μg/ml and 2μg/ml concentrations. A Tau standard (10^5pM) was used for the ELISA prepared in PBS. PBS only (0pM Tau) was used as a control. Microtitre plates were coated overnight with the different concentrations of 39E10 applied to the microwell plate in duplicates. The effect of these different capture antibody concentrations was investigated on zero (0 pM) Tau and Tau at high concentration (10^5pM). The Assay was further developed as described in section 4.1.2 2.

4.1.2.2 Optimization of Detector antibody (Biotinylated Anti-tau)

The effect of biotinylated detector antibody concentration for the detection of full length tau 441 was achieved by the use of different dilutions (1:1000 to 1:10000) of biotinylated tau antibody in the assay using 0.5 μg/ml of capture antibody, zero (0 pM) tau and high concentration (10^5pM) of tau. The assay ran in duplicates, was further developed as described in section 4.1.2

4.1.2.3 Optimisation of Standard curve range

Optimisation of the standard curve range for measuring tau was performed by using standards prepared in PBS, along with zero control of PBS only. The standard curve range was (0, 1, 10, 10^2, 10^3, 10^4 and 10^5) pM. Standards were applied to the well plate in duplicates. Absorbance of wells was captured at 450 nM and a standard curve was prepared with concentration (pM) on the X axis (log scale) vs absorbance at 450nm on the Y axis (linear).

4.1.2.4 Interference in the detection by anti tau of tau in HS

The degree of interference of assay by other molecules other than tau was achieved by performing the assay as described in section 4.1.2.3 (detection of Tau), except that the tau concentrations were achieved in 5% human serum. Absorbance was captured at 450nm

4.1.2.5 Intra- and inter- assay variability of optimal ELISA conditions for tau.

Intra-assay variability was determined by applying 6 replicates of each of the standards and zero tau (as control) of the optimized ELISA. Inter-assay variability was determined by applying 2 replicates of each standard to five individual plates

4.1.2.6 Improving sensitivity of ELISA assay for optimal detection of tau in CSF

In order to further increase the sensitivity of the assay, the effect of altering the volume of TMB substrate and stop solution was investigated using a range of Tau concentrations from to 1pM- 1280 pM. This range of concentrations more closely resembles those reported previously in CSF samples. The optimised ELISA was performed as described in section 3.2.2. The effect of different combinations of TMB and 2 M sulphuric acid dilutions made up in PBS were investigated on the sensitivity of the assay. The dilution combinations used were TMB 100 µl and 2M sulpuric acid (Stop solution) 100 µl, TMB 50 µl and 2 M sulphuric acid 100 µl, TMB 100 µl and 2 M sulphuric acid 50 µl, TMB 50 µl and 2 M sulphuric acid 50 µl, TMB 25µl and 2M sulphuric acid 75 µl. Each dilution combination was an individual experiment run in duplicates three times.

4.1.2.7 Detection of Tau in CSF samples

Seven CSF samples were applied to the optimized ELISA as described in section 4.1.2.3 using the Tau concentrations (10240, 5120, 2560, 1280, 640, 320, 160, 80, 40, 20, 10, 5, 2.5, 1.25) pM as standards.

4.2   Confirmation of detection of tau by Western blot
4.2.1 General method

Tau protein was reconstituted in PBS or 5% human serum and equal volumes of 20 µl containing 0 µg, 0.05 µg, 0.1 µg and 0.2 µg were pipetted out into microtubes. 5 µl of 2X laemmli sample buffer was added into each microtube to make the volume up to 25 µl. Each microtube was shaken thoroughly before boiling for 5minutes at 99°C to shear protein. 5 µl of prestained protein ladder and 25 µl of each tau sample were electrophoresed through a premade gel in 1X running buffer at 0.02A for 1 hour. Proteins were then transferred unto a nitrocellulose membrane by means of a trans-blot transfer system for 7 mins at 2.5A, 22V. Membrane was rinsed in diH$_2$O and soaked in Ponceau red for 5 mins to check transfer efficiency.

Subsequently, the membrane was placed in blocking solution containing 5% (w/v) dried skimmed milk powder diluted in phosphate buffer saline (PBS) containing 0.1% Tween-20 (0.1% PBST) for one hour and probed over night at 4°C with primary antibody (39E10) in the same blocking solution. The next day, the membrane was washed three times in PBS containing 0.3% Tween-20 (PBST) for 15 minutes each before incubation with horse radish peroxidase (HRP) conjugated secondary antibody, a goat anti-mouse antibody, in

blocking solution for one hour at room temperature. Following three more washes in 0.3% PBST, the membrane was placed on a tray and incubated with enhanced chemiluminescence (ECL) substrate for five minutes in the dark . Finally, results were visualised using an odyssey infrared imaging system scanner.

4.2.2 Western blot result Analysis

The image developed from ECL was opened in imageJ and the protein intensity quantified using the gel analysis option in image J software (http://rsbweb.nih.gov/ij) as shown in the example in Fig. 4.2. This involved images being converted into grayscale and using the rectangular selection tool, large rectangles were drawn around each band of interest in turn. Subsequently, a profile plot was created for each selected area and a straight line was drawn at the base of each peak, from one side to the other to enclose the area of the peak (the tails to either side of the peak were the background signal). Finally, using the wand tracing tool, the size could be expressed as a percentage of total size of all the measured peaks. The percentage value of the protein was divided by the loading control (0 µg tau) percentage to get relative intensity.
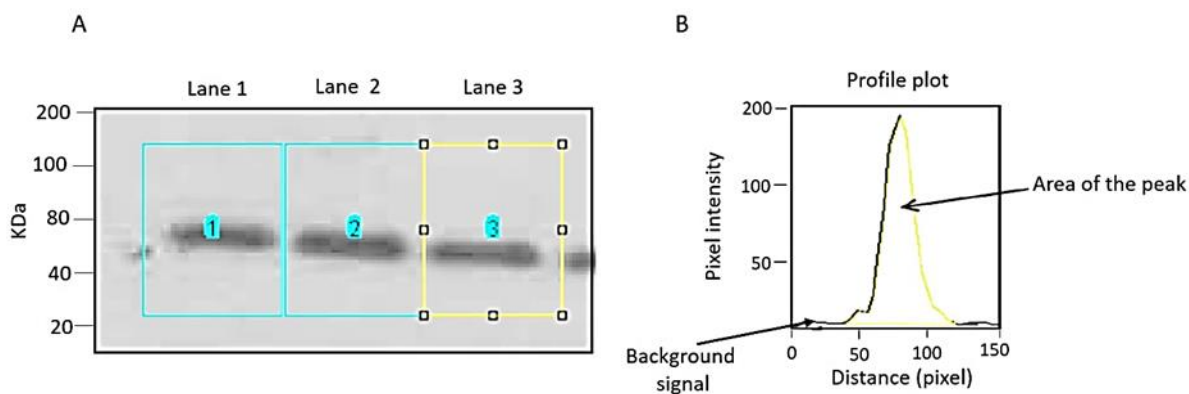
Figure 4.2 : Analysis of Western blots in image J. (A) Rectangles are drawn around the bands of interest and (B) a profile plot is then created for each band. A line is drawn at the base of each peak to enclose the area of the peak with tails on either side encompassing the background signal. Each peak is selected (yellow) and the size calculated.

4.3 RESULTS and Discussion

4.3.1 Results

4.3.1.1 Effect of Capture Antibody (CA)

The effect of 39E10 as capture antibody in the ELISA assay was investigated by coating the micro well plate with different concentrations (0.25 μg/ml, 0.5 μg/ml, 1 μg/ml and 2 μg/ml) of 39E10 in carbonate/bicarbonate buffer and exposed to Tau in PBS at 10^5 pM and 0 pM containing no tau as the control. Data was obtained from 3 sets of experiments run in duplicates and is presented as standard error of mean (SEM) of absorbance (x-axis) and CA concentration (μg/ml)
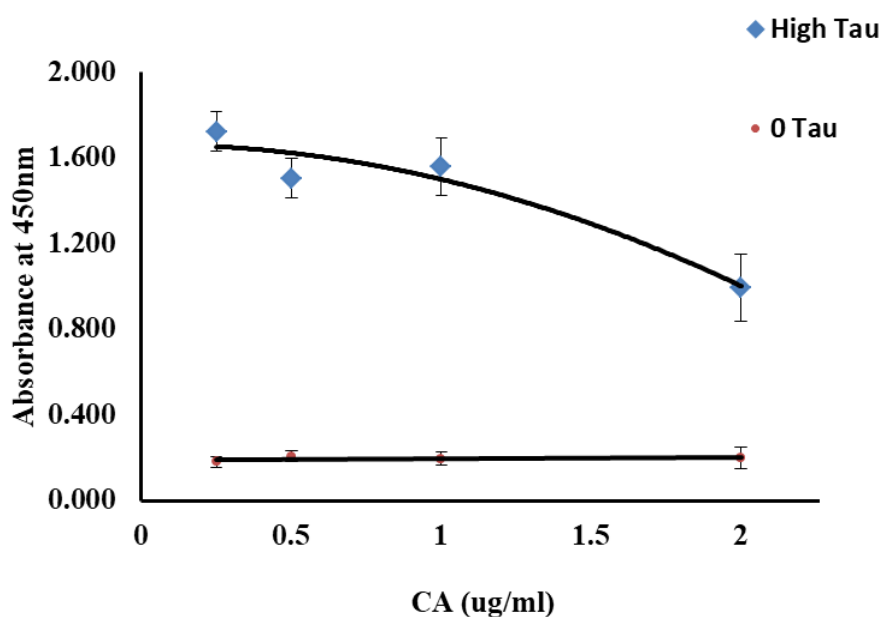
Figure 4.3: Effect of capture antibody (CA) on zero tau and high tau (10^5pM) by ELISA.

Looking at the difference in absorbance between high Tau concentration and 0 Tau across a range of CA concentrations (P >0.05), One-way analysis of variance revealed that there was no significant difference according to capture antibody concentration. However, post hoc analysis of individual CA concentrations showed that 2μg/ml CA results in a significantly decreased response. Therefore, any concentration of CA between 0μg/ml and

1μg/ml could be chosen for subsequent optimisation of the ELISA. 1μg/ml of CA was the concentration of choice.

4.3.1.2 Effect of Detector Antibody (DA)

Tau protein at 0pM (low) and 10^5pM (high) concentrations in PBS were captured using 1μg/ml of 39E10 and the effect of different dilutions (1:1000, 1:2000, 1: 5000, 1:10000) of DA in blocking buffer were investigated in the ELISA. Data was obtained from 3 sets of experiments run in duplicates and is present as standard error of mean (SEM) of absorbance (X axis) and DA concentration (μg/ml) (Y axis)
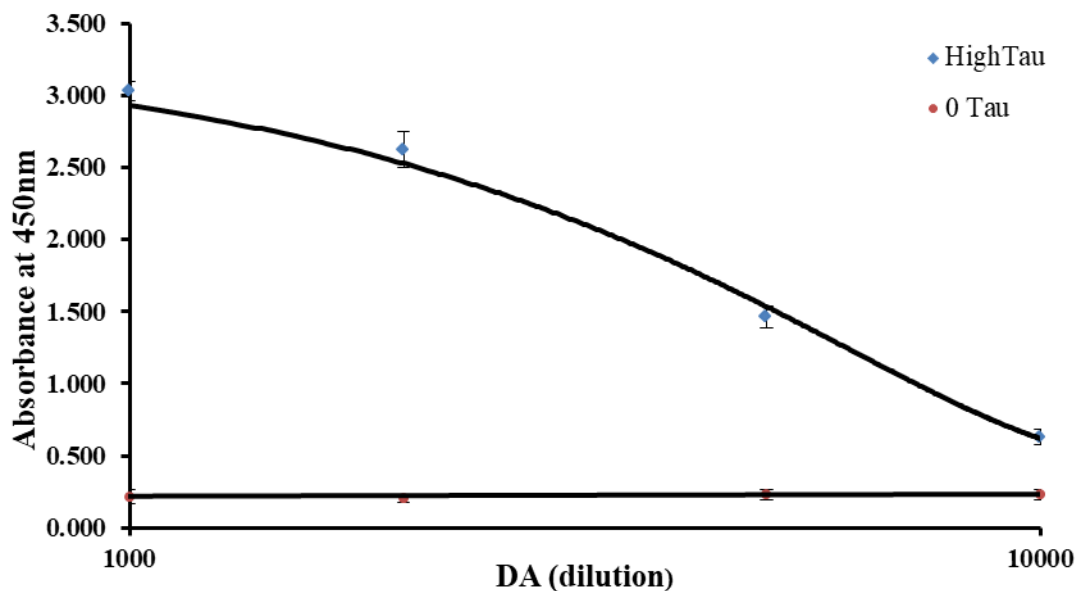
Figure 4.4: Effect of detector antibody (DA) on zero tau and high tau (10^5pM).

In order to analyse the effect of DA, the difference in absorbance between high tau concentration and 0 tau across a range of DA dilutions (P >0.05) was seen. One-way analysis of variance revealed that there was no significant difference according to detector antibody dilutions between 1:1000 and 1:2000, but significant difference (p <0.05) is seen across all dilutions of DA from 1:2000 upto 1:10000, 1:2000 DA was the dilution chosen for further optimisation of the ELISA assay.

4.3.1.3 Optimisation of Range of Standards

The plate was coated with 1μg/ml 39E10 and secondary antibody diluted at 1:2000 used as detection antibody. *** (P< 0.001), ** (P<0.01), using one tail t-test assuming unequal variances, ns: no significant difference. Data is plotted as mean ± SEM for n=3 (number of replicates)
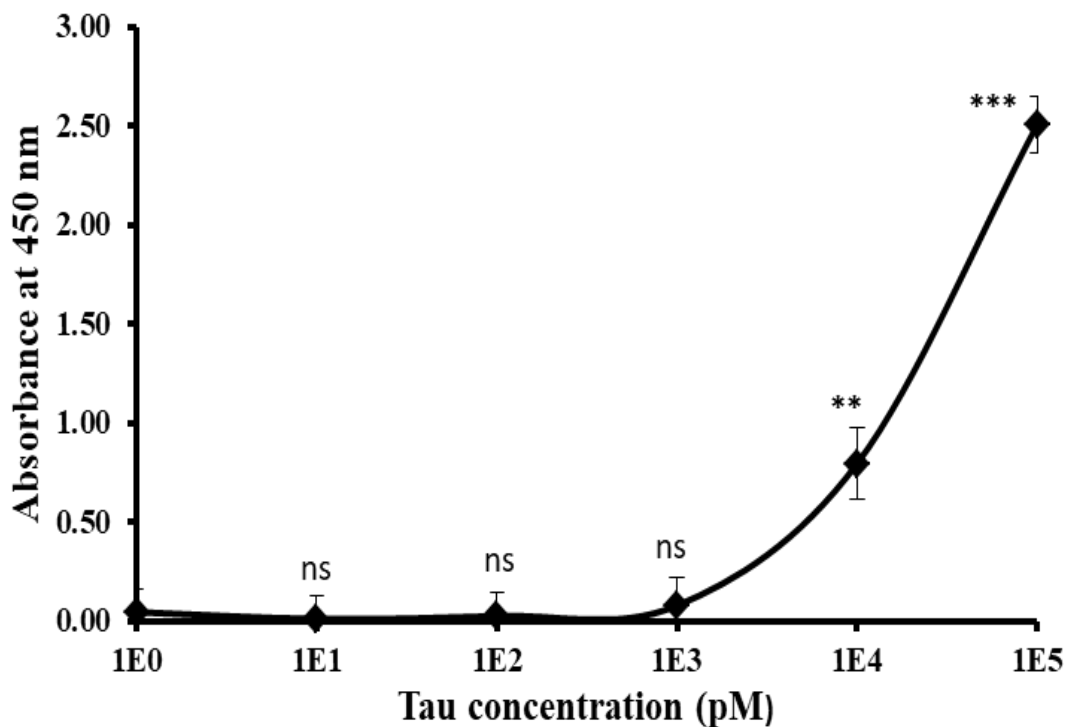
Figure 4.5: A typical Standard curve obtained from an optimised ELISA for measuring Tau in PBS using 39E10 as capture AB.

The assay range of the ELISA was 10^{-2} to 10^5 and the detection range was determined to be 10^4pM –10^5pM with a limit of detection of 10^4pM tau (P<0.05).

4.3.1.4 Detection of tau in human serum

The plate was coated with 1ug/ml 39E10 and secondary antibody diluted at 1:2000 used as detection antibody. *** (P< 0.001), ** (P<0.01), using one tail t-test assuming unequal variances, ns: significant difference. Data is plotted as mean ± SEM for n=3 (number of replicates)
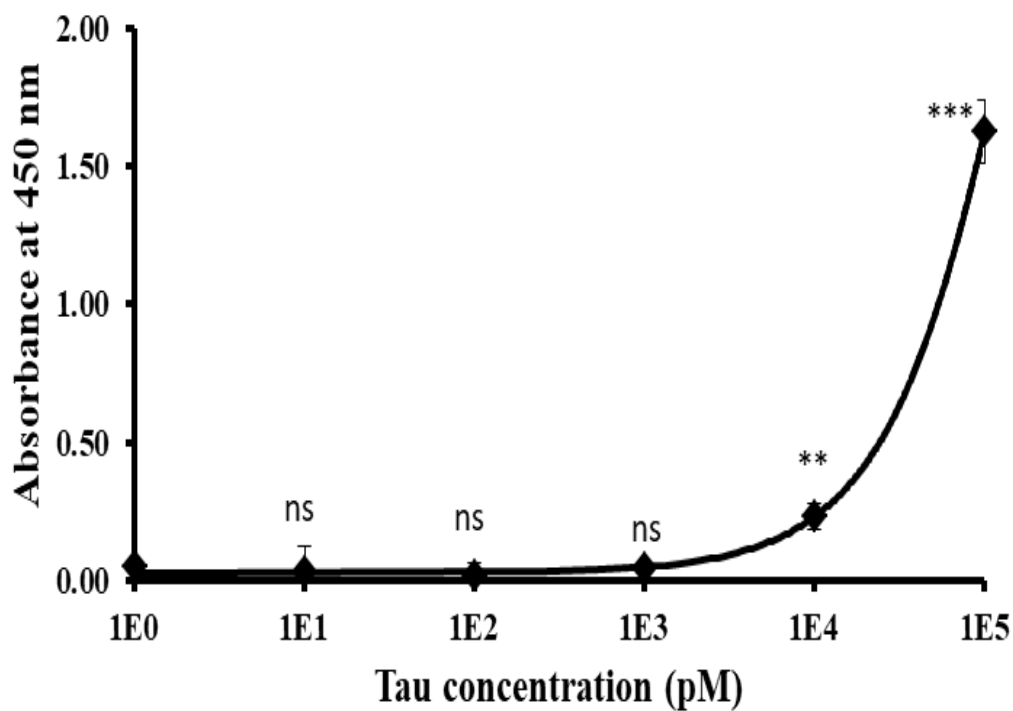
Figure 4.6: A typical Standard curve obtained from an optimised ELISA for measuring Tau spiked in Human serum (HS) using 39E10 as capture AB.

4.3.1.5 Comparison of tau detection in PBS and human serum

Data obtained from measurements of Tau in PBS and Tau spiked in human serum, were compared (Fig 4.7). Data is plotted as mean ± SEM for n= 3 (number of replicates)
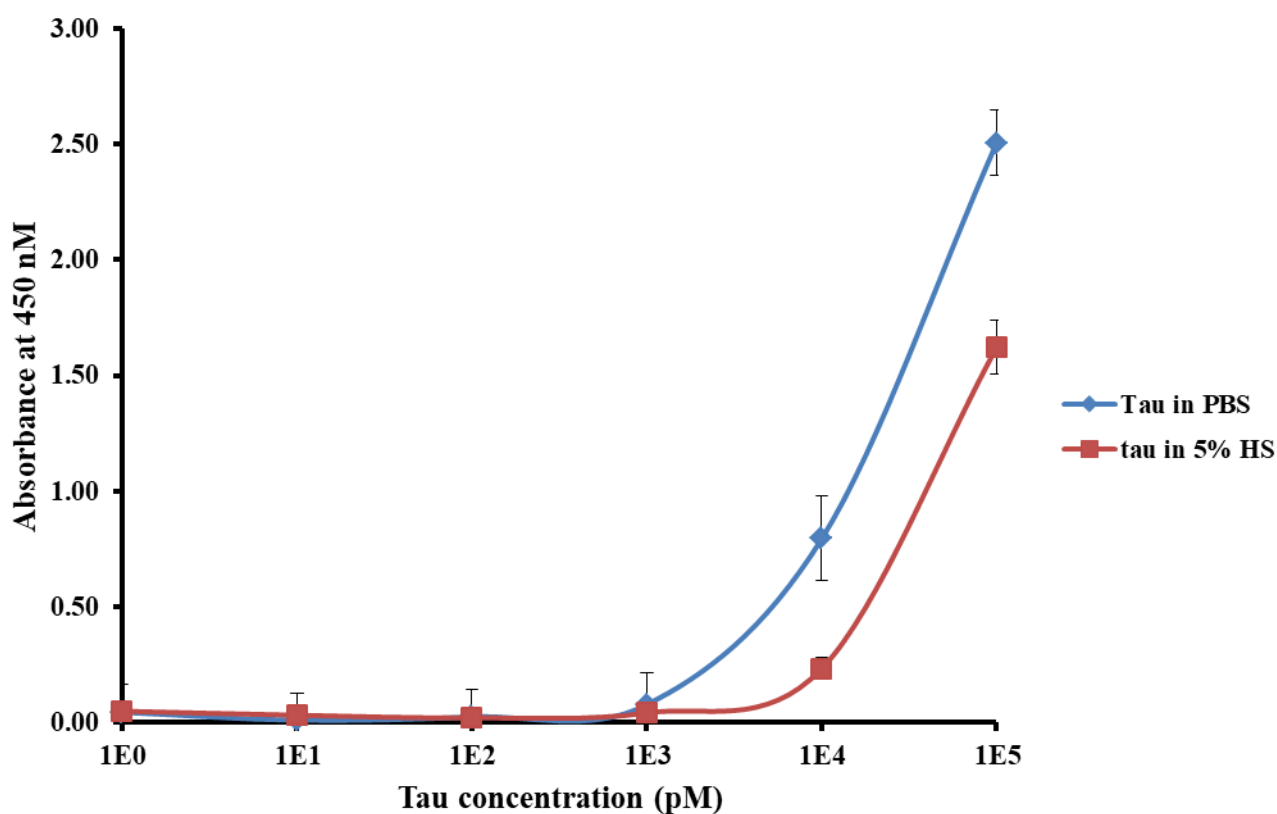
Figure 4.7: **ELISA results showing detection of different tau concentrations (1- 10^5 pM) in PBS or in 5% HS.**

4.3.1.6 Intra Assay Variability and inter-assay variability

Intra-assay variability of the optimised sandwich ELISA was determined using 6 replicates of each Tau standard concentration (0, 1, 10, 10^2, 10^3, 10^4 and 10^5) pM on one plate. The CVs were less 10% (Table 4.1).

Table 4.1: Intra assay variability from 6 different plates of different concentrations of Tau

Tau conc (pM)	% CV
0	8.498
1	6.899

10	9.467
10^2	8.440
10^3	4.101
10^4	9.507
10^5	9.806

Intra-assay CV (n=7) = average % CV = 8.1

The plate was coated with 1ug/ml 39E10 and secondary antibody diluted at 1:2500 used as detection antibody. Inter-assay variability was determined by comparing the different Tau standard concentrations (0, 1, 10, 10^2, 10^3, 10^4 and 10^5) pM from 5 individual plates, each concentration being run in duplicate and the mean obtained. CVs were less than 14% (Table 4.2)

Table 4.2: Inter-assay variability an optimised ELISA for measuring Tau in PBS.

Tau conc (pM)	% CV
0	13.114
1	11.609
10	10.204
10^2	11.821
10^3	13.566
10^4	11.309
10^5	10.412

4.3.1.7 Improving sensitivity of ELISA for measurement of tau CSF samples

For measurement of Tau concentration in human cerebrospinal fluid usually measured 1E4 pM which falls within the lower range of the assay developed, the assay was further optimized to extend the lower range of the and make it more sensitive by varying different combination volumes of TMB substrate (100 μl, 50 μl, and 25 μl) and 2M sulphuric acid stop solution (100 μl, 50 μl, and 75 μl)(Fig. 4.8A). For each time the TMB and stop solution volumes were altered, the final volume read by the plate reader was adjusted to 200μl by the addition of PBS. Tau concentrations (1 – 1280) pM were used as standards. The combination of TMB50 SS100 reported a higher signal across all concentrations of tau compared to the

other combination volumes TMB25 SS75, TMB50 SS50, TMB100 SS50 and TMB100 SS100. A one tail t-test revealed no significant difference (P>0.05) between 1E0 pM to 640 pM and control (0 pM) tau concentrations but a significance difference (P<0.05) is seen with the higher tau concentration above 1E3 and Control (0 pM) (Fig. 4.8A).

TMB50 SS100 conditions were used to quantify Tau in CSF from seven human samples. Wells with 0 tau were used as controls, while serial dilutions of commercial tau (10240, 5120, 2560, 1280, 640, 320, 160, 80, 40, 20, 10, 5, 2.5, 1.25) pM were used as standards. Sample volumes were maintained at 100ul to be consistent with standards and controls. Experiment was performed in duplicates (Fig. 4.8B)

(A)
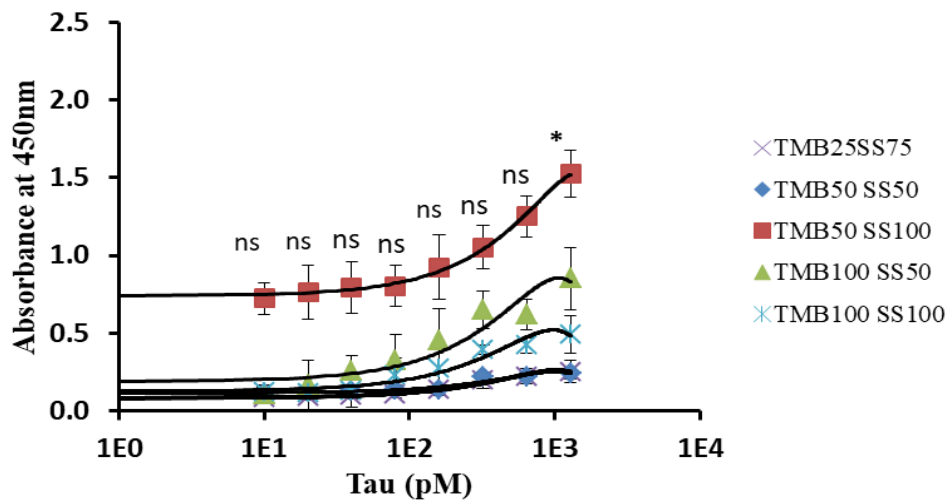
(B)
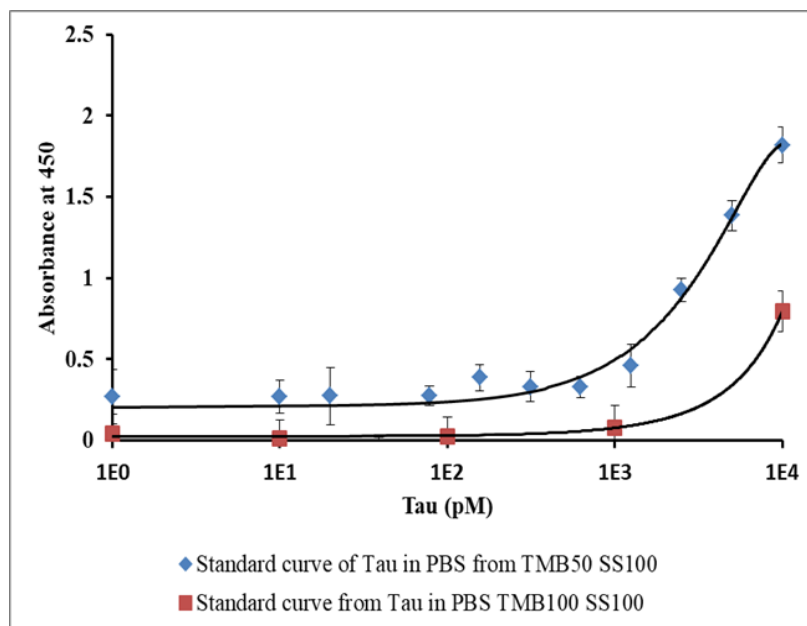
Figure 4.8: **Optimization of Standard curve to measure Tau in human CSF samples**. (A) Effect of different combinations of TMB and stop solution (SS) volumes. TMB is the substrate volume (µl) and SS is the stop solution volume (ul). Using T-Test assuming unequal variance *P<0.05, ns: no significance . (B) Comparison of standard curves achieved from Tau in PBS using TMB100 SS100 and TMB50 SS100. Data is plotted as mean ± SEM for n = 3 (number of replicates).

Comparing the standard curves from achieved using conditions TMB50 SS100 and TMB100 SS100, the standard curve from TMB50 SS100 provided a higher signal, however Tau protein was undetectable in all seven samples of CSF measured.

4.3.1.8 Comparison of ELISA and biosensor

The ELISA was carried out to determine the limit of detection (LOD) of tau. LOD was defined as the lowest concentration of tau that could be distinguished from HS in the absence of tau. The whole process of ELISA took a few hours while the electrochemical biosensor testing only took less than an hour for the incubation and measurement. The LOD by biosensor (10^{-2}pM) was greatly superior to that established by ELISA (10^4 pM). Similar to the biosensor, the LOD of Tau by the ELISA is unaltered by the presence of human serum. However, a difference can be observed in the absorbance signal at the concentrations of 10^4 pM and 10^5pM in the presence and absence of HS (Fig. 4.7) similar to the difference seen in percentage change in Rct for the biosensor in the presence and absence of HS (Fig. 3.18B). This difference is possibly due to matrix effect in the presence of HS.

Protein was undetectable in all seven samples of CSF measured.

(A)

(B)
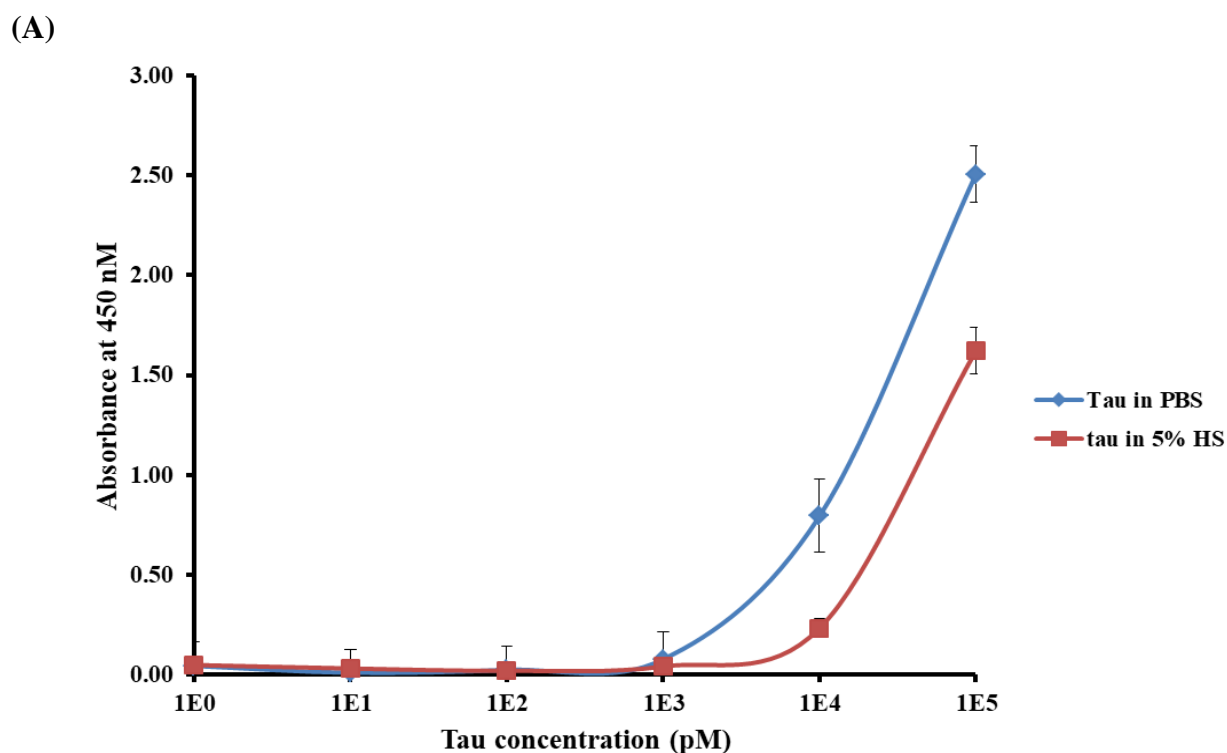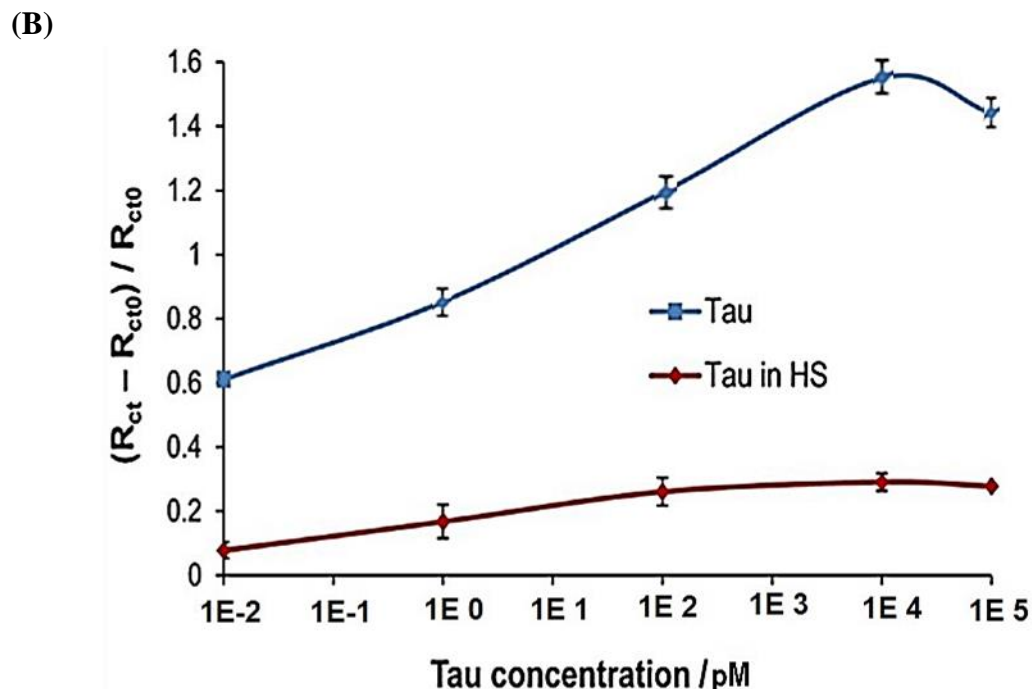
Figure 4:9: **Comparison of Tau in PBS and Tau spiked in HS by ELISA and electrochemical biosensor methods (Wang _et al._, 2017)** . (A) ELISA results showing detection of different concentrations from (1 to 10^5) pM of tau in PBS or tau spiked in 5% human serum (HS). (B) Biosensor results showing detection of different concentrations from (10^{-2} to 10^5) pM of tau in PBS or tau spiked in HS. Data was plotted as mean $\pm$ SEM for n = 3.

The LOD both as seen on the graphs and calculated from biosensor was six orders of

magnitude lower than that from ELISA.

Table 4.3: **Summary of Assay range and detection limit by the biosensor and ELISA**

Assay method	Limit of quantification (pM)	Assay range (pM)
Biosensor	10^{-2}	$1\sim10^5$
ELISA	10^4	$10^{-2}\sim10^5$

4.3.1.9 Western blot Analysis

Western blot analysis was performed to confirm the detection of full length tau and the specificity of 39E10 for full length tau.
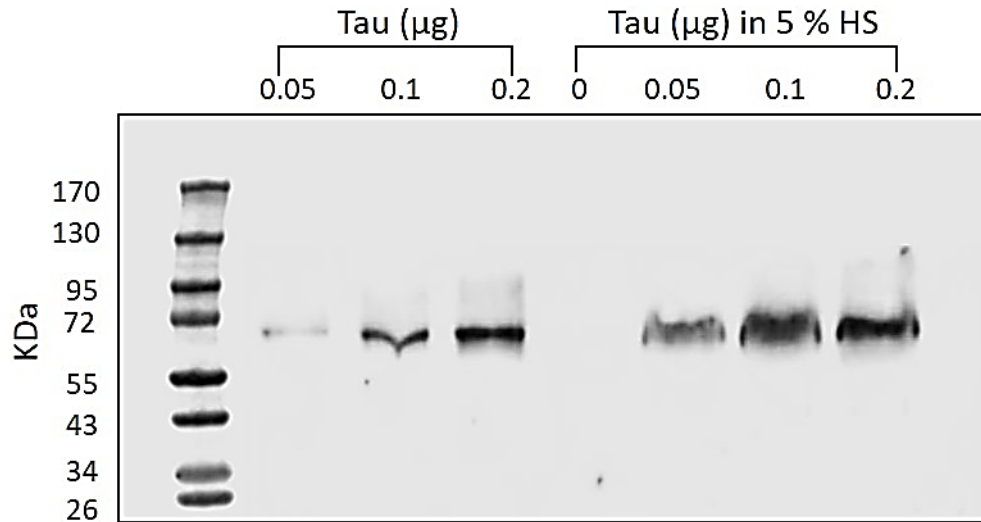
Figure 4.10: **SDS-PAGE gel and Western blot showing reactivity of full length Tau by detection of 0.05 -0.2 μg Tau in PBS and Tau in 5% HS by anti-tau**. The positions of the molecular mass standards (in kDa) are indicated on the left.

A Pre-cast gel was loaded with the following: First lane – Molecular weight standards; Second, third and fourth lanes - Tau in PBS concentrations 0.05, 0.1, 0.2 (μg) respectively; fifth lane- zero tau (HS only); sixth, seventh and eight lane – Tau in HS concentrations 0.05, 0.1 and 0.2 (μg) respectively. Blots were probed with enhanced chemiluminescence (ECL) substrate and captured using the odyssey infrared system scanner. Figure 4.10 shows the main band position of full length tau at; ~ 70 kDa when detected with 39E10 antibody. Lane five with no tau was used as the control, the intensity of the signal from immunoreactivity was seen to increase with increasing concentration (0.05, 0.1 and 0.2) μg of tau both in PBS and human serum but with more intense signals in human serum compared to tau in PBS for the same concentrations of tau.

Image J software was then used to generate the data displayed on the charts (Fig. 4.11) comparing Tau in PBS and HS on the blot as detected by 39E10.
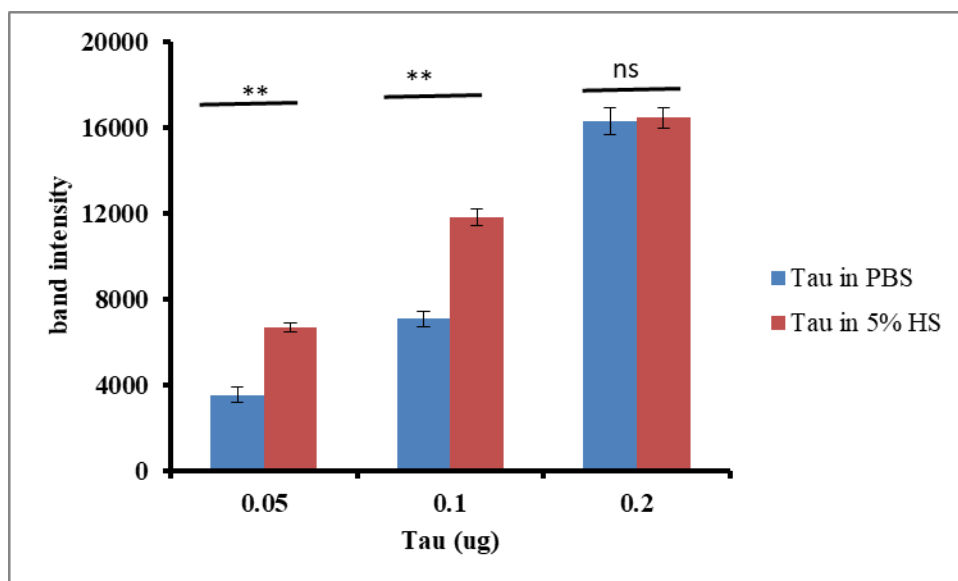
Figure 4.11: **Comparison of Tau detection in PBS and 5% Human Serum from Western blots analysed by Image J**. Data is presented as mean of three different experiments with standard error for n=3

The difference in the intensity of the signal detection of tau in PBS and Tau in HS is compared using a two tail t-test. The intensity of the signals are significantly different at lower concentrations of 0.05 and 0.1μg **(P< 0.001) and not significant (ns) at higher concentration of 0.2μg. Data was normalised by subtracting the value of signal intensity achieved by no tau from value of signal intensity achieved from all the concentrations of tau (0.05, 0.1 and 0.2) μg in PBS and in HS. The difference in signal detection of tau seen in PBS and HS could be due to non-specific binding of other proteins in HS.

4.3.2 Discussion

Alzheimer's disease (AD) is characterised by elevated levels of total tau (t-tau), test consistent benchmark levels to indicate AD have not yet been established. Using a sandwich enzyme-linked immunosorbent assay (ELISA), this study aimed to develop and optimise an ELISA capable of quantifying tau concentration in patients' cerebrospinal fluid (CSF) samples. The second aim of developing this ELISA assay was to compare with and validate the biosensor developed in chapter 3.

Firstly, conditions for the ELISA were optimised using 39E10 antibody, the bioreceptor component from the biosensor in chapter 3. It was found that a working range of 1 to 10^5 pM tau protein can be detected. Furthermore, interference with the assay was investigated. By comparing both results of the assay from tau in PBS and tau in human serum (HS) (Fig. 4.7),

the sensitivity (10^4 pM) was unaltered; however, a shift to the right of the standard curve derived from Tau in HS suggests a possible matrix effect / non-specific interference by other components in HS. The use of biotin-labelled secondary detection antibody took advantage of the avidin-biotin method of signal amplification. First exploited in the 1980s, the biotin-avidin complex increases sensitivity due to the high enzyme-to-antibody ratio as well as an exceptionally high affinity and stability ensuring the desired conjunction of binder and probe (Madri and Barwick, 1983).

Compared with other in-house, some ELISAs for Tau have reported limits of detection of tau down to attomolar range (Hu *et al.*, 2002), the assay developed in this study was less sensitive. It is noteworthy that most of these in-house ELISAs used enhanced methods such as magnetic capturing and digital detection, biotin-tyramide amplification and bienzyme substrate recycling. Sunderland and team in 2003 reported an ELISA with cut off of 195 pg/mL ~ 4.2pM for CSF tau with a sensitivity and specificity of 92% and 89%, respectively, to distinguish between AD patients and controls, which is comparable with rates with clinical diagnosis. The LoD of the ELISA developed for tau detection at 10^4pM is four magnitudes higher than the value of 4.2pM. This implies that the ELISA developed in this study has a high detection limit above the levels reported in CSf, human serum and plasma and therefore could not possibly be applied in clinical use.

Comparing the ELISA assay with the biosensor from chapter 3, it's LoD of 10^4 pM is 5 five magnitudes higher than that of the biosensor's, 0.2 pM, a value which is clinically relevant. Also with the biosensor, incubation and measurement was achieved in under 30min which is far less time compared to the ELISA assay which took 2 days to acquire measurements, implying that the ELISA compared to the sensor was more laborious and time consuming.

Sensitivity is the change in signal per unit of concentration or the slope of the dose/response curve. If an immunoassay produces a larger signal for a given concentration, it may be possible to detect lower concentrations above background. The lower range of the ELISA assay was extended for the detection of tau in CSF samples by altering volumes of TMB. The TMB reaction is routinely stopped by using an acid to convert the blue reaction product to a yellow product. The yellow product has a higher extinction coefficient that yields about 2.6 times the absorbance signal for a given concentration of the analyte. Furthermore, it is known that the conversion of TMB to the yellow product increases the ability to detect the analyte (Ekins, R. and Edwards, P., 1997). Therefore, varying the volumes of the TMB and stop solution affects the absorbance signal (Fig. 4:8A). The

detection limit is usually governed by the standard deviation of the signal measurements; the less error, the easier it is to to distinguish a low concentration from the background. From Fig. 4.10, the combination volumes of TMB and 2M sulphuric acid (stop solution) 50μl and 100μl respectively showed a very distinct increase in signal detection defined by the absorbance reading and the slope of the curve., however Tau was undetected in all seven CSF samples. Implying Tau in the samples was low below the detection limit of the optimised ELISA. Due to the limited amount of CSF, as well as the lack of electrodes for further studies, further ELISA measurements were not performed.

One major advantage of using 39E10 antibody is that it is raised against full-length tau (Tau 441). 39E10 antibody recognises the middle domain (amino acids 189–195 according to full-length tau) shared by all six isoforms of tau protein. This means that the biosensor and ELISA if clinically valid, could be used to measure total tau protein (all six isoforms) which is among the main markers for AD and could potentially be used for early diagnosis of AD. However, there is no published data on the use of 39E10 as a capture antibody in reported ELISA systems; one study has published 39E10 as detector antibody, and a few studies have used this antibody in biosensor development (Wang *et al.*, 2017; Li *et al.*, 2018), Western blotting (Michalski *et al.*, 2015) and Immunohistochemistry (IHC)(Mammadova *et al.*, 2017; Li *et al.*, 2019). There is very limited information about 39E10 and its use is recommended mainly for WB and IHC by Biolegend, the exclusive provider of the antibody product. Therefore this study suggests further investigations into the use of 39E10 for detection of total tau protein.

It is recommended that one uses a commercial ELISA or other methods as reference/validation. The availability of several commercial kits for detection of tau makes ELISA an excellent method for tau detection. Despite this advanatges there are some drawbacks, including extensive incubation and washing steps and the use of multiple antibodies. Immuno-PCR (iPCR) related techniques have also proven successful in measuring low concentrations of tau protein. One such technique is a nano-iPCR technique which was used to detect tau concentrations via immobilisation of tau-specific antibody (Tau-5) directly in PCR wells, followed by real-time PCR detection in combination with Au-nanoparticles functionalised with tau-specific monoclonal antibody HT7 and a single-stranded thiolated oligonucleotide (Stegurová *et al.*, 2014). An impressive detection range at pM level attributed to the effectiveness of this method. However, PCR amplification is very sensitive and in the case of nonspecific interference by detection elements that bind to the PCR well walls, signal will be greatly amplified, increasing the background, which may

become a drawback. Alternative methods of detection of various tau forms are required, these methods need to be simple, sensitive and user friendly, to allow for the detection of AD and differential diagnosis between related neurodegenerative disorders.

Finally, Western blotting was used to confirm the specificity of the bioreceptor for tau binding (Fig. 4.10). The expected molecular weight (MW) of full-length tau under reducing conditions of SDS is ~ 70kDa equivalent to the signal captured on the blot as seen on Fig. 4.10. This result, therefore, confirms the results from the biosensor and indicates that the antibody does not bind significantly to other proteins in HS.

Chapter 5

5. General conclusions and future work

5.1. General Conclusions

The main objectives achieved in this project were

I.   Development and validation of a new tetrapolar biosensor for Tau protein

II.   Development of an ELISA for comparison of the biosensor performance

III.   Identification of limitations of ELISA for use in detecting low level of Tau which would limit early detection of AD

IV.   Identified limitations of antibody chemistry for detection of Tau

This project, focused on the development of a novel biosensor to detect tau protein using a tetrapolar impedance system, as tetrapolar electrode systems offer the advantage of reduced interfacial electrode polarization in contrast to bipolar and tripolar systems (Kassanos, Demosthenous and Bayford, 2008). Once the biosensor was constructed, it took 25 mins to achieve EIS readings of tau (incubation plus measurements).

The capture antibody anti tau used in the ELISA was the same antibody used as biomolecule on the bioreceptor of the sensor, to make the methods more comparable and also to confirm antigen (tau) capture by the specific antibodies (anti-tau), thus confirming antibody immobilisation on the surface of the biosensors. Some studies have reported enzyme-linked immunosorbent assays (ELISA) measuring tau concentration in patients' cerebrospinal fluid (CSF) samples estimated to be below 5 pM level, which is not the case with the ELISA in this study. The ability of ELISA to detect such low concentration levels, and its availability via commercially available kits make it an excellent method for tau detection. However, despite these advantages there are also drawbacks, such as use of multiple antibodies, extensive incubation and washing steps.

The specificity of the bioreceptor for tau binding was confirmed by Western blotting, which was unaltered by other components in human serum, particularly albumin which is the most-abundant serum protein. The sensor developed in this project can be used to assay tau in biological fluids such as CSF and serum due to it's low LoD. Compared to previous biosensor systems for the detection of tau (Jose O Esteves-Villanueva, Trzeciakiewicz and Martic, 2014; Carlin and Martic-Milne, 2018), the tetrapolar system is exquisitely sensitive, highly specific for tau and allows detection of tau spiked in human serum down to a concentration of 0.2 pM a value unaltered by BSA and components of HS and which is diagnostically important for AD. The preliminary results from the various experiments

carried out for this project have shed some light on important issues that need to be considered for the successful development of an impedance-based biosensor for the detection of the tau in this case, or any other biomarkers in future development. Experiments have proved DTSSP to be a good cross linker as through simple coupling procedures, it leads to the successful detection of tau following antibody immobilisation. One of the short comings of this project is the lack of investigation of the effect of protein G on the orientation of anti-tau on the sensor surface despite the varied conclusions in the literature on the use of protein G to aid antibody orientation for enhanced detection of antigen of interest, in this case tau. Some studies have reported that protein G does not ultimately lead to better detection of the antigen of interest (Kassanos *et al.*, 2008), tau in this case. Other orientation studies using thiolated antibodies have also proved unsuccessful, showing that the best coupling procedures could be through the coupling of the SAM layer followed by antibody immobilisation. It was noticed that adequate washing is important to maintain stability of the biosensors, and reduce variability between them, and further experiments have shown that the biosensors gain maximum stability when constructed with the antibody layer. The biosensors have shown the possibility of detecting tau protein at various concentrations, but through validation experiments, highlighted the problem of non-specific binding, which following further experiments was greatly reduced, through the use of ethanolamine as a blocking reagent.

High variability between the sensors was also possibly due to reusability of the electrodes and it construction as some of the Electrodes appeared to broken under the microscope.

5.2 Future work

For the purpose of this research, future work would seek to follow the chemistry in this work to construct the sensors on new electrodes which are under fabrication. The sensors will be used to validate the biosensor with patient CSF fluids obtained from AD and control patients. There is scope to further improve the sensitivity and specificity of the sensors and also decrease variability of the sensor for example, by changing the geometry of the electrodes.

The complexity of the system resulting from many layers makes it difficult to control every layer and maintain stability. Therefore, exploting diferrent avenues for reducing the number of layers such as (a) assessing the effect or relevance of protein G (b) Using anti tau $F(ab)_2$ directly on the electrode surface as bioreceptors for detection of tau protein (c) employing the use of nanoparticles (d) employ the use of aptamers

Considering that anitbodies are relatively large molecules, It might therefore be better to make use of a smaller capture layers, such as an antibody fragment to detect the specific antigen. Antibody fragments, (anti tau F(ab)$_2$ in this case) are small sections of antibodies containing the portion that binds antigen. For example, antibodies can be engineered such that only the Fab fragments are available, and their disulphide bonds exposed such that they bind directly to gold surfaces. The use of llama heavy chain variable region antibody fragment (VHH) (14kDa) bearing the specific antigen binding region would be interesting in the construction of biosensors for detection of Tau.

Although still being investigated, noble biosensing techniques are making use of nanomaterials through modification of biorecognition layers to enhance problems of conventional biosensors (e.g., sensitivity and selectivity) to provide more sensitive and highly accurate nanobiosensor platforms. One main advantage of nanomaterial is the high surface area to volume ratios which allow the surface to be used in a better and far more diversely functional manner. Various types of nanomaterials such as gold nanoparticles, magnetic nanoparticles, quantum dots and carbon nanotubes have been added to biosensors and due to their unique chemical and physical characteristics, enormous changes in identification of biomolecules have been made .Within the group of nanoparticles, gold nanoparticles are mostly used for electrochemical biosensor application due to their biocompatibility, their optical and electronic properties, and relatively simple production and modification.

Aptamers are synthetic molecules that can be raised against any kind of target. Although costly they have many advantages over the use of antibodies in biosensing. Aptamers have equal or superior affinity and specificity to the target compared antibodies, they are smaller in size, are easier to modify and immobilize. Furthermore, aptamers are stable at room temperature and have longer shelf life and offer higher reproducibility.

References

Acker, C. M., Forest, S. K., Zinkowski, R., Davies, P. and d'Abramo, C. (2013) 'Sensitive quantitative assays for tau and phospho-tau in transgenic mouse models', *Neurobiology of Aging*, 34(1), p 338–350.

Ackmann, M., Wiech, H. and Mandelkow, E. (2000) 'Nonsaturable binding indicates clustering of Tau on the microtubule surface in a paired helical filament-like conformation', *Journal of Biological Chemistry*, 275(39), p 30335–30343.

Adelina, C. (2019) 'The costs of dementia: advocacy, media and stigma.', *Alzheimer's Disease International: World Alzheimer Report 2019*, p 100–101.

Ahmadi, S., Ebralidze, I. I., She, Z. and Kraatz, H. B. (2017) 'Electrochemical studies of tau protein-iron interactions—Potential implications for Alzheimer's Disease', *Electrochimica Acta*, 236, p 384–393.

Akiyama, H., Barger, S., Barnum, S., Bradt, B., Bauer, J., Cole, G. M., Cooper, N. R., Eikelenboom, P., Emmerling, M., Fiebich, B. L., Finch, C. E., Frautschy, S., Griffin, W. S. T., Hampel, H., Hull, M., Landreth, G., Lue, L. F., Mrak, R., MacKenzie, I. R., McGeer, P. L., O'Banion, M. K., Pachter, J., Pasinetti, G., Plata-Salaman, C., Rogers, J., Rydel, R., Shen, Y., Streit, W., Strohmeyer, R., Tooyoma, I., Van Muiswinkel, F. L., Veerhuis, R., Walker, D., Webster, S., Wegrzyniak, B., Wenk, G. and Wyss-Coray, T. (2000) Inflammation and Alzheimer's disease, *Neurobiology of Aging*, 21, p 383–421

Algeciras-Schimnich, A., Bruns, D. E., Boyd, J. C., Bryant, S. C., La Fortune, K. A. and Grebe, S. K. G. (2013) 'Failure of current laboratory protocols to detect lot-to-lot reagent differences: Findings and possible solutions', *Clinical Chemistry*, 59, p 1187–1194

Aloisi, A., Torre, A. Della, De Benedetto, A. and Rinaldi, R. (2019) 'Bio-recognition in spectroscopy-based biosensors for *Heavy Metals-water and waterborne contamination analysis', *Biosensors*, 9.

Alves, G., Lange, J., Blennow, K., Zetterberg, H., Andreasson, U., Førland, M. G., Tysnes, O. B., Larsen, J. P. and Pedersen, K. F. (2014) 'CSF A??42 predicts early-onset dementia in Parkinson disease', *Neurology*, 82(20), p 1784–1790.

Alzheimer's Association (2014) '2014 Alzheimer's disease facts and figures.', *Alzheimer's & dementia : the journal of the Alzheimer's Association*. Elsevier Inc., 10(2), p 321–387.

Alzheimer's Society (Online). Available at: https://www.alzheimers.org.uk/about-dementia/symptoms-and-diagnosis/how-dementia-progresses/brain-dementia (Accessed 2017)

Ameri, M., Shabaninejad, Z., Movahedpour, A., Sahebkar, A., Mohammadi, S., Hosseindoost, S., Ebrahimi, M. S., Savardashtaki, A., Karimipour, M. and Mirzaei, H. (2020) 'Biosensors for detection of Tau protein as an Alzheimer's disease marker', *International Journal of Biological Macromolecules*. Elsevier B.V., 162, p 1100–1108.

Andreasen, N., Minthon, L., Davidsson, P., Vanmechelen, E., Vanderstichele, H., Winblad, B. and Blennow, K. (2001) 'Evaluation of CSF-tau and CSF-Aβ 42 as diagnostic markers for Alzheimer disease in clinical practice', *Archives of Neurology*, 58(3), p 373–379.

Arai, T., Ikeda, K., Akiyama, H., Shikamoto, Y., Tsuchiya, K., Yagishita, S., Beach, T., Rogers, J., Schwab, C. and McGeer, P. L. (2001) 'Distinct isoforms of tau aggregated in neurons and glial cells in brains of patients with Pick's disease, corticobasal degeneration and progressive supranuclear palsy.', *Acta neuropathologica*, 101(2), p 167–73.

Arya, S. K., Chornokur, G., Venugopal, M. and Bhansali, S. (2010) 'Dithiobis(succinimidyl propionate) modified gold microarray electrode based electrochemical immunosensor for ultrasensitive detection of cortisol', *Biosensors and Bioelectronics*, 25(10), 2296–2301.

Arya, S. K., Pandey, P., Singh, S. P., Datta, M. and Malhotra, B. D. (2007) 'Dithiobissuccinimidyl propionate self assembled monolayer based cholesterol biosensor.', *The Analyst*, 132(10), p 1005–1009.

Ates, M. (2011) 'Review study of electrochemical impedance spectroscopy and equivalent electrical circuits of conducting polymers on carbon surfaces', *Progress in Organic Coatings*. Elsevier B.V., 71(1), p 1–10.

Ballatore, C., Lee, V. M.-Y. and Trojanowski, J. Q. (2007) 'Tau-mediated neurodegeneration in Alzheimer's disease and related disorders.', *Nature reviews. Neuroscience*, 8(9), p 663–72.

Barbier, P., Zejneli, O., Martinho, M., Lasorsa, A., Belle, V., Smet-Nocca, C., Tsvetkov, P. O., Devred, F. and Landrieu, I. (2019) 'Role of tau as a microtubule-associated protein: Structural and functional aspects', *Frontiers in Aging Neuroscience*, 10

Bardai, F. H., Wang, L., Mutreja, Y., Yenjerla, M., Gamblin, T. C. and Feany, M. B. (2018) 'A conserved cytoskeletal signaling cascade mediates neurotoxicity of FTDP-17 tau mutations in vivo', *Journal of Neuroscience*, 38(1), p 108–119.

Bart, M., Stigter, E. C. A., Stapert, H. R., De Jong, G. J. and Van Bennekom, W. P. (2005) 'On the response of a label-free interferon-γ immunosensor utilizing electrochemical impedance spectroscopy', *Biosensors and Bioelectronics*, 21(1), p 49–59.

Barthélemy NR, Fenaille F, Hirtz C, Sergeant N, Schraen-Maschke S, Vialaret J, Buée L, Gabelle A, Junot C, Lehmann S, Becher F. (2016). Tau Protein Quantification in Human Cerebrospinal Fluid by Targeted Mass Spectrometry at High Sequence Coverage Provides Insights into Its Primary Structure Heterogeneity. *Journal of Proteome Research*, *15*(2), 667–676

Bejanin, A., Schonhaut, D. R., La Joie, R., Kramer, J. H., Baker, S. L., Sosa, N., Ayakta, N., Cantwell, A., Janabi, M., Lauriola, M., O'Neil, J. P., Gorno-Tempini, M. L., Miller, Z. A., Rosen, H. J., Miller, B. L., Jagust, W. J. and Rabinovici, G. D. (2017) 'Tau pathology and neurodegeneration contribute to cognitive impairment in Alzheimer's disease', *Brain*, 140(12), p 3286–3300.

Berg, J. M., Tymoczko, J. L. and Stryer, L. (2012) . *Biochemistry*. 9th ed. Basingstoke : W.H. Freeman

Blennow, K. (2004) 'Cerebrospinal Fluid Protein Biomarkers for Alzheimer's Disease', *NeuroRX*, 1(2), p 213–225.

Blennow, K. (2005) 'CSF biomarkers for Alzheimer's disease: use in early diagnosis and evaluation of drug treatment', *Expert Rev Mol Diagn*, 5(5), p 661–672.

Blennow, K. (2017a) 'A Review of Fluid Biomarkers for Alzheimer's Disease: Moving from

CSF to Blood', *Neurology and Therapy*. Springer Healthcare, 6(s1), p 15–24.

Blennow, K. (2017b) 'A Review of Fluid Biomarkers for Alzheimer's Disease: Moving from CSF to Blood', *Neurology and Therapy*, 6, p 15–24

Blennow, K., Wallin, A., Ågren, H., Spenger, C., Siegfried, J. and Vanmechelen, E. (1995) 'tau protein in cerebrospinal fluid - A biochemical marker for axonal degeneration in Alzheimer disease?', *Molecular and Chemical Neuropathology*, 26(3), p 231–245.

Bard, A. J. and Faulkner, L. R.. (2001) *Electrochemical Methods, Fundamentals and Applications*, 2nd ed.

Bloom, G. S. (2014) 'Amyloid-β and tau: The trigger and bullet in Alzheimer disease pathogenesis', *JAMA Neurology*, 71(4), p 505–508

Braak, H. and Braak, E. (1991) 'Neuropathological stageing of Alzheimer-related changes', *Acta Neuropathologica*, 82, p 239–259

Bros, P., Delatour, V., Vialaret, J., Lalere, B., Barthelemy, N., Gabelle, A., Lehmann, S. and Hirtz, C. (2015) 'Quantitative detection of amyloid-β peptides by mass spectrometry: State of the art and clinical applications', *Clinical Chemistry and Laboratory Medicine*, 53, p 1483–1493

Buckley, R. F., Hanseeuw, B., Schultz, A. P., Vannini, P., Aghjayan, S. L., Properzi, M. J., Jackson, J. D., Mormino, E. C., Rentz, D. M., Sperling, R. A., Johnson, K. A. and Amariglio, R. E. (2017) 'Region-specific association of subjective cognitive decline with tauopathy independent of global β-amyloid burden', *JAMA Neurology*, 74(12), p 1455–1463.

Buée, L., Bussière, T., Buée-Scherrer, V., Delacourte, A. and Hof, P. R. (2000) 'Tau protein isoforms, phosphorylation and role in neurodegenerative disorders', *Brain Research Reviews*, 33(1), p 95–130.

Buée, L. and Delacourte, A. (1999) 'Comparative biochemistry of tau in progressive supranuclear palsy, corticobasal degeneration, FTDP-17 and Pick's disease', in *Brain Pathology*, 9, p 681–693

Bunker, J. M., Kamath, K., Wilson, L., Jordan, M. A. and Feinstein, S. C. (2006) 'FTDP-17 mutations compromise the ability of Tau to regulate microtubule dynamics in cells', *Journal of Biological Chemistry*, 281(17), p 11856–11863.

Campbell, D. P. and McCloskey, C. J. (2002) 'Interferometric Biosensors', in *Optical Biosensors*, 60(1), p 91–100.

del Campo, M., Jongbloed, W., Twaalfhoven, H. A. M., Veerhuis, R., Blankenstein, M. A. and Teunissen, C. E. (2015) 'Facilitating the validation of novel protein biomarkers for dementia: An optimal workflow for the development of sandwich immunoassays', *Frontiers in Neurology*, 6

Cao, L. L., Guan, P. P., Liang, Y. Y., Huang, X. S. and Wang, P. (2019) 'Calcium ions stimulate the hyperphosphorylation of tau by activating microsomal prostaglandin E synthase 1', *Frontiers in Aging Neuroscience*, 11

Carlin, N. and Martic-Milne, S. (2018) 'Anti-Tau Antibodies Based Electrochemical Sensor for Detection of Tau Protein Biomarkers', *Journal of The Electrochemical Society*, 165(12), p

G3018–G3025.

Carneiro, P., Loureiro, J., Delerue-Matos, C., Morais, S. and do Carmo Pereira, M. (2017) 'Alzheimer's disease: Development of a sensitive label-free electrochemical immunosensor for detection of amyloid beta peptide', *Sensors and Actuators, B: Chemical*. Elsevier B.V., 239, p 157–165.

Cedazo-Minguez, A. and Winblad, B. (2010) 'Biomarkers for Alzheimer's disease and other forms of dementia: clinical needs, limitations and future aspects', *Experimental gerontology*, 45(1), p 5–14.

Chen, C., Liu, W., Tian, S. and Hong, T. (2019) 'Novel surface-enhanced raman spectroscopy techniques for DNA, protein and drug detection', *Sensors (Switzerland)*, 19.

Chen, J. H., Lin, K. P. and Chen, Y. C. (2009) 'Risk factors for dementia', *Journal of the Formosan Medical Association*, p 754–764.

Choices, N. (2015) *What causes dementia? - Dementia guide - NHS Choices, NHS UK*. Available at: http://www.nhs.uk/conditions/dementia-guide/pages/causes-of-dementia.aspx.(Accessed 17 November 2015)

Choudhury, D., Xavier, P. L., Chaudhari, K., John, R., Dasgupta, A. K., Pradeep, T. and Chakrabarti, G. (2013) 'Unprecedented inhibition of tubulin polymerization directed by gold nanoparticles inducing cell cycle arrest and apoptosis', *Nanoscale*, 5(10), p 4476–4489.

Clavaguera, F., Bolmont, T., Crowther, R. A., Abramowski, D., Frank, S., Probst, A., Fraser, G., Stalder, A. K., Beibel, M., Staufenbiel, M., Jucker, M., Goedert, M. and Tolnay, M. (2009) 'Transmission and spreading of tauopathy in transgenic mouse brain', *Nature Cell Biology*, 11(7), p 909–913

Colin, M., Dujardin, S., Schraen-Maschke, S., Meno-Tetang, G., Duyckaerts, C., Courade, J. P. and Buée, L. (2020) 'From the prion-like propagation hypothesis to therapeutic strategies of anti-tau immunotherapy', *Acta Neuropathologica*, 139, p 3–25

Coon, K. D., Myers, A. J., Craig, D. W., Webster, J. A., Pearson, J. V., Lince, D. H., Zismann, V. L., Beach, T. G., Leung, D., Bryden, L., Halperin, R. F., Marlowe, L., Kaleem, M., Walker, D. G., Ravid, R., Heward, C. B., Rogers, J., Papassotiropoulos, A., Reiman, E. M., Hardy, J. and Stephan, D. A. (2007) 'A high-density whole-genome association study reveals that APOE is the major susceptibility gene for sporadic late-onset Alzheimer's disease', *Journal of Clinical Psychiatry*, 68(4), p 613–618.

Correia dos Santos, M. M., Paes de Sousa, P. M., Simões Gonçalves, M. L., Krippahl, L., Moura, J. J. G., Lojou, É. and Bianco, P. (2003) 'Electrochemical studies on small electron transfer proteins using membrane electrodes', *Journal of Electroanalytical Chemistry*, 541, p 153–162.

Cogger, N.D. and Evans, N. J. (1999) An introduction to Electrochemical Impedance Measurement, Solartron Analytical.

Craig-Schapiro, R., Fagan, A. M. and Holtzman, D. M. (2009) 'Biomarkers of Alzheimer's disease', *Neurobiology of Disease*. Elsevier Inc., 35(2), p 128–140.

Cross, G. H., Reeves, A. A., Brand, S., Popplewell, J. F., Peel, L. L., Swann, M. J. and Freeman, N. J. (2003) 'A new quantitative optical biosensor for protein characterisation',

Biosensors and Bioelectronics.

Cunningham, E. L., McGuinness, B., Herron, B. and Passmore, A. P. (2015) 'Dementia.', *The Ulster medical journal*, 84(2), p 79–87.

D'Souza, S. F. (2001) 'Microbial biosensors', *Biosensors and Bioelectronics*, 16(6), p 337–353.

Damborský, P., Švitel, J. and Katrlík, J. (2016) 'Optical biosensors', *Essays in Biochemistry*, 60(1), p 91–100.

Daniels, J. S. and Pourmand, N. (2007) 'Label-free impedance biosensors: Opportunities and challenges', *Electroanalysis*, p 1239–1257.

Dear, A. J., Michaels, T. C. T., Meisl, G., Klenerman, D., Wu, S., Perrett, S., Linse, S., Dobson, C. M. and Knowles, T. P. J. (2020) 'Kinetic diversity of amyloid oligomers', *Proceedings of the National Academy of Sciences of the United States of America*, 117(22).

Delaère, P., Duyckaerts, C., Masters, C., Beyreuther, K., Piette, F. and Hauw, J. J. (1990) 'Large amounts of neocortical βA4 deposits without neuritic plaques nor tangles in a psychometrically assessed, non-demented person', *Neuroscience Letters*, 116(1–2), p 87–93.

DeLoache, W. C., Russ, Z. N., Narcross, L., Gonzales, A. M., Martin, V. J. J. and Dueber, J. E. (2015) 'An enzyme-coupled biosensor enables (S)-reticuline production in yeast from glucose', *Nature Chemical Biology*, 11, p 465–471.

Doody, R. S., Thomas, R. G., Farlow, M., Iwatsubo, T., Vellas, B., Joffe, S., Kieburtz, K., Raman, R., Sun, X., Aisen, P. S., Siemers, E., Liu-Seifert, H. and Mohs, R. (2014) 'Phase 3 trials of solanezumab for mild-to-moderate alzheimer's disease', *New England Journal of Medicine*, 370(4), p 311–321.

Drummond, E. and Wisniewski, T. (2017) 'Alzheimer's disease: experimental models and reality', *Acta Neuropathologica*, 133, p 155–175

DuBoff, B., Götz, J. and Feany, M. B. (2012) 'Tau Promotes Neurodegeneration via DRP1 Mislocalization In Vivo', *Neuron*, 75(4), p 618–632.

Ellington, A. D. and Szostak, J. W. (1990) 'In vitro selection of RNA molecules that bind specific ligands', *Nature*, 346(6287), p 818–822.

Esteves-Villanueva, Jose O, Trzeciakiewicz, H. and Martic, S. (2014) 'A protein-based electrochemical biosensor for detection of tau protein, a neurodegenerative disease biomarker.', *The Analyst*, 139(11), p 2823–31.

Esteves-Villanueva, Jose O., Trzeciakiewicz, H. and Martic, S. (2014) 'A protein-based electrochemical biosensor for detection of tau protein, a neurodegenerative disease biomarker', *Analyst*, 139(11), p 2823–2831.

Fan, X., White, I. M., Shopova, S. I., Zhu, H., Suter, J. D. and Sun, Y. (2008) 'Sensitive optical biosensors for unlabeled targets: A review', *Analytica Chimica Acta*, 620(1–2), p 8–26.

Farrer, L. A., Myers, R. H., Cupples, L. A., St. George-Hyslop, P. H., Bird, T. D., Rossor, M. N., Mullan, M. J., Polinsky, R., Nee, L., Heston, L., Van Broeckhoven, C., Martin, J. J.,

Crapper-McLachlan, D. and Growdon, J. H. (1990) 'Transmission and age-at-onset patterns in familial alzheimer's disease: Evidence for heterogeneity', *Neurology*, 40(3), p 395–403.

Fossati, S., Ramos Cejudo, J., Debure, L., Pirraglia, E., Sone, J. Y., Li, Y., Chen, J., Butler, T., Zetterberg, H., Blennow, K. and de Leon, M. J. (2019) 'Plasma tau complements CSF tau and P-tau in the diagnosis of Alzheimer's disease', *Alzheimer's and Dementia: Diagnosis, Assessment and Disease Monitoring*, 11, p 483–492.

Fowler, J. M., Stuart, M. C. and Wong, D. K. Y. (2007) 'Self-assembled layer of thiolated protein G as an immunosensor scaffold', *Analytical Chemistry*, 79(1), p 350–354.

Franks, W., Schenker, I., Schmutz, P. and Hierlemann, A. (2005) 'Impedance characterization and modeling of electrodes for biomedical applications', *IEEE Transactions on Biomedical Engineering*, 52(7), p 1295–1302.

Fulga, T. A., Elson-Schwab, I., Khurana, V., Steinhilb, M. L., Spires, T. L., Hyman, B. T. and Feany, M. B. (2007) 'Abnormal bundling and accumulation of F-actin mediates tau-induced neuronal degeneration in vivo', *Nature Cell Biology*, 9(2), p 139–148.

Geekiyanage, H., Jicha, G. A., Nelson, P. T. and Chan, C. (2012) 'Blood serum miRNA: Non-invasive biomarkers for Alzheimer's disease', *Experimental Neurology*. Elsevier B.V., 235(2), p 491–496.

Gelfanova, V., Higgs, R. E., Dean, R. a, Holtzman, D. M., Farlow, M. R., Siemers, E. R., Boodhoo, A., Qian, Y.-W., He, X., Jin, Z., Fisher, D. L., Cox, K. L. and Hale, J. E. (2007) 'Quantitative analysis of amyloid-beta peptides in cerebrospinal fluid using immunoprecipitation and MALDI-Tof mass spectrometry.', *Briefings in functional genomics & proteomics*, 6(2), p 149–158.

Giacobini, E. and Gold, G. (2013) 'Alzheimer disease therapy - Moving from amyloid-β to tau', *Nature Reviews Neurology*, 9, p 677–686

Goedert, M. (1993) 'Tau protein and the neurofibrillary pathology of Alzheimer's disease', *Trends in Neurosciences*, 16, p 460–465

Goedert, M., Eisenberg, D. S. and Crowther, R. A. (2017) 'Propagation of Tau Aggregates and Neurodegeneration', *Annual Review of Neuroscience*, 40(1), p 189–210.

Grieshaber, D., Mackenzie, R., Vörös, J. and Reimhult, E. (2008) 'Electrochemical Biosensors -Sensor Principles and Architectures', *Sensors*, 8(January), p 1400–1458.

Grimnes, S. and Martinsen, Ø. G. (2014) 'Electrodes', in *Bioimpedance and Bioelectricity Basics*. 3rd ed. Academic Press

Guan, Y. S., Hu, Y., Zhang, H., Wu, G., Yan, H. and Ren, S. (2019) 'A highly conductive, transparent molecular charge-transfer salt with reversible lithiation', *Chemical Communications*, 55(50), p 7179–7182.

Hammond, J. L., Formisano, N., Estrela, P., Carrara, S. and Tkac, J. (2016) 'Electrochemical biosensors and nanobiosensors', *Essays in Biochemistry*, 60(1), p 69–80.

Hampel, H., Blennow, K., Shaw, L. M., Hoessler, Y. C., Zetterberg, H. and Trojanowski, J. Q. (2010) 'Total and phosphorylated tau protein as biological markers of Alzheimer's disease', *Experimental Gerontology*, p 30–40.

Hardy, J. A. and Higgins, G. A. (1992) 'Alzheimer's disease: The amyloid cascade hypothesis', *Science*, 256, p 184–185

Hardy, J. and Selkoe, D. J. (2002) 'The amyloid hypothesis of Alzheimer's disease: progress and problems on the road to therapeutics.', *Science (New York, N.Y.)*, 297(5580), p 353–356.

Hasegawa, M. (2016) 'Molecular mechanisms in the pathogenesis of alzheimer's disease and Tauopathies-Prion-Like seeded aggregation and phosphorylation', *Biomolecules*, 6.

Hata, M., Tanaka, T., Kazui, H., Ishii, R., Canuet, L., Pascual-Marqui, R. D., Aoki, Y., Ikeda, S., Sato, S., Suzuki, Y., Kanemoto, H., Yoshiyama, K. and Iwase, M. (2016) 'Cerebrospinal Fluid Biomarkers of Alzheimers Disease Correlate With Electroencephalography Parameters Assessed by Exact Low-Resolution Electromagnetic Tomography (eLORETA)', *Clinical EEG and Neuroscience*, 48(5), p 338–347.

Haun, J. B., Yoon, T. J., Lee, H. and Weissleder, R. (2010) 'Magnetic nanoparticle biosensors', *Wiley Interdisciplinary Reviews: Nanomedicine and Nanobiotechnology*, 2, p 291–304

Hediger, S., Fontannaz, J., Sayah, A., Hunziker, W. and Gijs, M. A. M. (2000) 'Biosystem for the culture and characterisation of epithelial cell tissues', *Sensors and Actuators B: Chemical*, 63(1), p 63–73.

Holmes, C. and Amin, J. (2016) 'Dementia', *Medicine*, 44(11), p 687–690.

Holzinger, M., Goff, A. Le and Cosnier, S. (2014) 'Nanomaterials for biosensing applications: A review', *Frontiers in Chemistry*, 2.

Hu, Y. Y., He, S. S., Wang, X., Duan, Q. H., Grundke-Iqbal, I., Iqbal, K. and Wang, J. (2002) 'Levels of nonphosphorylated and phosphorylated tau in cerebrospinal fluid of Alzheimer's disease patients : an ultrasensitive bienzyme-substrate-recycle enzyme-linked immunosorbent assay.', *The American journal of pathology*, 160(4), p 1269–78.

Humpel, C. (2011) 'Identifying and validating biomarkers for Alzheimer's disease', *Trends in Biotechnology*. Elsevier Ltd, 29(1), p 26–32.

Ingram, E. M. and Spillantini, M. G. (2002) 'Tau gene mutations: Dissecting the pathogenesis of FTDP-17', *Trends in Molecular Medicine*, p 555–562.

Iqbal, K., Liu, F. and Gong, C. X. (2016) 'Tau and neurodegenerative disease: The story so far', *Nature Reviews Neurology*, 12, p 15–27

Ittner, L. M. and Götz, J. (2011) 'Amyloid-β and tau--a toxic pas de deux in Alzheimer's disease.', *Nature reviews. Neuroscience*, 12(2), p 65–72.

Jacobs, C. B., Peairs, M. J. and Venton, B. J. (2010) 'Review: Carbon nanotube based electrochemical sensors for biomolecules', *Analytica Chimica Acta*, 662, p 105–127

Jahshan, A., Esteves-Villanueva, J. O. and Martic-Milne, S. (2016) 'Evaluation of ferritin and transferrin binding to tau protein', *Journal of Inorganic Biochemistry*, 162, p 127–134.

Jaworski, T., Dewachter, I., Lechat, B., Croes, S., Termont, A., Demedts, D., Borghgraef, P., Devijver, H., Filipkowski, R. K., Kaczmarek, L., Kügler, S. and Van Leuven, F. (2009) 'AAV-tau mediates pyramidal neurodegeneration by cell-cycle re-entry without

neurofibrillary tangle formation in wild-type mice', *PLoS ONE*, 4(10).

Jaworski, T., Dewachter, I., Seymour, C. M., Borghgraef, P., Devijver, H., Kügler, S. and Van Leuven, F. (2010) 'Alzheimer's disease: Old problem, new views from transgenic and viral models', *Biochimica et Biophysica Acta - Molecular Basis of Disease*, 1802, p 808–818

Jia, C. P., Zhong, X. Q., Hua, B., Liu, M. Y., Jing, F. X., Lou, X. H., Yao, S. H., Xiang, J. Q., Jin, Q. H. and Zhao, J. L. (2009) 'Nano-ELISA for highly sensitive protein detection', *Biosensors and Bioelectronics*, 24(9), p 2836–2841.

Jiang, Y., Mullaney, K. A., Peterhoff, C. M., Che, S., Schmidt, S. D., Boyer-Boiteau, A., Ginsberg, S. D., Cataldo, A. M., Mathews, P. M. and Nixon, R. A. (2010) 'Alzheimer's-related endosome dysfunction in Down syndrome is Abeta-independent but requires APP and is reversed by BACE-1 inhibition.', *Proceedings of the National Academy of Sciences of the United States of America*, 107(4), p 1630–5.

K'Owino, I. O. and Sadik, O. A. (2005) 'Impedance spectroscopy: A powerful tool for rapid biomolecular screening and cell culture monitoring', *Electroanalysis*, 17, p 2101–2113

Kadavath, H., Hofele, R. V., Biernat, J., Kumar, S., Tepper, K., Urlaub, H., Mandelkow, E. and Zweckstetter, M. (2015) 'Tau stabilizes microtubules by binding at the interface between tubulin heterodimers', *Proceedings of the National Academy of Sciences of the United States of America*, 112, p 7501–7506

Kametani, F. and Hasegawa, M. (2018) 'Reconsideration of amyloid hypothesis and tau hypothesis in Alzheimer's disease', *Frontiers in Neuroscience*, 12.

Kang, C. C., Lin, J. M. G., Xu, Z., Kumar, S. and Herr, A. E. (2014) 'Single-cell western blotting after whole-cell imaging to assess cancer chemotherapeutic response', *Analytical Chemistry*, 86(20), p 10429–10436.

Karunakaran, C., Rajkumar, R. and Bhargava, K. (2015) 'Introduction to Biosensors', *Biosensors and Bioelectronics*, p 1–68.

Kassanos, P., Demosthenous, A. and Bayford, R. H. (2008) 'Comparison of tetrapolar injection-measurement techniques for coplanar affinity-based impedimetric immunosensors', *2008 IEEE-BIOCAS Biomedical Circuits and Systems Conference,* p 317–320.

Kassanos, P., Iles, R. K., Bayford, R. H. and Demosthenous, A. (2008) 'Towards the development of an electrochemical biosensor for hCGbeta detection.', *Physiological measurement*, 29(6), p S241-54.

Kim, H. J., Chae, S. C., Lee, D. K., Chromy, B., Lee, S. C., Park, Y. C., Klein, W. L., Krafft, G. A. and Hong, S. T. (2003) 'Selective neuronal degeneration induced by soluble oligomeric amyloid beta protein.', *The FASEB journal : official publication of the Federation of American Societies for Experimental Biology*, 17(1), p 118–120.

Kim, J., Chakrabarty, P., Hanna, A., March, A., Dickson, D. W., Borchelt, D. R., Golde, T. and Janus, C. (2013) 'Normal cognition in transgenic BRI2-Aβ mice', *Molecular Neurodegeneration*, 8(1).

Kim, S., Wark, A. W. and Lee, H. J. (2016) 'Femtomolar Detection of Tau Proteins in Undiluted Plasma Using Surface Plasmon Resonance', *Analytical Chemistry*, 88(15), p 7793–7799.

Kissinger, P. T. (2005) 'Biosensors - A perspective', *Biosensors and Bioelectronics*, 20(12), p 2512–2516.

Kathryn J. B., Hyoung-gon L., George P., Mark A. S. and Gemma C. (2009). Behavioral Testing and Considerations.' 2nd ed. CRC Press/Taylor & Francis

Knudsen, S. M., Lee, J., Ellington, A. D. and Savran, C. A. (2006) 'Ribozyme-mediated signal augmentation on a mass-sensitive biosensor', *Journal of the American Chemical Society*, 128(50), p 15936–15937.

Knutson, S., Raja, E., Bomgarden, R., Nlend, M., Chen, A., Kalyanasundaram, R. and Desai, S. (2016) 'Development and evaluation of a fluorescent antibody-drug conjugate for molecular imaging and targeted therapy of pancreatic cancer', *PLoS ONE*, 11(6).

Komarova, N. L. and Thalhauser, C. J. (2011) 'High degree of heterogeneity in Alzheimer's disease progression patterns', *PLoS Computational Biology*, 7(11).

Kovacs, G. G. (2015) 'Invited review: Neuropathology of tauopathies: Principles and practice', *Neuropathology and Applied Neurobiology*, 41, p 3–23

Koyama, A., O'Brien, J., Weuve, J., Blacker, D., Metti, A. L. and Yaffe, K. (2013) 'The role of peripheral inflammatory markers in dementia and Alzheimer's disease: a meta-analysis.', *The journals of gerontology. Series A, Biological sciences and medical sciences*, 68(4), p 433–40.

Kunzelmann, S., Solscheid, C. and Webb, M. R. (2014) 'Fluorescent biosensors: design and application to motor proteins.', *EXS*, 105, p 25–47

LaFerla, F. M., Green, K. N. and Oddo, S. (2007) 'Intracellular amyloid-beta in Alzheimer's disease.', *Nature reviews. Neuroscience*, 8(7), p 499–509.

Lai, R. Y., Seferos, D. S., Heeger, A. J., Bazan, G. C. and Plaxco, K. W. (2006) 'Comparison of the signaling and stability of electrochemical DNA sensors fabricated from 6- or 11-carbon self-assembled monolayers', *Langmuir*, 22(25), p 10796–10800.

Lee, E. G., Park, K. M., Jeong, J. Y., Lee, S. H., Baek, J. E., Lee, H. W., Jung, J. K. and Chung, B. H. (2011) 'Carbon nanotube-assisted enhancement of surface plasmon resonance signal', *Analytical Biochemistry*, 408(2), p 206–211.

Lee, V. M.-Y., Goedert, M. and Trojanowski, J. Q. (2001) 'Neurodegenerative Tauopathies', *Annual Review of Neuroscience*, 24, p 1121–1159

Lenigk, R., Lam, E., Lai, A., Wang, H., Han, Y., Carlier, P. and Renneberg, R. (2000) 'Enzyme biosensor for studying therapeutics of Alzheimer's disease', *Biosensors and Bioelectronics*, 15(9–10), p 541–547.

Leroy, K., Ando, K., Laporte, V., Dedecker, R., Suain, V., Authelet, M., Héraud, C., Pierrot, N., Yilmaz, Z., Octave, J. N. and Brion, J. P. (2012) 'Lack of tau proteins rescues neuronal cell death and decreases amyloidogenic processing of APP in APP/PS1 mice', *American Journal of Pathology*. Elsevier Inc., 181(6), p 1928–1940.

Li, D., Scarano, S., Lisi, S., Palladino, P. and Minunni, M. (2018) 'Real-time tau protein detection by sandwich-based piezoelectric biosensing: Exploring tubulin as a mass enhancer', *Sensors (Switzerland)*, 18(4).

Li, G. and Miao, P. (2013) 'Electrochemical Analysis of Proteins and Cells', *Electrochemical Analysis of Protein and Cells*, p 1–18.

Li, R., Huang, H., Zhang, X., Ye, S. and Li, Q. (2017) 'Monoclonal antibody based Dot-ELISA and indirect fluorescence antibody technique for detecting Edwardsiella ictaluri infection in yellow catfish (Pelteobagrus fulvidraco)', *Aquaculture and Fisheries*, 2(5), p 207–212.

Li, S. S., Lin, C. W., Wei, K. C., Huang, C. Y., Hsu, P. H., Liu, H. L., Lu, Y. J., Lin, S. C., Yang, H. W. and Ma, C. C. M. (2016) 'Non-invasive screening for early Alzheimer's disease diagnosis by a sensitively immunomagnetic biosensor', *Scientific Reports*, 6.

Li, Y., Schluesener, H. J. and Xu, S. (2010) 'Gold nanoparticle-based biosensors', *Gold Bulletin*, 43(1), p 29–41.

Li, L., Jiang, Y., Hu, W., Tung, Y. C., Dai, C., Chu, D., … Liu, F. (2019). Pathological Alterations of Tau in Alzheimer's Disease and 3xTg-AD Mouse Brains. *Molecular Neurobiology*, 56(9), p 6168–6183.

Li, Z., Deng, M., Huang, F., Jin, C., Sun, S., Chen, H., Liu, X., He, L., Sadek, A. H. and Zhang, C. C. (2020) 'Correction to: LILRB4 ITIMs mediate the T cell suppression and infiltration of acute myeloid leukemia cells, *Cellular and Molecular Immunology*, 17(3), p 272-282 .

Lifke, V., Kollmorgen, G., Manuilova, E., Oelschlaegel, T., Hillringhaus, L., Widmann, M., von Arnim, C. A. F., Otto, M., Christenson, R. H., Powers, J. L., Shaw, L. M., Hansson, O., Doecke, J. D., Li, Q. X., Teunissen, C., Tumani, H. and Blennow, K. (2019) 'Elecsys® Total-Tau and Phospho-Tau (181P) CSF assays: Analytical performance of the novel, fully automated immunoassays for quantification of tau proteins in human cerebrospinal fluid', *Clinical Biochemistry*, 72, p 30–38.

Lisdat, F. and Schäfer, D. (2008) 'The use of electrochemical impedance spectroscopy for biosensing', *Analytical and Bioanalytical Chemistry*, 391(5), p 1555–1567.

Lisi, S., Scarano, S., Fedeli, S., Pascale, E., Cicchi, S., Ravelet, C., Peyrin, E. and Minunni, M. (2017) 'Toward sensitive immuno-based detection of tau protein by surface plasmon resonance coupled to carbon nanostructures as signal amplifiers', *Biosensors and Bioelectronics*, 93, p 289–292.

Liu, A., Wang, K., Weng, S., Lei, Y., Lin, L., Chen, W., Lin, X. and Chen, Y. (2012) 'Development of electrochemical DNA biosensors', *TrAC - Trends in Analytical Chemistry*, p 101–111.

Liu, F. and Gong, C. X. (2008) 'Tau exon 10 alternative splicing and tauopathies', *Molecular Neurodegeneration*, 3(1).

Liu, Y., Qing, H. and Deng, Y. (2014) 'Biomarkers in Alzheimer's disease analysis by mass spectrometry-based proteomics', *International Journal of Molecular Sciences*, 15(5), p 7865–7882.

Love, J. C., Estroff, L. A., Kriebel, J. K., Nuzzo, R. G. and Whitesides, G. M. (2005) 'Self-assembled monolayers of thiolates on metals as a form of nanotechnology', *Chemical Reviews*, 105, p 1103–1169

Loy, C. T., Schofield, P. R., Turner, A. M. and Kwok, J. B. J. (2014) 'Genetics of dementia', *The Lancet*, p 828–840.

Luk, C., Giovannoni, G., Williams, D. R., Lees, A. J. and de Silva, R. (2009) 'Development of a sensitive ELISA for quantification of three- and four-repeat tau isoforms in tauopathies', *Journal of Neuroscience Methods*, 180(1), p 34–42.

Luppa, P. B., Sokoll, L. J. and Chan, D. W. (2001) 'Immunosensors—principles and applications to clinical chemistry', *Clinica Chimica Acta*, 314(1–2), p 1–26.

Ma, F., Li, C. chen and Zhang, C. yang (2018) 'Development of quantum dot-based biosensors: principles and applications', *Journal of Materials Chemistry B*, 6, p 6173–6190

Ma, H., Su, Y. and Nathan, A. (2015a) 'Cell constant studies of bipolar and tetrapolar electrode systems for impedance measurement', *Sensors and Actuators, B: Chemical*. Elsevier B.V., 221, p 1264–1270.

Ma, H., Su, Y. and Nathan, A. (2015b) 'Cell constant studies of bipolar and tetrapolar electrode systems for impedance measurement', *Sensors and Actuators, B: Chemical*, 221, p 1264–1270.

Mahmood, T. and Yang, P. C. (2012) 'Western blot: Technique, theory, and trouble shooting', *North American Journal of Medical Sciences*, 4(9), p 429–434.

Manickam, A., Johnson, C. A., Kavusi, S. and Hassibi, A. (2012) 'Interface design for CMOS-integrated Electrochemical Impedance Spectroscopy (EIS) biosensors', *Sensors (Switzerland)*, 12(11), p 14467–14488.

Mariani, S., Scarano, S., Spadavecchia, J. and Minunni, M. (2015) 'A reusable optical biosensor for the ultrasensitive and selective detection of unamplified human genomic DNA with gold nanostars', *Biosensors and Bioelectronics*, 74, p 981–988.

Martić, S., Beheshti, S., Kraatz, H. B. and Litchfield, D. W. (2012) 'Electrochemical investigations of tau protein phosphorylations and interactions with pin1', *Chemistry and Biodiversity*, 9(9), p 1693–1702.

Martić, S., Beheshti, S., Rains, M. K. and Kraatz, H. B. (2012) 'Electrochemical investigations into Tau protein phosphorylations', *Analyst*, 137(9), p 2042–2046.

Martic, S., Rains, M. K. and Kraatz, H. B. (2013) 'Probing copper/tau protein interactions electrochemically', *Analytical Biochemistry*. Elsevier Inc., 442(2), p 130–137.

Mammadova, N., Ghaisas, S., Zenitsky, G., Sakaguchi, D. S., Kanthasamy, A. G., Greenlee, J. J., & West Greenlee, M. H. (2017). Lasting Retinal Injury in a Mouse Model of Blast-Induced Trauma. *American Journal of Pathology*, 187(7), p 1459–1472.

Masson, J. F., Battaglia, T. M., Cramer, J., Beaudoin, S., Sierks, M. and Booksh, K. S. (2006) 'Reduction of nonspecific protein binding on surface plasmon resonance biosensors', *Analytical and Bioanalytical Chemistry*, 386(7–8), p 1951–1959.

Mattsson, N., Andreasson, U., Persson, S., Carrillo, M. C., Collins, S., Chalbot, S., Cutler, N., Dufour-Rainfray, D., Fagan, A. M., Heegaard, N. H. H., Hsiung, G.-Y. R., Hyman, B., Iqbal, K., Lachno, D. R., Lleó, A., Lewczuk, P., Molinuevo, J. L., Parchi, P., Regeniter, A., Rissman, R., Rosenmann, H., Sancesario, G., Schröder, J., Shaw, L. M., Teunissen, C. E.,

Trojanowski, J. Q., Vanderstichele, H., Vandijck, M., Verbeek, M. M., Zetterberg, H., Blennow, K. and Käser, S. A. (2013) 'CSF biomarker variability in the Alzheimer's Association quality control program on behalf of the Alzheimer's Association QC Program Work Group', *Alzheimers Dement*, 9(3), p 251–261.

Mayeux, R. and Schupf, N. (2011) 'Blood-based biomarkers for Alzheimer's disease: Plasma Aβ40 and Aβ42, and genetic variants', *Neurobiology of Aging*, p S10–S19.

McGeer, P. L. and McGeer, E. G. (2013) 'The amyloid cascade-inflammatory hypothesis of Alzheimer disease: Implications for therapy', *Acta Neuropathologica*, 126, p 479–497

Mirsky, V. M., Riepl, M. and Wolfbeis, O. S. (1997) 'Capacitive monitoring of protein immobilization and antigen-antibody reactions on monomolecular alkylthiol films on gold electrodes', *Biosensors and Bioelectronics*, 12(9–10), p 977–989.

Mishra, G. K., Sharma, V. and Mishra, R. K. (2018) 'Electrochemical aptasensors for food and environmental safeguarding: A review', *Biosensors*, 8.

Michalski, B., Corrada, M. M., Kawas, C. H., & Fahnestock, M. (2015). Brain-derived neurotrophic factor and TrkB expression in the "oldest-old," the 90+ Study: Correlation with cognitive status and levels of soluble amyloid-beta. *Neurobiology of Aging*, 36(12), p 3130–3139.

Mohanty, S. P. (2015) 'Biosensors : A Tutorial Review Biosensors : A Tutorial Review', *IEEE Potentials*, 25, p 35–40.

Moore, B. C. (2009) 'Your first choice for antibodies! Introduction to Western Blotting'. Oxford :MorphoSys UK Ltd.

Nakamura, A., Kaneko, N., Villemagne, V. L., Kato, T., Doecke, J., Doré, V., Fowler, C., Li, Q. X., Martins, R., Rowe, C., Tomita, T., Matsuzaki, K., Ishii, Kenji, Ishii, Kazunari, Arahata, Y., Iwamoto, S., Ito, K., Tanaka, K., Masters, C. L. and Yanagisawa, K. (2018) 'High performance plasma amyloid-β biomarkers for Alzheimer's disease', *Nature*, 554(7691), p 249–254.

Neubert, H., Jacoby, E. S., Bansal, S. S., Iles, R. K., Cowan, D. A. and Kicman, A. T. (2002) 'Enhanced affinity capture MALDI-TOF MS: Orientation of an immunoglobulin G using recombinant protein G', *Analytical Chemistry*, 74(15), p 3677–3683.

Ng, S. Y., Reboud, J., Wang, K. Y. P., Tang, K. C., Zhang, L., Wong, P., Moe, K. T., Shim, W. and Chen, Y. (2010) 'Label-free impedance detection of low levels of circulating endothelial progenitor cells for point-of-care diagnosis', *Biosensors and Bioelectronics*, 25(5), p 1095–1101.

Nguyen, H. H., Park, J., Kang, S. and Kim, M. (2015) 'Surface plasmon resonance: A versatile technique for biosensor applications', *Sensors (Switzerland)*, 15, p 10481–10510

Ocvirk, G., Buck, H. and DuVall, S. H. (2017) 'Electrochemical glucose biosensors for diabetes care', *Bioanalytical Reviews*, 6.

Oh, B. K., Lee, W., Kim, Y. K., Lee, W. H. and Choi, J. W. (2004) 'Surface plasmon resonance immunosensor using self-assembled protein G for the detection of Salmonella paratyphi', *Journal of Biotechnology*, 111(1), p 1–8.

Okamura, N., Harada, R., Furumoto, S., Arai, H., Yanai, K. and Kudo, Y. (2014) 'Tau PET Imaging in Alzheimer's Disease', *Current Neurology and Neuroscience Reports*, 14.

Olczak, M., Niderla-Bielińska, J., Kwiatkowska, M., Samojłowicz, D., Tarka, S. and Wierzba-Bobrowicz, T. (2017) 'Tau protein (MAPT) as a possible biochemical marker of traumatic brain injury in postmortem examination', *Forensic Science International*, 280, p 1–7.

Olsen, B., Axelsson-Olsson, D., Thelin, A. and Weiland, O. (2006) 'Unexpected high prevalence of IgG-antibodies to hepatitis E virus in Swedish pig farmers and controls', *Scandinavian Journal of Infectious Diseases*, 38(1), p 55–58.

Ono, K., Condron, M. M. and Teplow, D. B. (2009) 'Structure-neurotoxicity relationships of amyloid β-protein oligomers', *Proceedings of the National Academy of Sciences of the United States of America*, 106(35), p 14745–14750.

Ono, T., Yamauchi, L., Miyasaka, T., Takashima, A. and Noji, H. (2014) 'Single-Molecule Assay for Tau Protein Using Digital Elisa System', p 2566–2567.

Ostrowitzki, S., Deptula, D., Thurfjell, L., Barkhof, F., Bohrmann, B., Brooks, D. J., Klunk, W. E., Ashford, E., Yoo, K., Xu, Z. X., Loetscher, H. and Santarelli, L. (2012) 'Mechanism of amyloid removal in patients with Alzheimer disease treated with gantenerumab', *Archives of Neurology*, 69(2), p 198–207.

Ou, L., Song, B., Liang, H., Liu, J., Feng, X., Deng, B., Sun, T. and Shao, L. (2016) 'Toxicity of graphene-family nanoparticles: a general review of the origins and mechanisms', *Particle and Fibre Toxicology*. Particle and Fibre Toxicology, 13(1), p. 57.

Palop, J. J. and Mucke, L. (2010) 'Amyloid-beta-induced neuronal dysfunction in Alzheimer's disease: from synapses toward neural networks.', *Nature neuroscience*, 13(7), p 812–818.

Park, S. (2003) 'With impedance data, a complete description of an electrochemical system is possible.', *Society*, p 455–461.

Parsons, C. G., Danysz, W., Dekundy, A. and Pulte, I. (2013) 'Memantine and cholinesterase inhibitors: Complementary mechanisms in the treatment of Alzheimer's disease', *Neurotoxicity Research*, 24, p 358–369

Pekeles, H., Qureshi, H. Y., Paudel, H. K., Schipper, H. M., Gornistky, M. and Chertkow, H. (2018) 'Development and validation of a salivary tau biomarker in Alzheimer's disease', *Alzheimer's & Dementia: Diagnosis, Assessment & Disease Monitoring*, p 1–8.

Pérez-Ruiz, E., Decrop, D., Ven, K., Tripodi, L., Leirs, K., Rosseels, J., van de Wouwer, M., Geukens, N., De Vos, A., Vanmechelen, E., Winderickx, J., Lammertyn, J. and Spasic, D. (2018) 'Digital ELISA for the quantification of attomolar concentrations of Alzheimer's disease biomarker protein Tau in biological samples', *Analytica Chimica Acta*, 1015, p 74–81.

Pohanka, M. (2018) 'Overview of piezoelectric biosensors, immunosensors and DNA sensors and their applications', *Materials*, 11.

Porcelli, E. B. and Filho, V. S. (2018) 'Induction of Forces at Distance Performed by Piezoelectric Materials', *Journal of Power and Energy Engineering,* 06(01), p 33–50.

Portelius, E., Hansson, S. F., Tran, A. J., Zetterberg, H., Grognet, P., Vanmechelen, E., Höglund, K., Brinkmalm, G., Westman-Brinkmalm, A., Nordhoff, E., Blennow, K. and Gobom, J. (2008) 'Characterization of tau in cerebrospinal fluid using mass spectrometry', *Journal of Proteome Research*, 7(5), p 2114–2120.

Ranga, n. (2011) *5 Types of Elisa Tests | Their Differences and Principle Explained.* Available at: http://www.studyread.com/types-of-elisa. (Accessed 11th December 2015)

Rahman, A. R. A., Lo, C. M. and Bhansali, S. (2006) 'A micro-electrode array biosensor for impedance spectroscopy of human umbilical vein endothelial cells', *Sensors and Actuators B-Chemical*, 118(1–2), p 115–120.

Rains, M. K., Martić, S., Freeman, D. and Kraatz, H. B. (2013) 'Electrochemical investigations into kinase-catalyzed transformations of tau protein', *ACS Chemical Neuroscience*, 4(8), p 1194–1203.

Ramalingam, V. (2019) 'Multifunctionality of gold nanoparticles: Plausible and convincing properties', *Advances in Colloid and Interface Science*, 271.

Ramanathan, K. and Danielsson, B. (2001) 'Principles and applications of thermal biosensors', *Biosensors and Bioelectronics*, 16(6), p 417–423.

Rapoport, M., Dawson, H. N., Binder, L. I., Vitek, M. P. and Ferreira, A. (2002) 'Tau is essential to β-amyloid-induced neurotoxicity', *Proceedings of the National Academy of Sciences of the United States of America*, 99(9), p 6364–6369.

Ricciarelli, R. and Fedele, E. (2017) 'The Amyloid Cascade Hypothesis in Alzheimer's Disease: It's Time to Change Our Mind', *Current Neuropharmacology*, 15(6).

Rio-Echevarria, I. M., Ponti, J., Urbán, P. and Gilliland, D. (2019) 'Vial sonication and ultrasonic immersion probe sonication to generate stable dispersions of multiwall carbon nanotubes for physico-chemical characterization and biological testing', *Nanotoxicology*, 13(7), p 923–937.

Rissin, D. M., Kan, C. W., Campbell, T. G., Howes, S. C., Fournier, D. R., Song, L., Piech, T., Patel, P. P., Chang, L., Rivnak, A. J., Ferrell, E. P., Randall, J. D., Provuncher, G. K., Walt, D. R. and Duffy, D. C. (2010) 'Single-molecule enzyme-linked immunosorbent assay detects serum proteins at subfemtomolar concentrations', *Nature Biotechnology*, 28(6), p 595–599.

Roberson, E. D., Scearce-Levie, K., Palop, J. J., Yan, F., Cheng, I. H., Wu, T., Gerstein, H., Yu, G. Q. and Mucke, L. (2007) 'Reducing endogenous tau ameliorates amyloid β-induced deficits in an Alzheimer's disease mouse model', *Science*, 316(5825), p 750–754.

Rushworth, J. V., Ahmed, A., Griffiths, H. H., Pollock, N. M., Hooper, N. M. and Millner, P. A. (2014) 'A label-free electrical impedimetric biosensor for the specific detection of Alzheimer's amyloid-beta oligomers', *Biosensors and Bioelectronics*, 56, p 83–90.

Rusmini, F., Zhong, Z. and Feijen, J. (2007) 'Protein immobilization strategies for protein biochips', *Biomacromolecules*, p 1775–1789.

Salloway, S., Sperling, R., Fox, N. C., Blennow, K., Klunk, W., Raskind, M., Sabbagh, M., Honig, L. S., Porsteinsson, A. P., Ferris, S., Reichert, M., Ketter, N., Nejadnik, B., Guenzler, V., Miloslavsky, M., Wang, D., Lu, Y., Lull, J., Tudor, I. C., Liu, E., Grundman, M., Yuen,

E., Black, R. and Brashear, H. R. (2014) 'Two phase 3 trials of Bapineuzumab in mild-to-moderate Alzheimer's disease', *New England Journal of Medicine*, 370(4), p 322–333.

Schemmerer, M., Rauh, C., Jilg, W. and Wenzel, J. J. (2017) 'Time course of hepatitis E-specific antibodies in adults', *Journal of Viral Hepatitis*, 24(1), p 75–79.

Schönheit, B., Zarski, R. and Ohm, T. G. (2004) 'Spatial and temporal relationships between plaques and tangles in Alzheimer-pathology', *Neurobiology of Aging*, 25, p 697–711

Sergeant, N., Bussiere, T., Vermersch, P., Lejeune, J. P. and Delacourte, A. (1995) 'Isoelectric point differentiates PHF-tau from biopsy-derived human brain tau proteins', *Neuroreport*, p 2217–2220.

Sergeant, N., Delacourte, A. and Buée, L. (2005) 'Tau protein as a differential biomarker of tauopathies', *Biochimica et Biophysica Acta - Molecular Basis of Disease*, 1739(2), p 179–197.

Shabaninejad, Z., Yousefi, F., Movahedpour, A., Ghasemi, Y., Dokanehiifard, S., Rezaei, S., Aryan, R., Savardashtaki, A. and Mirzaei, H. (2019) 'Electrochemical-based biosensors for microRNA detection: Nanotechnology comes into view', *Analytical Biochemistry*, 581.

Sharma, S. K., Sehgal, N. and Kumar, A. (2003) 'Biomolecules for development of biosensors and their applications', *Current Applied Physics*, 3(2–3), p 307–316.

Shui, B., Tao, D., Florea, A., Cheng, J., Zhao, Q., Gu, Y., Li, W., Jaffrezic-Renault, N., Mei, Y. and Guo, Z. (2018) 'Biosensors for Alzheimer's disease biomarker detection: A review', *Biochimie*, 147, p 13–24

Sjögren, M, Vanderstichele, H., Agren, H., Zachrisson, O., Edsbagge, M., Wikkelsø, C., Sjögren, M., Vanderstichele, H., Ågren, H., Zachrisson, O., Edsbagge, M., Wilkkelsø, C., Skoog, I., Wallin, A., Wahlund, L. O., Marcusson, J., Nägga, K., Andreasen, N., Davidsson, P., Vanmechelen, E. and Blennow, K. (2001) 'Tau and Aβ42 in cerebrospinal fluid from healthy adults 21-93 years of age: Establishment of reference values', *Clinical Chemistry*, 47, p 1776–1781.

Snyder, H. M., Carrillo, M. C., Grodstein, F., Henriksen, K., Jeromin, A., Lovestone, S., Mielke, M. M., O'Bryant, S., Sarasa, M., Sjøgren, M., Soares, H., Teeling, J., Trushina, E., Ward, M., West, T., Bain, L. J., Shineman, D. W., Weiner, M. and Fillit, H. M. (2014) 'Developing novel blood-based biomarkers for Alzheimer's disease', *Alzheimer's and Dementia*. Elsevier Ltd, 10(1), p 109–114.

Sok, V. and Fragoso, A. (2019) 'Amperometric biosensor for glyphosate based on the inhibition of tyrosinase conjugated to carbon nano-onions in a chitosan matrix on a screen-printed electrode', *Microchimica Acta*, 186 (6).

Sparks, D. L., Kryscio, R. J., Sabbagh, M. N., Ziolkowski, C., Lin, Y., Sparks, L. M., Liebsack, C. and Johnson-Traver, S. (2012) 'Tau is reduced in AD plasma and validation of employed ELISA methods', *Am J Neurodegener Dis*, 1(1), p 99–106.

Spillantini, M. G. and Goedert, M. (1998) 'TAU PROTEIN PATHOLOGY IN NEURODEGENERATIVE DISEASES [Review]', *Trends in Neurosciences*, 21(10), p 428–433.

Spillantini, M. G., Goedert, M., Crowther, R. A., Murrell, J. R., Farlow, M. R. and Ghetti, B.

(1997) 'Familial multiple system tauopathy with presenile dementia: a disease with abundant neuronal and glial tau filaments.', *Proceedings of the National Academy of Sciences of the United States of America*, 94(8), p 4113–8.

Spillantini, M. G., Murrell, J. R., Goedert, M., Farlow, M. R., Klug, A. and Ghetti, B. (1998) 'Mutation in the tau gene in familial multiple system tauopathy with presenile dementia', *Proceedings of the National Academy of Sciences of the United States of America*, 95(13), p 7737–7741

Spitznagel, T. M. and Clark, D. S. (1993) 'Surface-density and orientation effects on immobilized antibodies and antibody fragments.', *Bio/technology (Nature Publishing Company)*, 11(7), p 825–9.

Špringer, T., Hemmerová, E., Finocchiaro, G., Krištofiková, Z., Vyhnálek, M. and Homola, J. (2020) 'Surface plasmon resonance biosensor for the detection of tau-amyloid β complex', *Sensors and Actuators, B: Chemical*, 316.

St-Amour, I., Paré, I., Alata, W., Coulombe, K., Ringuette-Goulet, C., Drouin-Ouellet, J., Vandal, M., Soulet, D., Bazin, R. and Calon, F. (2013) 'Brain bioavailability of human intravenous immunoglobulin and its transport through the murine blood-brain barrier', *Journal of Cerebral Blood Flow and Metabolism*, 33(12), p 1983–1992.

Stacey, W. (2015) 'Clearly, graphene is the new gold', *Epilepsy Currents*, 15(6), p 351–352.

Stegurová, L., Dráberová, E., Bartos, A., Dráber, Pavel, Řípová, D. and Dráber, Petr (2014) 'Gold nanoparticle-based immuno-PCR for detection of tau protein in cerebrospinal fluid', *Journal of Immunological Methods*, 406, p 137–142.

Stephen, S., Gunasekaran, D. and Anitharaj, V. (2018) 'Application of enzyme linked immunosorbent assay (Elisa) and indirect fluorescent antibody test for serodiagnosis of acute scrub typhus in and around Puducherry, India', *Journal of Clinical and Diagnostic Research*, 12(11).

Stopford, C. L., Snowden, J. S., Thompson, J. C. and Neary, D. (2008) 'Variability in cognitive presentation of Alzheimer's disease', *Cortex*, 44(2), p 185–195.

Stravalaci, M., Beeg, M., Salmona, M. and Gobbi, M. (2011) 'Use of surface plasmon resonance to study the elongation kinetics and the binding properties of the highly amyloidogenic Aβ1-42 peptide, synthesized by depsi-peptide technique', *Biosensors and Bioelectronics*, 26(5), p 2772–2775.

Strimbu, K. and Tavel, J. a (2011) 'What are Biomarkers?', *Curr Opin HIV AIDS*, 5(6), p 463–466.

Stryer, L. (1995) *Biochemistry*, 4th ed. New York: W.H.Freeman & Colorado LTD

Stulík, K., Amatore, C., Holub, K., Marecek, V. and Kutner, W. (2000) 'Microelectrodes. Definitions, characterization, and applications (Technical report)', *Pure and Applied Chemistry*, 72(8), p 1483–92.

Su, L., Jia, W., Hou, C. and Lei, Y. (2011) 'Microbial biosensors: A review', *Biosensors and Bioelectronics*. Elsevier B.V., 26(5), p 1788–1799.

Suni, I. I. (2008) 'Impedance methods for electrochemical sensors using nanomaterials',

TrAC - Trends in Analytical Chemistry, 27(7), p 604–611

Takahashi, M., Miyata, H., Kametani, F., Nonaka, T., Akiyama, H., Hisanaga, S. ichi and Hasegawa, M. (2015) 'Extracellular association of APP and tau fibrils induces intracellular aggregate formation of tau', *Acta Neuropathologica*, 129(6), p 895–907.

Takeda, S. (2019) 'Tau Propagation as a Diagnostic and Therapeutic Target for Dementia: Potentials and Unanswered Questions', *Frontiers in Neuroscience*, 13, p 1–8.

Tang, H., Chen, J., Nie, L., Kuang, Y. and Yao, S. (2007) 'A label-free electrochemical immunoassay for carcinoembryonic antigen (CEA) based on gold nanoparticles (AuNPs) and nonconductive polymer film', *Biosensors and Bioelectronics*, 22(6), p 1061–1067.

Tao, D., Shui, B., Gu, Y., Cheng, J., Zhang, W., Jaffrezic-Renault, N., Song, S. and Guo, Z. (2019) 'Development of a label-free electrochemical aptasensor for the detection of Tau381 and its preliminary application in AD and non-AD patients' sera', *Biosensors*, 9(3).

Tektronix. (2015). Performing Cyclic Voltammetry Measurements Using Model 2450 or 2460, p 1–8.

Thévenot, D. R., Toth, K., Durst, R. A. and Wilson, G. S. (2001) 'Electrochemical biosensors: Recommended definitions and classification', *Biosensors and Bioelectronics*, 16(1–2), p 121–131.

The University of Arizona (College of medicine phoenix). 2019, Molecular Discovery Core - Pioneer FE SPR System. Available at: https://phoenixmed.arizona.edu/mcd/instrumentation/pioneer: (Accessed 23rd october 2020)

Tombelli, S., Minunni, M. and Mascini, M. (2005) 'Piezoelectric biosensors: Strategies for coupling nucleic acids to piezoelectric devices', *Methods*, 37(1), p 48–56.

Trazzi, S., Fuchs, C., Valli, E., Perini, G., Bartesaghi, R. and Ciani, E. (2013) 'The amyloid precursor protein (APP) triplicated gene impairs neuronal precursor differentiation and neurite development through two different domains in the ts65dn mouse model for down syndrome', *Journal of Biological Chemistry*, 288(29), p 20817–20829.

Trushina, N. I., Bakota, L., Mulkidjanian, A. Y. and Brandt, R. (2019) 'The Evolution of Tau Phosphorylation and Interactions', *Frontiers in Aging Neuroscience*, 11, p 1–18.

Trzeciakiewicz, H., Esteves-Villanueva, J. O., Carlin, N. and Martić, S. (2015) 'Electrochemistry of heparin binding to tau protein on Au surfaces', *Electrochimica Acta*, 162, p 24–30.

Tuerk, C. and Gold, L. (1990) 'Systematic evolution of ligands by exponential enrichment: RNA ligands to bacteriophage T4 DNA polymerase', *Science*, 249(4968), p 505–510.

Tung, V. C., Huang, J. H., Tevis, I., Kim, F., Kim, J., Chu, C. W., Stupp, S. I. and Huang, J. (2011) 'Surfactant-free water-processable photoconductive all-carbon composite', *Journal of the American Chemical Society*, 133(13), p 4940–4947.

Vashist, S. K. and Vashist, P. (2011) 'Recent advances in quartz crystal microbalance-based sensors', *Journal of Sensors*.

Villemagne, V. L., Pike, K. E., Chételat, G., Ellis, K. A., Mulligan, R. S., Bourgeat, P.,

Ackermann, U., Jones, G., Szoeke, C., Salvado, O., Martins, R., O'Keefe, G., Mathis, C. A., Klunk, W. E., Ames, D., Masters, C. L. and Rowe, C. C. (2011) 'Longitudinal assessment of Aβ and cognition in aging and Alzheimer disease', *Annals of Neurology*, 69(1), p 181–192.

Vives, A. A. (2008) *Piezoelectric transducers and applications*. 2nd ed. Springer Berlin Heidelberg

Vogel, J., Iturria-Medina, Y., Strandberg, O. T., Smith, R., Evans, A. C., Hansson, O., Initiative, for the A. D. N. and Study, the S. B. (2019) 'Pathological tau spreads through communicating brain regions in human Alzheimer's disease', *bioRxiv*, p. 555821.

Vogel, J. W., Iturria-Medina, Y., Strandberg, O. T., Smith, R., Levitis, E., Evans, A. C. and Hansson, O. (2020) 'Spread of pathological tau proteins through communicating neurons in human Alzheimer's disease', *Nature communications*, 11(1), p. 2612.

Vu Nu, T. T., Tran, N. H. T., Nam, E., Nguyen, T. T., Yoon, W. J., Cho, S., Kim, J., Chang, K. A. and Ju, H. (2018) 'Blood-based immunoassay of tau proteins for early diagnosis of Alzheimer's disease using surface plasmon resonance fiber sensors', *RSC Advances*, 8(14), p 7855–7862.

Wang, J. (2006) 'Electrochemical biosensors: Towards point-of-care cancer diagnostics', *Biosensors and Bioelectronics*, 21(10), p 1887–1892.

Wang, J. Z. and Liu, F. (2008) 'Microtubule-associated protein tau in development, degeneration and protection of neurons', *Progress in Neurobiology*, 85(2), p 148–175.

Wang, S. X., Acha, D., Shah, A. J., Hills, F., Roitt, I., Demosthenous, A. and Bayford, R. H. (2017) 'Detection of the tau protein in human serum by a sensitive four-electrode electrochemical biosensor', *Biosensors and Bioelectronics*, 92, p 482–488.

Wang, W., Singh, S., Zeng, D. L., King, K. and Nema, S. (2007) 'Antibody structure, instability, and formulation', *Journal of Pharmaceutical Sciences*, 96, p 1–26

Wang, Y. and Mandelkow, E. (2015) 'Tau in physiology and pathology.', *Nature reviews. Neuroscience*, 17(1), p 22–35.

Wimo, A., Jönsson, L., Bond, J., Prince, M. and Winblad, B. (2013) 'The worldwide economic impact of dementia 2010', *Alzheimer's and Dementia*, 9(1), p 1–11.

Wu, L., Rosa-Neto, P., Hsiung, G.-Y. R., Sadovnick, a D., Masellis, M., Black, S. E., Jia, J. and Gauthier, S. (2012) 'Early-onset familial Alzheimer's disease (EOFAD).', *The Canadian journal of neurological sciences. Le journal canadien des sciences neurologiques*, 39(4), p 436–45.

Yang, L., Li, Y. and Erf, G. F. (2004) 'Interdigitated Array Microelectrode-Based Electrochemical Impedance Immunosensor for Detection of Escherichia coli O157:H7', *Analytical Chemistry*, 76(4), p 1107–1113.

Yang, N., Chen, X., Ren, T., Zhang, P. and Yang, D. (2015) 'Carbon nanotube based biosensors', *Sensors and Actuators, B: Chemical*, 207, p 690–715

Yang, Z., Castrignanò, E., Estrela, P., Frost, C. G. and Kasprzyk-Hordern, B. (2016) 'Community Sewage Sensors towards Evaluation of Drug Use Trends: Detection of Cocaine in Wastewater with DNA-Directed Immobilization Aptamer Sensors.', *Scientific reports.*

Nature Publishing Group, 6, p. 21024.

Yang, Z., Zhang, C., Zhang, J. and Bai, W. (2014) 'Potentiometric glucose biosensor based on core-shell Fe3O4-enzyme-polypyrrole nanoparticles', *Biosensors and Bioelectronics*, 51, p 268–273.

Yuan, Y., Panwar, N., Yap, S. H. K., Wu, Q., Zeng, S., Xu, J., Tjin, S. C., Song, J., Qu, J. and Yong, K. T. (2017) 'SERS-based ultrasensitive sensing platform: An insight into design and practical applications', *Coordination Chemistry Reviews*, 337, p 1–33

Zanoli, L. M., D'Agata, R. and Spoto, G. (2012) 'Functionalized gold nanoparticles for ultrasensitive DNA detection', *Analytical and Bioanalytical Chemistry*, 402, p 1759–1771

Zempel, H. and Mandelkow, E. (2014) 'Lost after translation: Missorting of Tau protein and consequences for Alzheimer disease', *Trends in Neurosciences*, 37, p 721–732

Zengin, A., Tamer, U. and Caykara, T. (2013) 'A SERS-based sandwich assay for ultrasensitive and selective detection of Alzheimer's tau protein', *Biomacromolecules*, 14(9), p 3001–3009.

Zetterberg, H., Wilson, D., Andreasson, U., Minthon, L., Blennow, K., Randall, J. and Hansson, O. (2013) 'Plasma tau levels in Alzheimer's disease', *Alzheimer's Research and Therapy*, 5.

Zhang, S., Huang, F., Liu, B., Ding, J., Xu, X. and Kong, J. (2007) 'A sensitive impedance immunosensor based on functionalized gold nanoparticle-protein composite films for probing apolipoprotein A-I', *Talanta*, 71(2), p 874–881.

Zhang, X., Guo, Q. and Cui, D. (2009) 'Recent advances in nanotechnology applied to biosensors', *Sensors*, 9, p 1033–1053

Zhang, Y., Thompson, R., Zhang, H. and Xu, H. (2011) 'APP processing in Alzheimer's disease.', *Molecular brain*, 4, p. 3.

Zheng, T., Zhang, Q., Feng, S., Zhu, J. J., Wang, Q. and Wang, H. (2014) 'Robust nonenzymatic hybrid nanoelectrocatalysts for signal amplification toward ultrasensitive electrochemical cytosensing', *Journal of the American Chemical Society*, 136(6), p 2288–2291.

Zhu, G., Ye, M., Donovan, M. J., Song, E., Zhao, Z. and Tan, W. (2012) 'Nucleic acid aptamers: An emerging frontier in cancer therapy', *Chemical Communications*, 48(85), p 10472–10480.
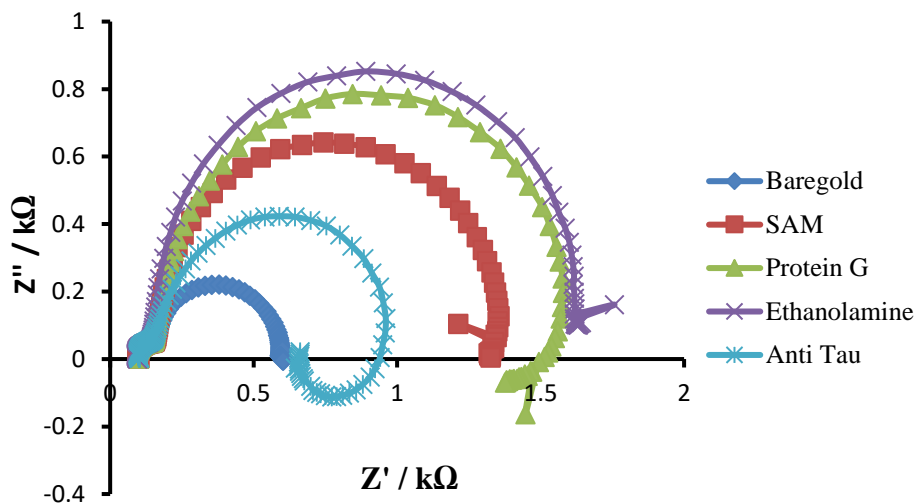
Appendix 1:

Figure shows build-up of sensor, measurement for full frequency range 10 Hz -1 MHz. Plots appear noisy at the extremes of the frequency range.

Appendix 2: (Table 4.1) EIS parameters obtained from fitting the Nyquist plots shown in Figure 3. to the Randles circuit model (Alternative presentation of data with standard error in Appendix 2)

Electrode	Rs (Ω)	Cp (nF)	Rct (Ω)
Biosensor	130.6±1.9	159.7±2.9	592.3±14.3
tau 10^{-2} pM	139.2±2.0	159.7±2.8	647.1±16.9
tau 1 pM	150.0±2.2	156.6±2.6	844.1±24.5
tau 10^2 pM	142.8±1.8	154.6±2.0	1266.0±39.4
tau 10^4 pM	125.6±1.5	128.5±1.3	1789.0±53.0
tau 10^5 pM	119.0±1.1	123.5±9.3	1739.0±37.8

Appendix 3: Table showing Rp (Rct) values extracted from 3 different sets of experiments measuring tau protein

Tau (pM)	Rp Rct(Ω)	Rp Rct(Ω)	Rp Rct(Ω)	Mean
Biosensor	592.3	474	1205.9	757.4
1E-2	647.1	1235	1451	1111.033
1E 0	844.1	1388	1548	1260.033
1E 2	1266	1467	1727	1486.667
1E 4	1789	1480	1921	1730
1E 5	1739	1543	1457	1579.667

Appendix 4: Table showing Rp (Rct) values extracted from 3 different sets of experiments measuring BSA

BSA (pM)	Rp Rct(Ω)	Rp Rct(Ω)	Rp Rct(Ω)	Mean
Biosensor	1078	1032	441.6	850.5333
1E-2	1107	954.7	397.8	819.8333
1E 0	896.8	1004	361.5	754.1
1E 2	1043	948.8	390.7	794.1667
1E 4	1025	960.2	462.4	815.8667
1E 5	1236	767	499.2	834.0667